MODULATION OF THE HOST UNFOLDED PROTEIN RESPONSE BY *LEGIONELLA PNEUMOPHILA*

A thesis

submitted by

Andrew D. Hempstead

In partial fulfillment of the requirements
for the degree of

Doctor of Philosophy

in

Molecular Microbiology

TUFTS UNIVERSITY

Sackler School of Graduate Biomedical Sciences

August, 2015

ADVISOR: RALPH R. ISBERG PH.D.

Abstract

Legionella pneumophila, the causative agent of Legionnaires′ disease, is a Gram-negative intracellular pathogen that replicates within alveolar macrophages during disease. The ability of *L. pneumophila* to replicate within a host cell is dependent on the Icm/Dot type IV secretion system (T4SS), which delivers Icm/Dot translocated substrates (IDTS) into the host cell cytosol. Many of these IDTS are involved in the generation of the *Legionella*-containing vacuole (LCV), which is composed of endoplasmic reticulum (ER)-derived membrane. Here, I report the identification and characterization of MavT, an IDTS that, when expressed in eukaryotic cells, induces the dramatic reorganization of ER structure. MavT binds to members of the Hsp70 family and contains a J domain, which stimulates ATP hydrolysis and substrate binding by Hsp70, consistent with MavT functioning through the manipulation of host cell chaperones. Furthermore, the J domain is clearly functional, as it is shown here to be able to rescue a thermosensitive *E. coli* mutant.

L. pneumophila manipulation of host cell chaperone function and its downstream effects on protein folding led to the hypothesis that the bacterium targets folding pathways associated with the host ER. Many intracellular pathogens that interact with the ER induce or modulate an ER stress response to misfolded proteins, termed the unfolded protein response (UPR). During host cell challenge, I show that *L. pneumophila* inhibits chemical induction of the IRE1 branch of the UPR, in a manner dependent on the Icm/Dot T4SS and, specifically, five translocated substrates that inhibit host cell translation elongation. *L. pneumophila*-derived pathogen associated molecular products (PAMPs), as well as a strain lacking the five translocated elongation inhibitors, induced

this branch of the UPR, indicating the functionality of mechanisms to inhibit UPR during host cell challenge. As many pathogens inhibit translation elongation, this may be a common strategy to inhibit the host UPR. These studies further our knowledge of the broad ways by which *Legionella* modulates the host cell ER and its signaling pathways during disease.

Acknowledgements

Throughout my time at Tufts, there have been numerous individuals who have played an invaluable role in my development as a scientist. Without their support, I would not have been able to achieve many of the goals I had set out to accomplish as a graduate student. The Molecular Microbiology Program has been a wonderful place to call home, providing me with the foundation necessary to become a scientific researcher, while also challenging me to continue to improve.

I specifically would like to thank my advisor, Ralph Isberg PhD. His example of what can be accomplished as a scientist, and the positive impact one can have on the lives of others, has been inspiring. I am also grateful for his guidance, support, and positive outlook, which have helped me to overcome obstacles during my thesis research.

Furthermore, I am greatly appreciative of my Thesis Advisory Committee: Andy Camilli PhD, Katya Heldwein PhD, and Sasha Poltorak PhD. The direction and advice they provided me with as my thesis project progressed vastly improved my research and helped me to think about my work from different perspectives. I would also like to thank Wayne Lencer MD for coming to Tufts to serve as my outside examiner.

My time in the Isberg Lab was a great experience because of the people who comprised the lab during my time there. I am especially indebted to the postdoctoral researchers who were more than willing to provide mentorship and advice, even though they had their own projects and goals to focus on. The graduate students and technicians have also been greatly supportive of me and I thank each of them for this.

I have formed many great friendships during graduate school. Whether this was playing softball with the Microbes, basketball with the Elephants, or just hanging out at tea. I am especially thankful for the friendship and support of Jared Pitts, Neil Greene, Dennise de Jesús and Greg Crimmins.

My family has been especially influential in my path to pursuing a PhD. Education has always been highly valued in my family and for this I am greatly appreciative. Thank you to my Mom, Dad, and sister for your love and support as well as you continued interest in my work.

Most importantly, I would like to thank my wife Megan who has been there for me throughout this journey. I am incredibly grateful for your encouragement, patience, and love, each and every day.

Table of Contents

List of Tables

List of Figures

List of Abbreviations

12-tetradecanoyl phorbol 13-acetate (TPA), ACES buffered yeast extract (AYE), activating transcription factor 6 (ATF6), ADP ribosyltransferases (ADPRTs), ADP-ribosylation factor 1 (Arf1), ATF/cAMP response elements (CRE), atlastin (ATL), basic leucine zipper (bZIP), bone marrow-derived macrophages (BMDMs), brefeldin A (BFA), *Brucella* containing vacuole (BCV), c-Jun-N-terminal kinase (JNK), C/EBP homologous protein (CHOP), calnexin (CNX), calreticulon (CRT), carbenicillin (Carb), ceramide transfer protein (CERT), charcoal buffered yeast extract (CYE), chloramphenicol (Cm), cholera toxin (CT), cycloheximide (CHX), effector triggered response (ETR), endoplasmic reticulum (ER), endoribonuclease (RNase), ER exit sites (ERES), ER stress elements (ERSE), ER-associated degredation (ERAD), ER-degredation-enhancing 1,2-mannosidase-like protein (EDEM), ER-Golgi intermediate compartment (ERGIC), eukaryotic translation initiation factor 2-α (eIF2α), general control non-derepressible-2 (GCN2), Golgi localization signal (GLS), GTP dissociation inhibitor (GDI), GTPase activating protein (GAP), guanine nucleotide exchange factor (GEF), Hank's balanced salt solution (HBSS), heat killed *Escherchia coli* (HKEc), heat killed *L. pneumophila* (HKLp), heat killed *Yersinia pseudotuberculosis* (HKYpt), heme-regulated inhibitor (HRI), Homogolous to Atf/Creb1 (HAC1), hours post infection (hpi), Icm/Dot translocated substrates (IDTS), inhibitor of κB (IκB), inositol requiring kinase 1 (IRE1), integrated stress response (ISR), intracellular multiplication/defect in organelle trafficking (Icm/Dot), IRE1-Dependent Decay (RIDD), isopropyl-β-D-thiogalactopyranoside (IPTG), IκB kinases (IKKs), kanamycin (Kan), L-azidohomoalanine (AHA), *Legionella* glucosyltransferase (Lgt), *Legionella*-containing vacuole (LCV), Lysogeny Broth (LB), mammalian target of rapamycin (mTOR), microtubule organizing center (MTOC), mitogen-activated protein kinase (MAPK), more regions allowing vacuolar colocalization (Mav), mouse embryonic fibroblast (MEF), mRNA-ribosome-nascent chain (R-RNC), N-(2-acetamido)-2-aminoethanesulfonic acid (ACES), nuclear factor kappa-light-chain-enhancer of activated B cells (NF-κB), pathogen associated molecular products (PAMPs), pattern recognition receptor (PRR), peptone-yeast extract-glucose (PYG), PKR-like endoplasmic reticulum kinase (PERK), protein disulfide isomerase (PDI), protein kinase activated by double-stranded RNA (PKR), reactive oxygen species (ROS), replicative BCV (rBCV), reticulon (RTN), retinoic acid-inducible gene 1 (RIG-I), RNA interference (RNAi), rough ER (RER), Shiga toxin 1 (Stx1), signal recognition particle (SRP), *Simkania* containing vacuole (SCV), Single nucleotide polymorphism (SNP), site 1 protease (S1P), site 2 protease (S2P), smooth ER (SER), subtilase (SubAB), ternary complex (TC), thapsigargin (Tp), thymidine (Thy), Toll-like receptor (TLR), Toll/interleukin 1 (IL-1)-receptor (TIR),

transitional ER (tER), transposon (Tn), tunicamycin (Tm), type III secretion systems (T3SS), type IV secretion system (T4SS), UDP-glucose:glycoprotein glucosyltransferase (UGGT), unfolded protein response (UPR), upstream ORF (uORF), X-box-binding protein 1 (XBP1s)

Chapter 1: Introduction

Sections of this chapter were adapted, with permission, from the following review article:

Hempstead AD, Isberg RR. Host signal transduction and protein kinases implicated in *Legionella* infection. Current topics in microbiology and immunology 376:249-69

1.1 ROLE OF THE ENDOPLASMIC RETICULUM IN CELLULAR FUNCTION

The endoplasmic reticulum (ER), the largest membrane bound organelle in the vast majority of eukaryotic cells, plays important roles in many activities key to the life of the cell. The ER functions in the folding and modification of membrane bound and secreted proteins, storage of Ca^{2+}, and lipid synthesis. Maintaining proper ER function is of paramount importance, as dysfunction can lead to disease progression or, if persistent, cell death. As a result, the cell encodes numerous mechanisms to cope with perturbations to the ER, allowing for a return to normal cell function.

1.1.1 Structure and function of the ER

While the ER is a continuous structure, extending from the nuclear envelope to the plasma membrane, it is composed of subdomains, dynamic structures that undergo rapid rearrangements to meet the needs of the cell. The largest categorical grouping of subdomains within the ER is into the smooth ER (SER), rough ER (RER), and nuclear

envelope. The rough ER is a sheet-like structure that is bounded by ribosomes, responsible for the translation of secretory or membrane bound proteins, which are folded in the ER lumen. The smooth ER is devoid of ribosomes and composed of tubular structures that extend out towards the periphery of the cell. The nuclear membrane is composed of two membrane sheets that surround the cells genetic material and are joined at nuclear pores, allowing for movement of substrates across the double membrane. Each of these subregions contains a subset of proteins specific to the function of the domain, allowing for specialization of function.

The tubular network of the smooth ER is a dynamic structure, undergoing continuous modifications and distinct interactions. Two families of proteins are responsible for the formation of ER tubules, the reticulons (RTN1-4) and DP1/Yop1p (Voeltz et al 2006). These proteins insert into the membrane forming a hairpin structure, resulting in membrane curvature and inducing tubule formation. ER tubules fuse with each other at structures termed three-way junctions, resulting in the mesh-like network of the peripheral ER. Three-way junction formation is mediated by dynamin-like membrane bound GTPases known as atlastins (Hu et al 2009, Rismanchi et al 2008). Proper tubule shaping and regulation of fission and fusion is necessary for cellular health, as mutations in proteins regulating these processes result in disease manifesting as hereditary spastic paraplegia (Park et al 2010).

Tubular ER forms extensive contacts with other organelles throughout the cell. Peripheral ER contacts the plasma membrane, which is important for lipid exchange, as well as calcium flux into the ER during conditions of luminal calcium depletion. Nonvesicular transport between the ER and peroxisomes is also important as many of the

lipids and integral membrane proteins required for formation and function of peroxisomes initiate from the ER (Kim et al 2006, Lam et al 2010, Raychaudhuri & Prinz 2008). Similar phenomena are observed at the interface of the ER-mitochondria, as there is no vesicular transport between these organelles (Voeltz et al 2002). Sites of ER-mitochondria interaction are also important for mitochondrial fission, which occurs in an actin mediated process (Friedman et al 2011, Korobova et al 2013), and flux of Ca^{2+} from the ER to the intermembrane space and matrix of the mitochondria, which has been shown to play roles in apoptosis as well as mitochondrial mobility and division (Rizzuto et al 1998, Scorrano et al 2003).

The border of the SER and RER, termed the transitional ER (tER), is the site of formation of vesicles bound for the ER-Golgi intermediate compartment (ERGIC), then to the Golgi, and finally secretion (Appenzeller-Herzog & Hauri 2006, Bannykh et al 1996). This occurs at ER exit sites (ERES), where COPII vesicles are formed (Hobman et al 1998). COPII vesicle formation is mediated by the action of Sar1, a small GTPase that induces membrane deformation (Bielli et al 2005, Lee et al 2005). Sar1 then recruits the Sec23-24 heterodimer that binds to cargo proteins to be transported (Miller et al 2002, Yoshihisa et al 1993). This is followed by the recruitment of the coat proteins Sec13-Sec31 that, with Sar1, drive vesicle formation and eventual fission (Lederkremer et al 2001, Yoshihisa et al 1993). After budding, uncoating of the vesicle occurs due to GTP hydrolysis by Sar1 as it traffics along the secretory pathway (Antonny et al 2001).

The RER is characterized by the presence of ribosomes associated with its surface that were readily observed during early electron microscopy studies of this organelle (Palade 1955). The RER is contiguous with the nuclear envelope with ribosomes found

on the nuclear outer membrane (Gerace & Burke 1988). In contrast to much of the SER, the RER is characterized by regions of little membrane curvature know as sheets. Sheet formation and width is regulated by Climp-63, which also plays a role in the binding of ribosomes to the RER (Sandoz & van der Goot 2015). Ribosomes on the RER cytosolic membrane surface are responsible for translation of secretory and membrane bound proteins, which are folded after translocation into the ER lumen.

1.1.2 Eukaryotic protein translation

Eukaryotic protein translation is divided into three distinct phases: initiation, elongation, and termination. These processes are accomplished by a large number of factors, which are further regulated by numerous other mechanisms. Regulation of translation plays an important role in gene expression and, as such, allows the cell to rapidly respond to changing environmental conditions.

Translation initiation occurs by two parallel processes in which separate initiation complexes interact with mRNA and the small 40S ribosomal subunit (for review see (Sonenberg & Hinnebusch 2009)). mRNA is bound by the eIF4F complex, which includes the cap binding factor eIF4E and the poly-A binding protein (PABP). This results in the recruitment of the 43S preinitiation complex after unwinding of the mRNA secondary structure by the eIF4F complex. The 43S preinitiation complex is composed of the 40S ribosomal small subunit and eIFs 1, 1A, 3, and 5 as well as the ternary complex (TC), which is composed of eIF2 in its GTP bound state and the methionyl-tRNA specialized for initiation (Met-tRNA$_i$). Once the preinitiation complex has been formed

on the mRNA, it begins scanning for an AUG start codon, which once in the P site is bound by Met-rRNA$_i$. eIF5 and eIF5B then induce the hydrolysis of GTP bound by eIF2α, resulting in the recruitment of the 60S ribosome and dissociation of many of the eIFs (Figure 1.1).

The energy state and nutrient availability of a cell is constantly monitored to regulate translation initiation through the control of the eIF4F complex formation. This is accomplished by the Ser/Thr kinase, mammalian target of rapamycin (mTOR), which is downstream of signaling pathways such as that of PI3K/Akt, which are responsible for sensing cellular conditions (Fingar & Blenis 2004). When activated by these pathways, mTOR phosphorylates 4E-BP1, which is an inhibitor of the cap binding protein eIF4E (Gingras et al 1999). 4E-BP1 inhibits eIF4F complex formation by competitive binding to the region of eIF4E that is responsible for its recruitment to the complex (Hay & Sonenberg 2004). Phosphorylation of 4E-BP1 by mTOR limits the affinity of 4E-BP for this domain, resulting in eIF4E recruitment to eIF4F and its subsequent binding to mRNA during translation initiation (Figure 1.1).

The cell is also able to regulate the other parallel pathway of translation initiation, the generation of a productive 43S complex. This is accomplished by inhibition of ternary complex formation through the phosphorylation of eIF2α-GDP on Ser51. eIF2α~P is a competitive inhibitor of eIF2B, the eIF2α guanine nucleotide exchange factor (GEF). This limits the pool of eIF2α-GTP and its subsequent ternary complex formation by the binding to Met-tRNA$_i$ (Sonenberg & Hinnebusch 2009). eIF2α phosphorylation is regulated by four kinases in a process that has been termed the integrated stress response

Figure 1.1 Mechanism of eukaryotic translation initiation and its regulation (1) The exchange of GDP, bound by eIF2, for GTP is mediated by the guanine nucleotide exchange factor eIF2B. (2) eIF2α, a component of the eIF2 complex, recruits the initiator tRNA (Met-$tRNA_i^{Met}$) to form the ternary complex. (3) The 40S ribosomal subunit is bound by eIF1, 1A, 3, and 5. (4) Incorporation of the ternary complex to form the 43S preinitiation complex. (5) Concomitant to steps 1-4, the eIF4 complex binds to mRNA through interaction with the methylated cap, by the cap binding protein eIF4E, and the poly A-tail, through the PABP. (6) The 43S complex is recruited to the mRNA by interactions of eIF3 and eIF5 with eIF4G and eIF4B. (7) The complex scans the 5′ UPR until an AUG start codon is reached. (8) This results in the hydrolysis of GTP bound by eIF2. (9) eIF2-GDP is released, followed by the release of eIF1, 3, and 5, as well as eIF4 complex members. (10) The release of these factors is induced by eIF5B recruitment during the joining of the 60S ribosomal subunit. (11) Hydrolysis of eIF5B-GTP and release of eIF1A results in the translation elongation competent 80S ribosome. (A) Regulation of ternary complex formation through phosphorylation of eIF2α. The eIF2α kinases (PERK, HRI, GCN2, PKR), initiators of the integrated stress response (ISR), phosphorylate eIF2α, which then acts as an inhibitor of eIF2B, preventing the exchange of eIF2 bound GDP for GTP. (B) Regulation of eIF4 complex formation. mTOR activation results in the phosphorylation of 4E-BP, causing it to dissociate from eIF4E, the cap binding protein, leading to eIF4 complex formation.

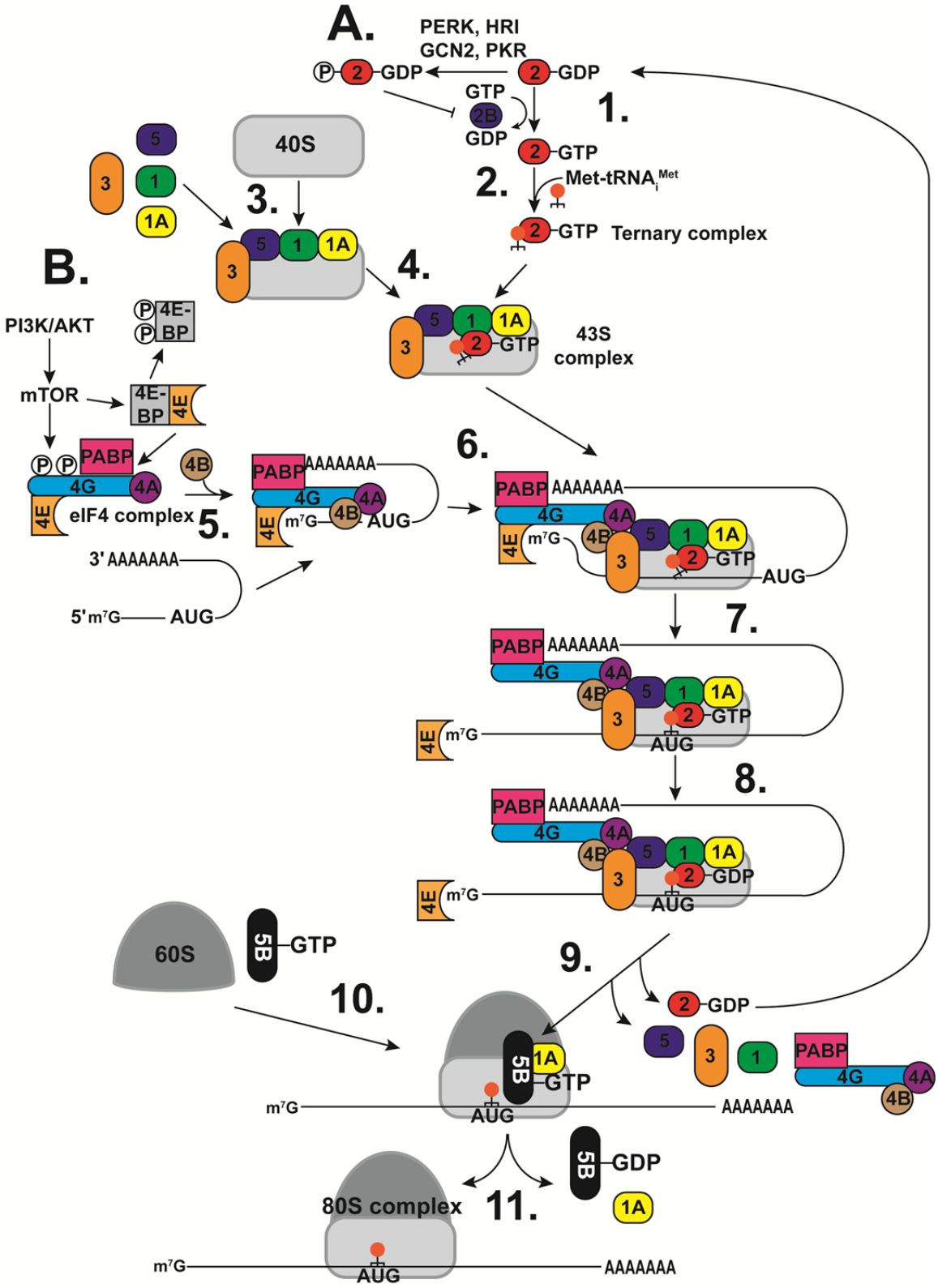
A.
PERK, HRI
GCN2, PKR
GDP
GTP
GDP
1.
GTP
2.
Met-tRNA$_i^{Met}$
GTP
Ternary complex
40S
3.
4.
43S
complex
B.
PI3K/AKT
4E-BP
mTOR
4E-BP
4E
PABP
4G
4A
4B
4E
eIF4 complex
5.
AAAAAAA
m^{7}G
AUG
3' AAAAAAA
5' m^{7}G
AUG
6.
7.
8.
GDP
60S
5B
GTP
9.
10.
11.
80S complex
m^{7}G
AUG
AAAAAAA

(ISR) as these kinases become active in response to a wide variety of cellular insults (Figure 1.1) (Harding et al 2003).

Relative to the complex process of translation initiation, translation elongation requires fewer factors and is a relatively simpler process (for review see (Dever & Green 2012)). Two elongation factors, eEF1A and eEF2 are the major players in this process. Once Met-tRNA$_i$ has bound to the P site, the A-site becomes occupied by the second codon of the ORF. GTP bound eEF1A binds to amino-acylated-tRNA and presents it to the A-site where, if it matches the codon, eEF1A is released following GTP hydrolysis. Once accommodated in the A-site, a peptide bond is formed to the P-site peptidyl-tRNA. This is followed by ratcheting of the ribosome, resulting in localization of tRNAs to hybrid E/P and P/A states. At this point eEF2 binds the 80S ribosome and promotes the translocation of the tRNAs to the E- and P-sites following GTP hydrolysis, thus freeing the A-site and allowing elongation to continue (Figure 1.2).

Termination of translation at stop codons is mediated by two release factors, eRF1 and eRF3 (Zhouravleva et al 1995). eRF1 recognizes the stop codon through its N-terminal domain while the C-terminus of this factor interacts with eRF3 (Song et al 2000). When this complex interacts with the ribosome, GTP is hydrolyzed, resulting in eRF3 release and the middle region of eRF1 extending into the peptide transfer region, causing the peptide to release from the ribosome (Frolova et al 1996, Song et al 2000).

Figure 1.2 Mechanism of translation elongation by eukaryotic cells. Translation elongation occurs by the addition of amino acids to an elongating peptide chain. Aminoacylated-tRNA (orange circle with attached tRNA) is recruited to the A-site of the ribosome by GTP bound eEF1A, which is activated by the GEF eEF1B. Once bound, the aminoacylated-tRNA forms a peptide bond with the aminoacylated-tRNA in the P-site. This is then acted upon by eEF2, which results in translocation of the elongating peptide chain to the E and P site. Following this, deacylated-tRNA is released from the E site, allowing for the cycle to continue until translation termination.

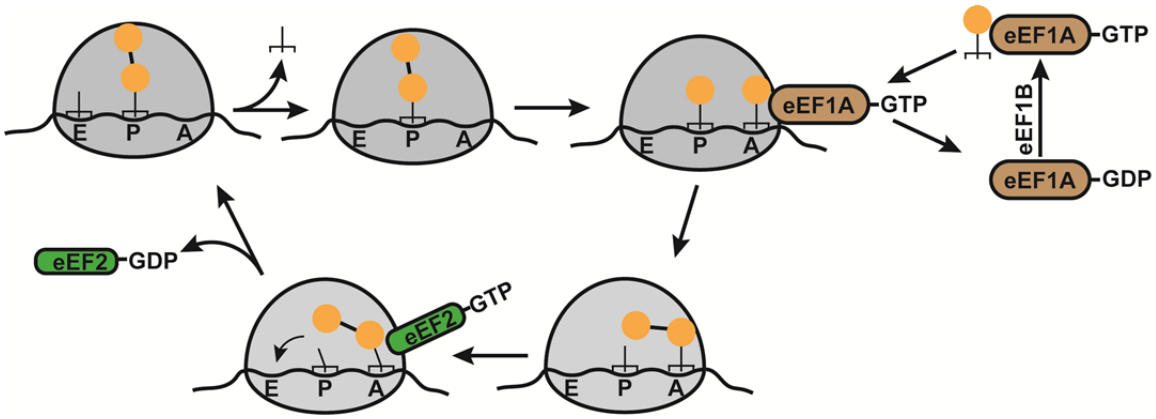
E P A
eEF1A
GTP
eEF1B
eEF1A
GDP
eEF2
GDP
eEF2
GTP

1.1.3 Protein translocation and folding in the ER lumen

During translation, proteins to be folded in the ER lumen are targeted to the RER by a signal sequence, usually found in the N-terminus of the protein that is identified by the signal recognition particle (SRP), a complex composed of 6 protein components and 7S RNA (Walter & Blobel 1980, Walter & Blobel 1982). The SRP is bound by the SRP receptor on the cytosolic surface of the ER where the ribosome then comes in contact with the Sec61 translocon (Halic et al 2006). The Sec61 complex directs the movement of the translating peptide into the ER lumen where folding begins, concurrent with translation (Sanders et al 1992). Folding in the ER lumen is a tightly regulated process in which folding factors ensure that only proteins that have folded properly are allowed to exit the ER. Proteins that are unable to reach their final folded state are retrotranslocated out of the ER where they undergo ubiquitin-mediated proteasomal degradation, a process termed ER-associated degradation (ERAD) (Needham & Brodsky 2013).

One of the most important folding factors found in the ER lumen is the Hsp70 family member BiP. Hsp70 family members bind to exposed hydrophobic regions on unfolded proteins, preventing their aggregation, prior to their localization to the hydrophobic core of the protein during proper folding (Fourie et al 1994). Hsp70 binding is an ATP regulated process in which ATP bound Hsp70 binds to client peptides in a low-affinity state. Binding is enhanced by the action of members of the Hsp40 family of cochaperones. Hsp40 proteins, through the activity of a domain known as a J domain, stimulate the ATPase domain of Hsp70, inducing ATP hydrolysis, and subsequent Hsp70 structural rearrangements that enhance polypeptide substrate binding (Fan et al 2003, Wall et al 1994). Hsp40 proteins, through protein interaction domains, also play roles in

the presentation of specific substrates to Hsp70 family members, while also targeting Hsp70 to specific subcellular locations (Fan et al 2003). As such, there are numerous Hsp40 family members that are found in the ER, allowing for the regulation of protein folding specificity (Fan et al 2003, Shen et al 2002b). Completion of the folding process by Hsp70 is regulated by nucleotide exchange factors that allow for ADP exchange with ATP, resulting in release of the client peptide.

Another important process in the regulation of protein folding is mediated by the lectin proteins calnexin and calreticulon (CNX/CRT). In the ER, N-linked glycosylation of elongating peptides transfers a core oligosaccharide to the nascent chain, which is then cleaved down to generate a monoglucosylated protein by glucosidases I and II (Hebert et al 1995). Monoglucosylated peptides are recognized by CNX/CRT, which maintain the protein in the ER lumen and also facilitate the interaction of the client peptide with ERp57, which is a protein disulfide isomerase (PDI) that assists with protein folding (Oliver et al 1999). Glucosidase II then acts to cleave the remaining glucose, resulting in disassociation of the protein from CNX/CRT (Hebert et al 1995) and the subsequent trafficking down the secretory pathway. If, after CNX/CRT dissociation, the protein is not properly folded, it is recognized by UDP-glucose:glycoprotein glucosyltransferase (UGGT) (Ritter & Helenius 2000), which adds back a monoglucose to the peptide, that can again be recognized by CNX/CRT to restart the cycle. Under circumstances in which a native structure is not achieved, a mannose is removed from the core oligosaccharide by ER α1,2-mannosidase, resulting in its recognition by the ER-degradation-enhancing 1,2-mannosidase-like protein (EDEM), which results in ERAD of the unfolded protein (Hosokawa et al 2001, Jakob et al 2001).

1.2 THE UNFOLDED PROTEIN RESPONSE

Varying environmental conditions encountered by the cell can induce the large scale mis- or unfolding of proteins within the ER lumen, termed ER stress. Because of the importance of protein folding and modification within the ER, eukaryotic cells possess a system, termed the unfolded protein response (UPR), to adapt to, and alleviated ER stress (Figure 1.3). In mammalian cells, UPR initiates from three transmembrane signaling proteins in the ER membrane: PKR-like endoplasmic reticulum kinase (PERK), inositol requiring kinase 1 (IRE1), and activating transcription factor 6 (ATF6) (Ron & Walter 2007, Schroder & Kaufman 2005). Each of these signaling complexes is able to sense misfolded proteins in the ER lumen and initiate a specific response to alleviate the stress. The combined end result of activation of these pathways is the upregulation of chaperones, to assist in the refolding of mis- or unfolded proteins, an expansion of the ER through the increased production of membrane lipids, and a decrease of the protein folding burden on the ER, through the degradation of cytosolic mRNA and the global inhibition of translation initiation (Maurel et al 2014, Ron & Walter 2007).

The ATF6 pathway is initiated in response to ER stress when two Golgi localization signals (GLS1 and GLS2) become exposed (Shen et al 2002a). A model for how this is believed to occur is that during unstressed cellular conditions GLS1 is bound by BiP and, in response to stress conditions, BiP dissociates in order to bind to unfolded proteins in the ER lumen, releasing ATF6 (Shen et al 2002a). When this occurs, GLS2 directs ATF6 to the Golgi where it is cleaved by site 1 and site 2 proteases (S1P and

Figure 1.3 Unfolded protein response (UPR) pathways. ER stress results in the misfolding of proteins within the ER lumen. Three transmembrane sensors: PERK, IRE1, and ATF6 detect misfolded proteins, through either their direct binding to the sensors, or when the ER chaperone BiP dissociates from the sensors, to bind to unfolded proteins. PERK activation occurs by its oligomerization and phosphorylation. PERK then phosphorylates the translation initiation factor eIF2α, which inhibits global translation, while allowing for the translation of specific factors, such as the transcription factor ATF4. IRE1 activation also occurs through its oligomerization and transphosphorylation. The kinase domain of IRE1 induces the phosphorylation of JNK, activating downstream pathways. The activated endonuclease domain of IRE1 serves two different activities: the degradation of multiple cytosolic mRNAs in a process termed RIDD, and the splicing of an intron in the mRNA encoding the transcription factor XBP1s, resulting in the translation of a functional transcriptional regulator. The ATF6 pathway is induced following BiP dissociation, which exposes a Golgi targeting domain, where ATF6 is cleaved by two proteases S1P and S2P. This releases the soluble N-terminus, ATF6f, a potent transcription factor. Each transcriptional regulator traffics to the nucleus where it binds ERSE or UPRE sites to upregulate the expression of target genes.

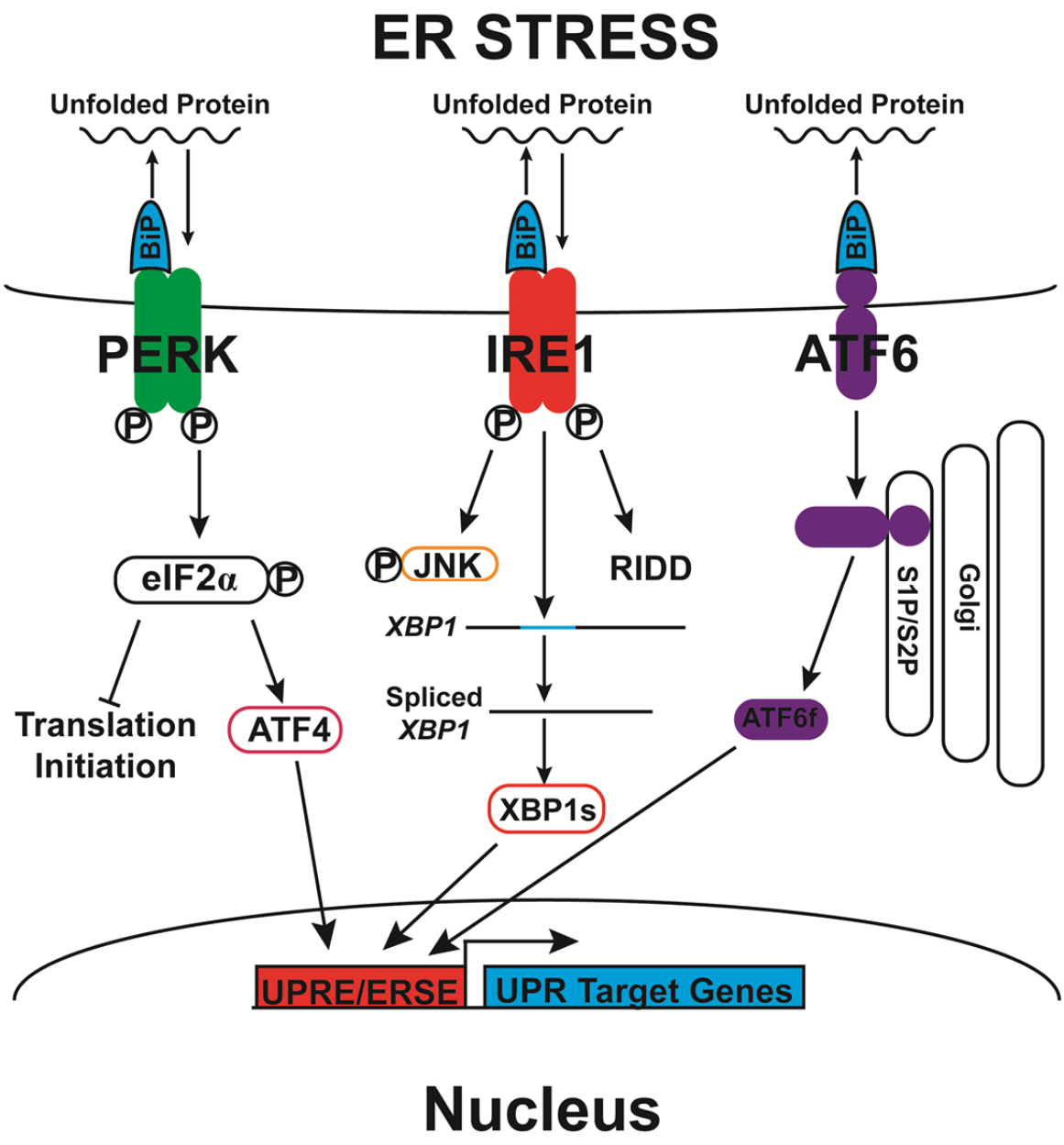
ER STRESS
Unfolded Protein
Unfolded Protein
Unfolded Protein
BiP
BiP
BiP
PERK
IRE1
ATF6
P
P
P
P
eIF2α
P
P JNK
RIDD
XBP1
Spliced
XBP1
S1P/S2P
Golgi
Translation
Initiation
ATF4
ATF6f
XBP1s
UPRE/ERSE
UPR Target Genes
Nucleus

S2P), resulting in the release of the N-terminal fragment, pATF6-N, a transcription factor that then localizes to the nucleus (Chen et al 2002, Haze et al 1999, Ye et al 2000). In the nucleus, pATF6-N induces the expression of genes regulated by ER stress elements (ERSE) I and II, and ATF/cAMP response elements (CRE) (Wang et al 2000, Yoshida et al 2000). Factors regulated by these elements include both chaperones and components of the ERAD system.

Activation of the PERK pathway occurs rapidly after induction of ER stress. PERK is a type I transmembrane protein containing a domain on the luminal side of the ER membrane that is able to sense ER stress (Harding et al 1999). The model for activation of PERK is similar to that of ATF6, in which BiP dissociation results in activation (Bertolotti et al 2000). PERK activation occurs through its oligomerization and trans-phosphorylation (Ma et al 2002). This results in the activation of its serine/threonine kinase domain on the cytosolic side of the ER membrane (Harding et al 1999).

Signaling downstream of PERK activation leads to the global inhibition of host protein translation (Harding et al 1999). PERK is a member of the eukaryotic translation initiation factor 2-α (eIF2α) kinase family that also consists of PKR (protein kinase activated by double-stranded RNA) that is induced by viral infection, HRI (heme regulated inhibitor) that is activated by heme deprivation or heat shock, and GCN2 (general control no derepressible-2) that is induced by amino acid limitation (Harding et al 1999, Raven & Koromilas 2008). Activation of this kinase family leads to the phosphorylation of eIF2α, reducing the binding to and delivery of Met-tRNA$_i$ to the initiation complex (Figure 1.1) (Sonenberg & Hinnebusch 2009). While this results in a

global limitation of protein translation initiation, select transcripts that contain an upstream ORF (uORF) are translated.(Palam et al 2011, Vattem & Wek 2004). One such factor, encoded downstream of a uORF in the transcripts 5′ UTR, is ATF4, a main target of PERK activation. This transcription factor is translated when initiation at the upstream uORF is unproductive, during conditions of eIF2α~P, resulting in ribosomal bypass of the uORF and subsequent translation of the downstream *ATF4* coding sequence (Vattem & Wek 2004). ATF4, a member of the basic leucine zipper (bZIP) superfamily, induces the expression of target genes, most notably the proapoptotic factor C/EBP homologous protein (CHOP) that is also translated in a uORF dependent manner (Palam et al 2011).

The IRE1 pathway is believed to be the most ancient and conserved pathway of the unfolded protein response (Ron & Walter 2007). There are two orthologs of IRE1 found in mammals, IRE1α and IRE1β, with IRE1α being ubiquitously expressed, while the expression of IRE1β is limited epithelial cells of the gastrointestinal tract (Bertolotti et al 2001). IRE1 is also a type I transmembrane protein with an ER luminal domain similar to that of PERK. Studies have shown that the luminal domain of PERK and IRE1 are interchangeable, pointing to a common mechanism of their activation (Bertolotti et al 2000). Notably, there appear to be multiple mechanisms by which IRE1 detects misfolded proteins in the ER lumen, either through dissociation of BiP (Bertolotti et al 2000), as seen for other sensors, or through the direct binding of misfolded protein (Cho et al 2013, Gardner & Walter 2011). Regardless of the mechanism by which IRE1 detects misfolded proteins, activation of IRE1 occurs through its oligomerization and trans-phosphorylation. This activation results in both the activation of a cytosolic kinase, which

induces signaling through the phosphorylation of c-Jun-N-terminal kinase (JNK), and an endoribonuclease (RNase) domain that acts on cytoplasmic mRNA.

Activation of the IRE1 RNase domain results in the expression of the potent bZIP transcription factor: X-box-binding protein 1 (XBP1s). In mammalian cells, *XBP1* mRNA is translated during unstressed conditions to generate an alternative form of the protein, XBP1u, which lacks the ability to bind DNA. XBP1u functions to direct the mRNA encoding XBP1 to the ER membrane, which is mediated by a hydrophobic stretch within the C-terminus of the protein (Yanagitani et al 2009). Ribosomal pausing, occurring after translation of this region, results in the entire mRNA-ribosome-nascent chain (R-RNC) complex localizing to the ER (Yanagitani et al 2011). During conditions of ER stress, the activated RNase domain of IRE1 mediates the unconventional cytoplasmic splicing of ER membrane targeted *XBP1* mRNA to cleave out a 26 nucleotide intron, resulting in a translational frameshift (Yoshida et al 2001). During splicing, the mRNA is ligated to generate a functional mRNA, by the ligase RtcB, from which XBP1s is translated (Lu et al 2014). Similarly, in yeast the XBP1 homolog, Homologous to Atf/Creb1 (HAC1), is encoded by mRNA containing a 252 nucleotide intron, which is spliced during ER stress (Mori et al 2000).

After translation, XBP1s traffics to the nucleus where it regulates the expression of an extensive number of genes. Like ATF6, XBP1s binds to ERSE sites to regulate the expression of factors involved in ERAD, protein folding, autophagy, lipid biogenesis, vesicle trafficking, and the translocation of proteins into the ER (Glimcher 2010). In yeast, HAC1 has been shown to be shown to induce the expression of 381 ORFs in response to ER stress inducing agents (Travers et al 2000). Expression of this large array

of factors by XBP1s or HAC1 allows the cell to cope with ER stress through activation of this pathway.

Activation of the RNase domain of IRE1 initiates an additional, XBP1s independent, mechanism to alleviate ER stress. This process, initially identified in *Drosophila*, is called IRE1-Dependent Decay (RIDD) of mRNA and results in the limiting of the cytosolic pool of mRNA, decreasing translation and the subsequent folding load placed upon the ER (Hollien & Weissman 2006). This system was later confirmed to also occur in higher eukaryotes, including mammals (Han et al 2009, Hollien et al 2009). RIDD shows sequence specificity for the consensus sequence 5′-CUGCAG-3′ that is identical, or similar, to that recognized in XBP1 encoding mRNA during splicing (Oikawa et al 2010). There are currently 37 putative targets of IRE1α that have been identified, with the sequence specificity determined for 21 of these (Maurel et al 2014). It appears that there is a preference for ER-localized and secretory proteins, consistent with the function of limiting the folding load on the ER, as they account for 64% of the IREα RIDD targets, while all of the identified IRE1β RIDD targets are ER-localized or secretory proteins (Maurel et al 2014).

If UPR pathway activation fails to alleviate ER stress, these pathways induce an apoptotic response in the cell. The JNK and RIDD pathways downstream of IRE1 activation result in proapoptotic signaling, which is in contrast to signaling emanating from XBP1s that is thought to be prosurvival (Moenner et al 2007). RIDD activation results in the decreased expression of four miRNAs that are repressors of the proapoptotic caspase-2, leading to its increased expression (Upton et al 2012). Meanwhile, JNK activation leads to mitochondrial mediated caspase activation and

apoptosis. ATF4, which is selectively translated after PERK activation, induces the expression of the proapoptotic factor CHOP (Oyadomari & Mori 2004). CHOP signals through the downregulation of the antiapoptotic Bcl-2 regulator protein and induces the translocation of the proapoptotic factor Bax to the mitochondria (McCullough et al 2001).

1.3 PATHOGEN MANIPULATION OF THE ER AND UPR PATHWAYS

Many bacterial and viral pathogens manipulate cellular membranes, including that of the ER, to inhibit the host's ability to respond and clear the pathogen, or to form an intracellular niche (Asrat et al 2014a). As such, these pathogens come in contact with pathways emanating from the ER, including the UPR. UPR pathways are linked to the innate immune response, allowing the host to recognize pathogen manipulation of the ER. Furthermore, both viral and bacterial pathogens encode mechanisms to manipulate UPR pathways for their own benefit.

1.3.1 Manipulation of the ER by intracellular pathogens

The ER is a nutrient rich organelle that is devoid of cytosolic innate immune sensors and thus is an attractive niche for intracellular pathogens. Pathogens are able to gain access to this organelle either by trafficking through the endocytic pathway, interacting with ER tubules, or intercepting vesicles trafficking from the ER. These pathogens then form a replicative niche utilizing ER interaction to form vacuoles that contain ER membrane and integral membrane proteins. This is often accomplished by the translocation of effector proteins through specialized bacterial secretion systems.

Brucella spp replicate within an intracellular compartment known as the *Brucella* containing vacuole (BCV). After uptake, *Brucella* initially traffics down the endocytic pathway, where it transiently interacts with lysosomes (Starr et al 2012, Starr et al 2008). Acidification by lysosomes is believed to activate the major *Brucella* virulence factor, its VirB T4SS (Boschiroli et al 2002). This system translocates effector proteins that limit further progression of the bacterium down the endocytic pathway resulting in subsequent construction of the BCV. This is accomplished by the hijacking of vesicles from ERES to mediate the formation of a replicative BCV (rBCV), in which endocytic membrane is replaced with ER membrane (Celli et al 2005). This process is dependent on the host Sar1 GTPase, which regulates COPII vesicle budding from ERES, as well as Rab2, a GTPase involved in retrograde trafficking of Golgi-ER vesicles (Celli et al 2005, Fugier et al 2009).

There is mounting evidence that intracellular replication by *Chlamydia* spp. also involves interaction with the ER. Within a cell, *Chlamydia* replicates within a vacuole termed an inclusion, which traffics along microtubules to the microtubule organizing center (MTOC)/Golgi region and does not fuse with endosomes or lysosomes (Clausen et al 1997, Hackstadt 2000). Rab1, a GTPase involved with ER-Golgi trafficking, interacts with the inclusion, pointing to the importance of vesicle trafficking from the ER in inclusion formation (Rzomp et al 2003). Furthermore, the bacterial inclusion membrane protein IncD recruits the ceramide transfer protein (CERT), resulting in the recruitment of VAPA/B tubules, consistent with interaction of the inclusion with ER tubules (Derre et al 2011).

The *Chlamydial*-like organism *Simkania negevensis* forms extensive ER contact sites with its *Simkania* containing vacuole (SCV) (Mehlitz et al 2014). *S. negevensis* does not associate with endosomal markers, and instead recruits ribosome studded membrane and ER markers within 1-2 days of infection (Mehlitz et al 2014). The SCV consists of numerous interconnected smaller vacuoles harboring bacteria, with ER contact sites in both mammalian cells and the amoebal host *Acanthamoeba castellanii*, consistent with a common mechanism of intracellular replication (Mehlitz et al 2014).

1.3.2 Activation of UPR pathways by bacterial pathogens

As many pathogens interact with the ER during their life cycle, it has been observed that some activate UPR pathways. This mechanism by which a host can detect pathogens was first observed for viruses, including flaviviruses, which form a replication complex on the ER surface, then bud into the ER lumen, a lifecycle which induces UPR pathways (Su et al 2002, Tardif et al 2002). Bacterial pathogens have also been observed to induce the UPR, often through specific effector proteins, many of which target the ER. UPR activation in response to pathogens is evolutionarily conserved as it occurs in both plants and lower eukaryotes (Moreno et al 2012, Richardson et al 2010).

Toxins produced by numerous bacterial species induce ER stress and activation of UPR pathways. *Listeria monocytogenes*, in a process dependent on listeriolysin O (LLO), induces all branches of the UPR (Pillich et al 2012). It is likely that this may be caused by a disruption of Ca^{2+} homeostasis, due to the pore-forming ability of this toxin. Cell death, induced by the VacA toxin of *Helicobacter pylori*, is mediated through the activation of

the PERK pathway of the UPR, resulting in CHOP induced apoptosis (Akazawa et al 2013). Shiga toxin-producing *E. coli* produce two toxins that have been shown to induce UPR. The subtilase (SubAB) toxin degrades BiP, resulting in the induction of all pathways of the UPR (Paton et al 2006, Wolfson et al 2008). Treatment of cells with the Shiga toxin 1 (Stx1) also induced all branches of the UPR, with activation of ATF6 and PERK, but not IRE1, dependent on toxin activity (Lee et al 2008). This may point to alternate mechanisms for the induction of each pathway.

Study of the activation of UPR pathways by cholera toxin (CT) showed the first mechanism by which a toxin activated a specific branch of the response (Cho et al 2013). Cholera toxin is an AB_5 subunit toxin that travels through the Golgi to the ER (Sandvig et al 1992). In the ER, the A subunit of the toxin unfolds, is recognized by the ERAD system, and retrotranslocates to the cytosol where it refolds to exert its toxin activity (Tsai et al 2001). CT specifically induces activation of IRE1, with no detectable activation of either PERK or ATF6 (Cho et al 2013). Like Stx1, this was independent of the enzymatic activity of the toxin, as CT with an inactivating mutation induced IRE1 to levels similar to that of the wild type protein. The mechanism by which CT induces IRE1 is through direct binding of the unfolded protein to the ER luminal domain of IRE1 (Figure 1.4) (Cho et al 2013). It is possible that a similar binding of Stx1 to IRE1 may be the mechanism by which the enzymatically inactive Stx1 mutant induces IRE1 activity (Celli & Tsolis 2015).

Interrogation of UPR pathways, during challenge by *Brucella* spp., has shown how VirB T4SS translocated effector proteins that target the ER induce pathways of the UPR. The *B. abortus* T4SS substrate VceC was required for the induction of UPR during

challenge of mouse macrophages. This protein, when expressed in cells, localizes to the ER and results in its reorganization, while also binding to BiP, which may be responsible for the induced UPR activation (de Jong et al 2013). Furthermore, ectopic expression of other T4SS substrates (BspC, BspG, BspH, BspI, and BspK) induced UPR pathways, as measured by ERSE reporter activity, which may point to alternative mechanisms of UPR activation (Myeni et al 2013). *B. melitensis* challenge of mouse macrophages also induces UPR, but this is independent of the VirB T4SS and is instead dependent on the Toll/interleukin 1 (IL-1)-receptor (TIR) domain-containing protein, TcpB (Smith et al 2013).

Detection of pathogen-associated molecular products (PAMPs) has been shown to directly activate the IRE1 pathway of the UPR. Agonists of Toll-like receptor (TLR) 1, 2, and 4-6 activate XBP1 splicing (Figure 1.4), while also inhibiting the induction of the PERK and ATF6 pathways (Martinon et al 2010). Engagement of TRAF6 by TLR downstream signaling proteins results in the ubiquitination of IRE1. As a consequence, there is inhibition of recruitment of protein phosphatase 2A (PP2A), allowing for the maintenance of IRE1 phosphorylation and subsequent RNase activity (Qiu et al 2013). TRAF6 also activates the NADPH oxidase Nox2, which is required for TLR mediated XBP1 splicing (Martinon et al 2010). A potential explanation for this finding is that reactive oxygen species (ROS) generated by Nox2 could be inducing ER stress (Martinon et al 2010). These findings showed that activation of a UPR pathway may occur through signaling that does not directly cause the misfolding of proteins in the ER lumen, while also showing the interconnectedness of innate immunity and UPR pathways.

1.3.3 Role of UPR pathways in the immune response

Numerous studies have shown that misregulation of protein folding in the ER lumen, resulting in the induction of ER stress, induces disease pathologies due to activation of pathways of the immune response. Expression of a misfolding mutant of Muc2, which encodes for mucin expressed by intestinal goblet cells, results in ER stress in vitro (Heazlewood et al 2008). Furthermore, mice harboring Muc2 mutations exhibited symptoms similar to the pathologies observed in human ulcerative colitis, including enhanced expression of IL-1β, TNF-α, and IFN-γ (Heazlewood et al 2008). Also, the human leukocyte antigen-B27, which frequently misfolds during MHC class 1 complex folding, induces UPR. This, in complex with pattern recognition receptor (PRR) agonism, leads to IL-23 production, resulting in T-helper 17 cell activation and expansion, which may play roles in spondyloarthritis (Colbert et al 2010).

Induction of each pathway of the UPR has been shown to induce nuclear factor kappa-light-chain-enhancer of activated B cells (NF-κB) activation. Signaling through the regulated transcription factor NF-κB results in changes in the expression of hundreds of genes, including proinflammatory cytokines and regulators of cell survival and differentiation (Natoli 2009). In an unstimulated cell, NF-κB hetero- and homodimers are inhibited by interaction with the inhibitor of κB (IκB) family proteins. NF-κB signaling is initiated when IκB kinases (IKKs) are activated, leading to the phosphorylation of IκB,

Figure 1.4 Proinflammatory cytokine induction mediated by IRE1 signaling TLR-mediated detection of bacterial PAMPs signals to activate TRAF6. TRAF6 mediated ubiquitination of IRE1 inhibits its interaction with the phosphatase PP2A, inducing prolonged IRE1 phosphorylation and activation. TRAF6 also induces generation of ROS through the NADPH oxidase NOX2, which may induce IRE1 activation through induction of ER stress. IRE1 activation leads to XBP1 splicing and expression of XBP1s, which binds to the promoter regions of proinflammatory cytokines. XBP1s appears to enhance proinflammatory cytokine signaling, rather than being the sole inducer of the response, as TLR mediated induction of proinflammatory cytokines, through NF-κB or MAPK signaling, is also required. IRE1 activation also occurs directly through the binding of the cholera toxin A subunit. While this induces XBP1 splicing, another pathway, through IRE1-dependent decay (RIDD), is essential for the activation of proinflammatory cytokines. RIDD generates RNA fragments that are detected by the cytosolic sensor RIG-I, resulting in NF-κB activation and downstream transcriptional induction of target genes. Lastly, IRE1 recruits JNK and IKK, resulting in downstream NF-κB and AP-1 activation.

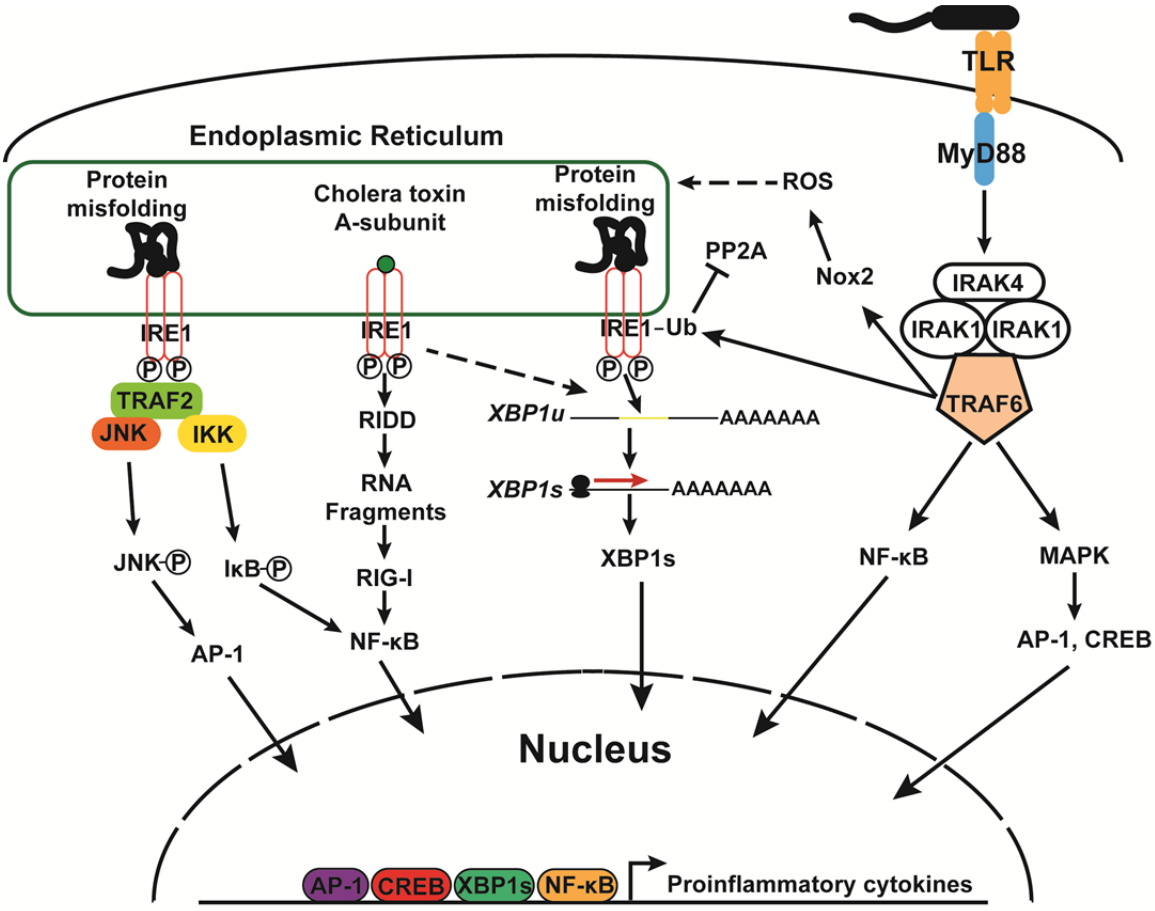
TLR
MyD88
Endoplasmic Reticulum
Protein misfolding
Cholera toxin A-subunit
Protein misfolding
ROS
PP2A
Nox2
IRAK4
IRAK1
IRAK1
IRE1
IRE1
IRE1-Ub
TRAF6
TRAF2
JNK
IKK
RIDD
XBP1u
AAAAAAA
RNA Fragments
XBP1s
AAAAAAA
JNK-P
IκB-P
RIG-I
XBP1s
NF-κB
MAPK
AP-1
NF-κB
AP-1, CREB
Nucleus
AP-1
CREB
XBP1s
NF-κB
Proinflammatory cytokines

which results in its ubiquitination and subsequent proteasomal degradation. Released NF-κB translocates to, and is maintained in the nucleus where it binds to κB sequences located in the promoter and enhancer regions of target genes (Li & Verma 2002). PERK mediated phosphorylation of eIF2α inhibits the translation of the short lived IκB, resulting in a lack of inhibitor necessary to inactivate NF-κB. ATF6 dependent transient activation NF-κB results from the phosphorylation of the kinase Akt, leading to IKK activation, during the early phase of the UPR (Yamazaki et al 2009)

Activation of the kinase domain of IRE1 results in downstream mitogen-activated protein kinase (MAPK) and NF-κB activation. The signaling pathways both go through the adaptor protein TRAF2, which is recruited to the ER membrane upon IRE1 activation. In the case of NF-κB activation, IRE1, through TRAF2, recruits IKK in a process dependent on IRE1 phosphorylation (Hu et al 2006, Kaneko et al 2003). This results in IKK mediated phosphorylation of the inhibitor of NF-κB, IκB and, consequently, translocation of NF-κB to the nucleus, leading to transcriptional upregulation of target genes. To induce MAPK signaling, IRE1 also recruits JNK to the ER membrane through TRAF2. Activation of JNK then leads to proinflammatory cytokine expression through the transcription factor AP-1(Karin 1995, Urano et al 2000).

While pathways of the UPR are directly interconnected with many innate immune signaling pathways, the largest role the UPR seems to have on immunity occurs when UPR pathways are activated in the context of PRR engagement. This is one of the best examples of the two-signal model of immunity, in which activation of two different pathways by a pathogen results in an enhanced cellular response (Vance et al 2009). It

appears that cells undergoing UPR pathway induction, while also detecting bacterial products, recognize this as a pathogen-specific signal, and respond accordingly.

Pharmacological induction of ER stress, in the presence of TLR agonists, induces a highly proinflammatory response. Treatment of cells with tunicamycin (Tm) or thapsigargin (Tp), chemical inducers of ER stress, induces limited induction of IL-6 or IL-23, but when combined with a TLR2 or TLR4 agonist induces a 10-100 fold induction in transcript levels, relative to the TLR agonist alone (Fontana et al 2011, Martinon et al 2010). Similar results are observed when secreted IL-6 is measured, showing that the transcriptional induction results proinflammatory cytokine production (Martinon et al 2010). The induction of IL-6 is largely dependent on XBP1s as shRNA knockdown of IRE1, or MEFs deficient in XBP1s, show a dramatic decrease in the two-signal, enhanced expression (Figure 1.4) (Martinon et al 2010). Furthermore, XBP1s has been shown to directly bind to the *Tnfα* and *Il6* promoters, consistent with XBP1s mediated transcriptional upregulation of these proinflammatory cytokines (Martinon et al 2010). It is likely that in the context of two signals, XBP1s collaborates with another innate immune transcriptional activator at these promoters to drive the enhanced expression of proinflammatory cytokines. In the case enhanced expression of IL-23, the induction is dependent on CHOP, rather than XBP1s, as CHOP binds to its promoter, and knockdown of *CHOP* inhibits the two-signal, enhanced response (Goodall et al 2010).

In addition to the role of XBP1s, downstream of IRE1 activation, the RIDD pathway also activates innate immune sensors (Figure 1.4). RIDD activation induces mRNA fragmentation that is recognized by the retinoic acid-inducible gene 1 (RIG-I), an RNA helicase that acts as a cytosolic sensor to detect double- and single-stranded

uncapped RNA (Cho et al 2013, Yoneyama et al 2004). This results in downstream expression of the proinflammatory cytokines IL-6 and IL-8 in response to NF-κB activation by RIG-I (Cho et al 2013). The mechanism by which IRE1 activates the innate immune response through RIDD was observed to be due to direct binding of CT to IRE1 (Cho et al 2013). This may point to the mechanism by which IRE1 is activated in determining the response, through XBP1s or the RIDD pathway, allowing for varying outputs from the same UPR sensor.

1.3.4 Inhibition of UPR pathways by pathogens

As activation of UPR pathways, in the context of PRR engagement, induces a strong proinflammatory response, it may be beneficial to pathogens to inhibit the response. This has been observed for the hepatitis C virus, which inhibits both the IRE1 and PERK pathways of the UPR (Pavio et al 2003, Tardif et al 2004). It has also been recently demonstrated that the chlamydial organism *Simkania negevensis* replicates in a vacuole that is closely associated with the ER and mitochondria (Mehlitz et al 2014). Interestingly, this pathogen does not induce an ER stress response, and furthermore, is able to inhibit chemically induced activation of UPR pathways, including that of IRE1α (Mehlitz et al 2014). While this appears to be beneficial to the bacterium, likely due to the limitation of an enhanced two-signal immune response, little is known about the mechanism by which it accomplishes this.

1.4 THE PATHOGENESIS OF *LEGIONELLA PNEUMOPHILA*

1.4.1 Legionnaires′ disease

A mysterious outbreak of severe pneumonia among attendees of the 58th American Legion Convention, held at the Bellevue Stratford Hotel in Philadelphia, Pennsylvania from July 21-24, 1976 would spark one of the most intense epidemiological studies ever conducted by the CDC to try to identify the causative agent. In all, 34 of the 221 infected individuals would die from this unknown disease. For months laboratory tests ruled out common causative agents of pneumonia, causing public criticism of the CDC by the media. A clue as to the causative agent of this disease came when Joseph McDade, a CDC scientist who specialized in *Rickettsia*, noticed that guinea pigs that had been inoculated with tissue of infected individuals had bacteria present in their livers (McDade et al 1977). Antibody testing confirmed that bacteria present in the guinea pig livers were also in both serum and lung tissues from infected individuals. This bacterium, the causative agent of Legionnaires′ disease, was named *Legionella pneumophila* to recognize the event which resulted in its discovery (Fraser 2005). Further testing revealed that *L. pneumophila* was responsible for causing unexplainable outbreaks as far back as 1947 (McDade et al 1979), as well as the 1968 outbreak in Pontiac, Michigan, which was characterized by a milder form of the illness, later termed Pontiac Fever (Glick et al 1978).

Current CDC estimates show that 8,000-18,000 individuals are hospitalized as a result of Legionnaires′ disease in the United States each year. Those most at risk for infection include the elderly, immunocompromised, and smokers. Symptoms including fever, chills, and a cough begin 2-10 days after exposure and are similar to those

observed with other pneumonias. This presents challenges for diagnosis, which is confirmed by a urinary antigen test. The common route of transmission is by aerosolization of a *Legionella* contaminated water source. There is currently no evidence for person-to-person transmission. Cell permeable antibiotics, such as erythromycin, are used to treat of *Legionella* infection (Edelstein 1995).

1.4.2 *Legionella pneumophila*

The genus *Legionella* is made up of 48 species, of which half have been shown to cause disease in humans (Dennis et al 1993, Fernandez et al 1989). Members of this genus are Gram-negative rods, which are obligate aerobes and require medium supplemented with iron and L-cysteine for growth (Feeley et al 1979). *Legionella* are found in the environment in freshwater sources as well as in the soil (Fields et al 2002). A defining characteristic of this genus is their ability to survive and replicate within protozoan hosts, though with different host specificities for each member of the genus (Fields 1996, Fields et al 1990).

Legionella pneumophila is the member of the genus *Legionella* most often associated with human disease (~85% of all *Legionella* infections) and conversely the best studied (Marston et al 1994). Interestingly, *L. pneumophila* is also believed to have the broadest host range (Fields 1996). This ability of *Legionella pneumophila* to replicate within freshwater protozoa was observed shortly after the initial outbreak in Philadelphia (Rowbotham 1980).

1.4.3 Intracellular replication of *Legionella pneumophila*

When nonpathogenic bacteria are taken up by protozoa in the environment, they are destroyed by low pH in lysosomes, a process that provides nutrients for the host. The ability of *L. pneumophila* to replicate within eukaryotic hosts is dependent on its ability to avoid fusion of the *Legionella* containing phagosome with secondary lysosomes (Horwitz 1983b). Instead *L. pneumophila* is found within an ever-changing replication niche in the host, which originates from the phagosome and is termed the *Legionella* containing vacuole (LCV). One hour after infection, smooth vesicles surround and begin to fuse with the LCV. Also at this time, mitochondria begin to associate with the LCV (Horwitz 1983a). At four hours after uptake, ribosomes, derived from the rough ER, begin to associate with the vacuole. Eight hours after uptake almost all (~95%) LCVs are studded with ribosomes and LCVs containing multiple bacteria are present, resulting from intracellular replication (Horwitz 1983a). Replication within a ribosome studded membrane is conserved in both protozoa and mammalian cells, pointing to a common lifecycle in the environment as well as during infection (Abu Kwaik 1996).

Further evidence that *Legionella* replicates within an ER derived vacuole came from the observation of the association of ER proteins with the LCV. Both Rab1, a small GTPase involved in the trafficking of vesicles from the ER to the Golgi, and Sec22b, a v-SNARE, found in ER derived vesicles, were observed associated with the LCV (Derre & Isberg 2004, Kagan et al 2004). Analysis of the LCV proteome by mass spectrometry has further revealed numerous other proteins involved in ER vesicle trafficking associated with the LCV (Bruckert & Abu Kwaik 2015, Urwyler et al 2009). Host ER proteins associated with the LCV are not limited to those involved in vesicle trafficking as luminal

ER proteins such as PDI, glucose-6-phosphate, and proteins containing the ER retention signal, KDEL are also observed (Robinson & Roy 2006). This indicates that the contents of ER derived vesicles mix with the luminal space of the LCV during its formation and may provide nutrients for the bacterium during intracellular replication.

The observation that the LCV resembled a vacuole derived from ER membrane and contained ER proteins, led to the search for vesicle trafficking pathways that were essential for *Legionella* replication. Treatment of cells with brefeldin A (BFA), which inhibits ER to Golgi trafficking by blocking the formation of COPII vesicles, limits the recruitment of ER markers to the LCV and strongly inhibits *L. pneumophila* replication, when added at the time of, or prior to, bacterial challenge (Kagan & Roy 2002). Overexpression of ADP-ribosylation factor 1 (Arf1), a small GTPase important for the formation of COPI vesicles, rescued the replication defect due to BFA treatment (Kagan & Roy 2002). Furthermore, expression of dominant negative mutants of Arf1 or Sar1 resulted in severe defects in *L. pneumophila* intracellular replication, indicating the importance of both COPI and COPII vesicle trafficking pathways (Kagan & Roy 2002). Rab1 activity was later shown to be required for high levels of intracellular replication but, interestingly, its recruitment was not affected by BFA treatment, which pointed to the possibility that multiple pathways of vesicle trafficking from the ER played roles in LCV biogenesis (Derre & Isberg 2004, Kagan et al 2004).

To address the prospect that multiple trafficking pathways were important for *L. pneumophila* replication, an RNA interference (RNAi) screen targeting factors involved in these processes was performed using *Drosophila* cells as a host. In this cell type, knockdown of *Sec22* had little effect on the ability of *Legionella* to replicate, while RNAi

targeted against *Arf1* resulted in an approximately 50% defect in intracellular replication (Dorer et al 2006). Intriguingly, RNAi treatment of cells targeting both *Arf1* and *Sec22* resulted in a much greater replication defect, relative to treatment with either alone (Dorer et al 2006). These results confirmed the hypothesis that multiple vesicle trafficking pathways played roles in LCV biogenesis. This also showed that the role of certain factors important for *L. pneumophila* replication could only be observed in the absence of other factors involved in similar functions, pointing to multiple, functionally redundant, processes involved in intracellular replication.

1.4.4 The Icm/Dot type IV secretion system

The ability of *Legionella* to replicate within a host cell, through the generation of a replication competent LCV, is dependent on its type IVb secretion system. This system, which is required for the translocation of effector proteins into the host, is encoded by ~27 genes termed *intracellular multiplication/defect in organelle trafficking* (*icm*/*dot*) (Berger & Isberg 1993, Marra et al 1992, Segal & Shuman 1997). Of these 27 genes, 19 show sequence homology to those required for conjugative transfer of the IncI conjugal plasmids Col1b-P9 and R64 (Segal & Shuman 1999, Vogel et al 1998). The other seven components do not show homology to this transfer system but are also responsible for the bacterium's ability to translocate ~300 effector proteins, known as Icm/Dot translocated substrates (IDTS), into the host.

The core complex of the Icm/Dot T4SS spans the bacterial membrane, forming a pore to allow the transfer of macromolecules. This complex is composed of DotC, DotD,

DotF, DotG, and DotH, with DotG forming the central channel that spans both the inner and outer membrane (Kubori et al 2014, Vincent et al 2006b). Of these, all but DotF are absolutely required for intracellular replication, with a strain lacking *dotF* showing a slight defect in replication and Icm/Dot dependent translocation (Kubori et al 2014). The integrity of this complex is important for the stability of the proteins that compose it as a deletion of *dotC* or *dotH* results in turnover of other Dot proteins (Vincent et al 2006b).

The Icm/Dot system also contains a second complex which contains the type IV coupling protein, DotL (Vincent et al 2012). The coupling protein provides energy for the system through the hydrolysis of ATP as well as binds to substrates that are to be translocated by the system. DotL interacts with DotM and DotN, which are also localized to the inner membrane (Vincent et al 2012). Interestingly, strains lacking the genes encoding for any of these proteins are either not viable or hypersensitive to NaCl (Buscher et al 2005). This is believed to occur due to toxicity from a partially assembled Icm/Dot T4SS, as deletions of other *icm/dot* genes can rescue the defect.

Two Icm/Dot soluble proteins, IcmS and IcmW, interact with translocated substrates, as well as DotL (Bardill et al 2005, Sutherland et al 2012). IcmS and IcmW form a stable complex, with IcmW rapidly degrading in the absence of IcmS (Ninio et al 2005). It has been observed that while some translocated substrates require IcmSW for translocation, others do not (Sutherland et al 2012). Multiple models for the function of IcmSW have been developed including: the recruitment of translocated substrates to the Icm/Dot system, regulating secretion through occlusion of IDTS secretion signals, or through the maintenance of translocated substrates in secretion competent form, prior to translocation (Cambronne & Roy 2007, Sutherland et al 2012).

1.4.5 IcmQ

Two Icm/Dot proteins that do not show homology to conjugal system components are IcmQ and IcmR, which are encoded by adjacent genes (Segal & Shuman 1997). IcmQ homologs are found in other intracellular pathogens such as *Coxiella*, *Rickettsia*, and *Bartonella* while there are no IcmR homologs, although potential partners of IcmQ, termed functional homologs of IcmR, are present in each genus (Feldman & Segal 2004, Feldman et al 2005). These proteins were predicted to act as a substrate-chaperone pair, similar to those seen in type III secretion systems (T3SS) and the type IV secretion system of *Agrobacterium tumefaciens* (Bennett & Hughes 2000, Deng et al 1999, Wattiau et al 1996), in which the chaperone (IcmR) binds to the substrate (IcmQ), preventing its aggregation.

As with many other Icm/Dot proteins, IcmQ/IcmR have been shown to play an important role during intracellular replication. Strains harboring in-frame deletions of *icmQ* or *icmR* were completely inhibited for intracellular replication in bone marrow-derived macrophages (BMDMs) (Coers et al 2000). In U937 cells, an *icmQ* mutant was unable to replicate, while a strain lacking *icmR* was able to replicate, but with a severe defect, relative to the wild type strain (Coers et al 2000). Furthermore, IcmQ was shown to be surface exposed on the bacterium only after contact with mammalian cells, consistent with the role of this protein during infection (Dumenil et al 2004).

Biochemical studies have begun to explore the role of IcmQ/IcmR during infection, and their interactions with each other. IcmQ/IcmR were determined to be soluble proteins that interact with a ratio of 2-3 IcmR molecules for each IcmQ protein

(Coers et al 2000, Dumenil & Isberg 2001). In the absence of IcmR, IcmQ forms high-molecular weight complexes, which can be dissociated by IcmR, consistent with IcmR playing the role of the chaperone in this pair (Dumenil & Isberg 2001). Furthermore, in the absence of IcmQ, *Legionella* lysates show a decrease in the levels of IcmR, pointing to IcmQ playing a role in the stability of IcmR (Dumenil & Isberg 2001). Insights into the role of IcmQ during infection come from lipid binding experiments in which IcmQ binds to lipids and forms pores that allow for the movement of small molecules across the membrane (Dumenil et al 2004). This is suggestive of IcmQ functioning in the formation of the pore through which substrates are translocated into the host.

The crystal structure of IcmQ, in complex with IcmR, has provided further insight into the role of these Icm/Dot proteins. The crystal structure revealed that the interaction between the two proteins occurred through a four-helix bundle with two helices being contributed by each protein (Farelli et al 2013, Raychaudhury et al 2009). This interaction occurred between the middle region of IcmR and the N-terminal region of IcmQ. Interestingly, the C-terminal region of IcmQ, which did not interact with IcmR, shows structural homology to the NAD^+ binding motifs of ADP ribosyltransferases (ADPRTs) of secreted bacterial toxins. In line with these findings, IcmQ was shown to specifically bind NAD^+, but not NADH, at concentrations in the physiological range (Farelli et al 2013).

To determine if the residues conserved in other ADPRTs were essential for the binding of NAD^+ by IcmQ, a mutational analysis was undertaken. A conserved residue, an aspartic acid at position 151, proved critical for binding to NAD^+ as a C-terminal construct of IcmQ encoded by the D151A mutation was unable to bind NAD^+.

Interestingly, the D151A mutation in full length IcmQ resulted in a protein with low expression levels, resulting from insolubility in both *E. coli* and *L. pneumophila*, indicating that NAD^+ binding may play a role in the proteins stability (Farelli et al 2013).

1.4.6 Translocated substrates of the Icm/Dot T4SS

Studies of translocated substrates of the Icm/Dot T4SS have revealed a vast amount of information about both the bacterium and the hosts that it infects. While ~300 IDTS have been identified, absence of a single substrate rarely results in a growth defect in tissue culture models of infection. This was most dramatically seen in a strain lacking 71 IDTS (31.4% of all identified translocated substrates) that was able to replicate in a BMDM tissue culture infection model (O'Connor et al 2011). Interestingly, strains lacking single, or families of, effectors have been shown to have defects in certain amoebal hosts in the absence of a defect in human or mouse macrophages (Bardill et al 2005, Fontana et al 2011, Liu & Luo 2007). Furthermore, challenge of cells knocked down for factors regulating host pathways has been shown to result in intracellular growth defects for single *idts* deletion strains, while showing no defect for the wild type strain (O'Connor et al 2012). These results show that many effectors may be required for intracellular replication in a single host, and having such a large cadre of effectors allows for the broad host range of *L. pneumophila*. They also show that IDTS may play functionally redundant roles in targeting multiple pathways to accomplish similar outcomes during infection.

Multiple bioinformatics analyses have been used to identify putative substrates of the Icm/Dot T4SS. Early studies to identify IDTS focused on the observation that many *L. pneumophila* genes encoded for putative proteins that contained motifs commonly found in eukaryotic proteins (de Felipe et al 2005, Nagai et al 2002). This pointed to the potential for their specific activity in eukaryotic hosts and also that they were likely acquired by horizontal gene transfer (de Felipe et al 2005). Many IDTS were found to be regulated by common transcriptional regulators, allowing for their identification by analysis of common regulatory sequences (Altman & Segal 2008, Zusman et al 2007). Another common feature of IDTS is that they are often found in close proximity within the genome, allowing for identification of multiple IDTS from the initial discovery of a single IDTS by other methods (Luo & Isberg 2004). Lastly, it was observed that multiple IDTS contained a common C-terminal motif that allowed for Icm/Dot dependent translocation. This led to large-scale identification of additional IDTS due to their homology to the translocation signal in their C termini (Burstein et al 2009, Huang et al 2011, Kubori et al 2008).

To verify the translocation of IDTS that were identified by bioinformatics analyses, multiple approaches have been undertaken. The earliest confirmation that a protein was translocated in an Icm/Dot dependent manner was through direct observation of protein localization in host cells by immunofluorescence microscopy utilizing an antibody specific to the protein (Nagai et al 2002). After the C-terminal translocation signal was identified, fusions of the C-termini of putative IDTS to a known IDTS, SidC, to which an antibody had been generated, were used to visualize if the SidC fusion proteins were localized to the host cell (Huang et al 2011, Luo & Isberg 2004). Fusion

constructs of putative IDTS to protein domains with enzymatic function that are only active in the target host cell have also been utilized, with enzymatic outputs measured by either ELISA or immunofluorescence microscopy (Huang et al 2011, Zhu et al 2011). IDTS have also been identified and characterized by differential fractionation of host cells to determine the localization of putative substrates after solubilization with detergents that target host cell membranes, but not the bacterial cells (Amyot et al 2013, Derre & Isberg 2005). Lastly, it was observed that the Icm/Dot T4SS allowed for the translocation of proteins into other bacterial cells. This allowed for the development of a Cre/*loxP* system that was used to identify IDTS through Cre-IDTS fusion proteins that resulted in antibiotic resistance of the recipient (Luo & Isberg 2004).

The first IDTS to be characterized, named RalF, was identified due to its Sec7 homology domain in the N-terminal region of the protein, which is commonly found in ADP ribosylation factor guanine nucleotide exchange factors (ARF-GEF) (Jackson & Casanova 2000, Nagai et al 2002). RalF was shown to be a functional ARF-GEF and was also required for the previously observed localization of ARF1 to the LCV (Nagai et al 2002). The C-terminal region of RalF contains a capping domain, which regulates the activity of the Sec7 homology domain. This region targets RalF to membrane of the LCV where its interaction with membranes relieves the auto-inhibitory activity of the capping domain (Folly-Klan et al 2013).

Some of the best described functions of IDTS have come through the study of the manipulation of the Rab family of small GTPases. This family of proteins is involved in trafficking of membrane vesicles through the secretory and endocytic pathways. The Rab1 subfamily specifically plays roles in the trafficking of vesicles from the ER to the

Golgi (Stenmark 2009). Rab1 is acted upon by at least 5 IDTS during the intracellular replication of *Legionella* (Figure 1.5). Recruitment of Rab1 to the LCV is mediated by SidM (also known as DrrA) early during infection (Machner & Isberg 2006, Murata et al 2006). SidM is a Rab1 GEF, which mediates the exchange of GDP for GTP, activating Rab1, while also displacing the Rab GTP dissociation inhibitor (GDI), which maintains Rab1 in an inactive state (Machner & Isberg 2006, Machner & Isberg 2007, Murata et al 2006). Furthermore, SidM induces the covalent attachment of an AMP moiety to Rab1, through a process known as AMPylation, preventing its inactivation by Rab1 GTPase activating proteins (GAPs) resulting in its maintenance on the LCV (Hardiman & Roy 2014, Muller et al 2010). Once on the LCV, Rab1 is bound by another IDTS, LidA. LidA acts by enhancing the interaction of Rab1 with SNARE proteins which interact with Sec22b that is found on vesicles, and thus promoting their recruitment to the LCV (Machner & Isberg 2006). Another modification that occurs to Rab1 on the LCV is the attachment of a phosphocholine moiety, a process termed PCylation (Mukherjee et al 2011). This is mediated by the effector AnkX, through its FIC domain, and may prevent Rab1 inactivation by GAPs. Interestingly, two IDTS SidD and Lem3 reverse the AMPylation and PCylation respectively (Neunuebel et al 2011, Tan et al 2011, Tan & Luo 2011). These effectors may serve to temporally regulate the activity of Rab1 during the later stages of infection. Lastly, the effector LemB serves as a Rab1GAP and as LemB is observed on the LCV only during late time points during infection, it likely acts to inactivate Rab1 during this time (Ingmundson et al 2007).

While study of IDTS that modify Rab1 have provided insight into the biochemical complexity of manipulation of the host cell by *Legionella*, the absence of any of these

Figure 1.5 Hijacking of ER membrane by *Legionella pneumophila*. *L. pneumophila* replicates within a vacuole derived from ER membrane. Multiple Icm/Dot translocated substrates (IDTS) (red circles) act on host factors (varying color circles) to mediate recruitment of ER derived membrane to the *Legionella* containing vacuole (LCV). The IDTS SidM recruits the host GTPase Rab1 to the LCV where it is acted upon further by SidM, as well as other IDTS (See text). LCV bound Rab1 mediates the recruitment of Sec22, a v-SNARE protein found on Golgi destined vesicles. COPI and COPII vesicles are also important for *L. pneumophila* intracellular replication as depletion of *ARF1* and *SAR1*, respectively, results in decreased bacterial growth.

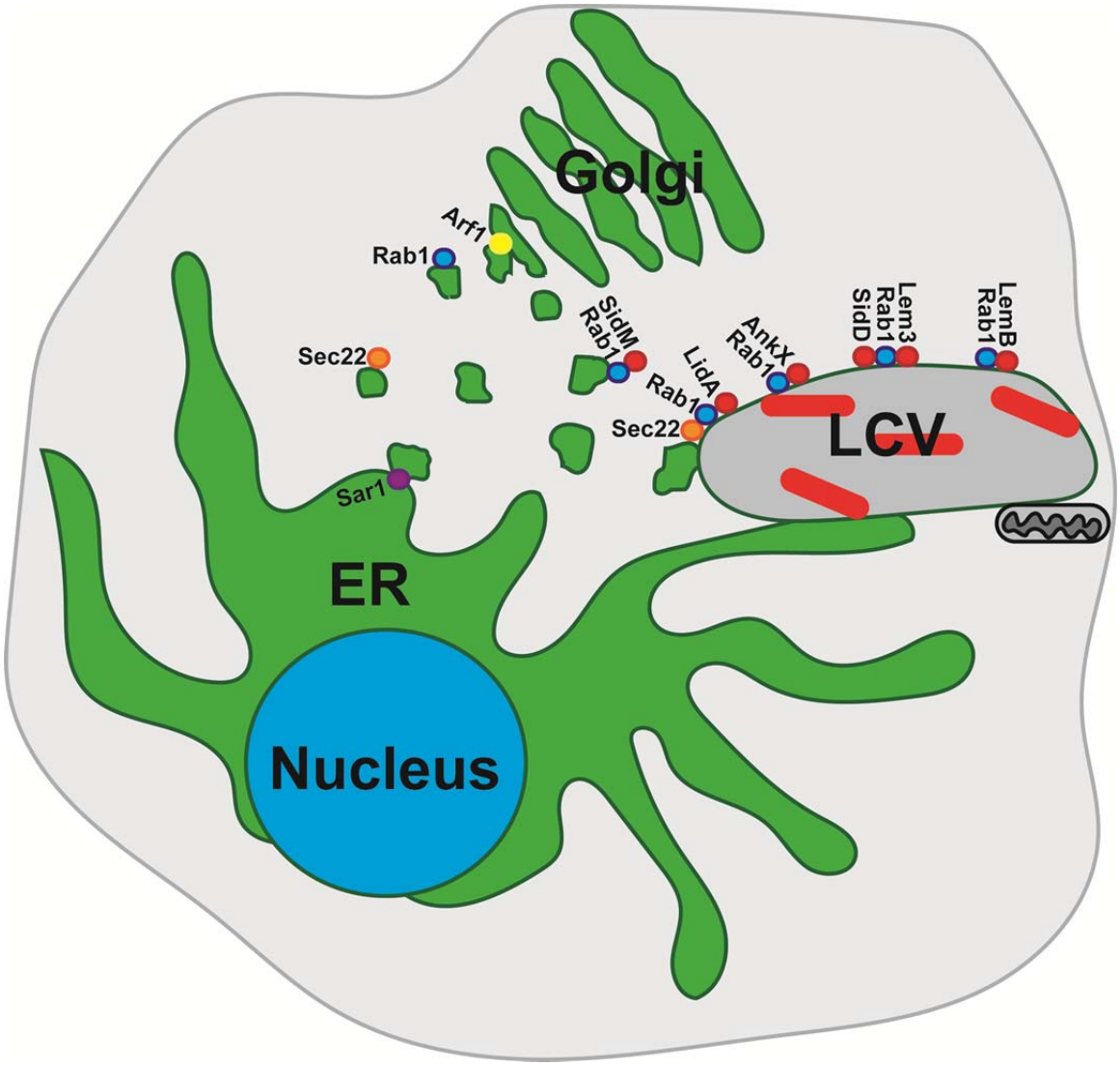
Golgi
Arf1
Rab1
Sec22
SidM
Rab1
LidA
Rab1
Sec22
AnkX
Rab1
Lem3
Rab1
SidD
LemB
Rab1
LCV
Sar1
ER
Nucleus

effector proteins does not result in a significant growth defect in tissue culture models of intracellular replication (Machner & Isberg 2006, Tan et al 2011). Interestingly, two IDTS were shown to be required for intracellular replication through a screen to identify non *icm*/*dot* genes important for growth in macrophages (Laguna et al 2006). These IDTS, SdhA and MavN, each perform unique functions for the bacterium, allowing for replication within a vacuolar niche.

Absence of *sdhA* results in a profound intracellular defect during replication in macrophages, while the defect is less severe in amoebal hosts (Laguna et al 2006). Strains harboring a deletion of *sdhA* are found within vacuoles that are permeable to the cytosol (Creasey & Isberg 2012). In macrophages, this results in recognition by cytosolic innate immune effectors, resulting in a caspase dependent host cell death (Aachoui et al 2013, Monroe et al 2009). *L. pneumophila* mutations that partially suppress the defect observed in *sdhA* mutants were identified in *plaA*, which encodes for a phospholipase, indicating that bacterial remodeling of the lipids of the LCV results in the exposure of the bacterium to the cytosol (Creasey & Isberg 2012).

L. pneumophila strains lacking MavN show a different intracellular growth defect than that seen of strains harboring an *sdhA* mutation. These mutants replicate within host cells for one or two divisions before their replication is arrested (Isaac, *et al*., submitted). This led to the hypothesis that the bacterium may be starved of an essential growth factor that was provided by MavN. Insight into this came when it was shown that *mavN* mutants upregulated genes involved in iron acquisition during intracellular replication. Furthermore, similar to other genes involved in iron acquisition, *mavN* is transcriptionally regulated by Fur, an iron sensitive negative regulator of gene expression. Lastly, while

MavN does not seem to play a role of iron acquisition during growth in broth culture, intracellular replication of the *mavN* mutant can be rescued by the addition of exogenous iron to the tissue culture medium during host cell challenge, pointing to it role in providing iron to intravacuolar *L. pneumophila* (Isaac, *et al*., submitted).

1.4.7 Host cell protein synthesis during challenge by *Legionella pneumophila*

Early studies on the challenge of Chinese hamster ovary cells by *Legionella* revealed that there is limited host cell translation (McCusker et al 1991). More recently, this has been shown to be mediated by both Icm/Dot translocated effectors and a host cellular response to the bacterium, resulting in limiting translation by two different mechanisms (Asrat et al 2014b, Fontana et al 2011, Ivanov & Roy 2013). While global translation is inhibited, there are some factors that are able to bypass this inhibition, although the mechanism behind this bypass is unclear (Asrat et al 2014b, Ivanov & Roy 2013).

The ability of the *Legionella* to inhibit host cell translation through IDTS was first observed when it was determined that the bacterium encoded glucosyltransferases that targeted the host elongation factor eEF1A (Belyi et al 2003, Belyi et al 2006). Three *Legionella* glucosyltransferases (Lgt1-3) have been identified that have domains showing sequence similarity to the enzymatic domain of the *Clostridial* glucosyltransferase toxins A and B (Sadretdinova et al 2012). Most strains other than *Legionella pneumophila* Philadelphia 1 encode only Lgt1 and Lgt3. Although the three predicted *Legionella* glucosyltransferases show significant similarity in this region, including conserved amino

acids that are important for activity, Lgt1-3 show only 15-30% sequence identity to each other. Initial studies identified eEF1A as the target of Lgt1 when it was incubated with eukaryotic lysates (Belyi et al 2006). Later studies confirmed that Lgt2 and Lgt3 also targeted this elongation factor. Each of these proteins glucosylate serine-53 of eEF1A, located within the 1G domain of eEF1A (Belyi et al 2006). This region is responsible for the binding and hydrolysis of GTP that occurs during the delivery of aminoacyl-tRNA to the ribosome in the process of translation elongation. Interestingly, the prokaryotic eEF1A homolog, EF-Tu, lacks the serine in this position and cannot be targeted by the Lgts, allowing for host elongation factor specificity (Belyi et al 2013). While eEF1A has been shown to be the primary target of the Lgts, another substrate, Hbs1 (Belyi et al 2009), which with Dom34 is involved in rescue of stalled elongation complexes, resulting in no-go mRNA decay (Doma & Parker 2006), has also been identified.

Another IDTS, SidI, also targets eEF1A (Shen et al 2009), as well as the translation elongation factor eEF1Bγ, although there is no homology between eEF1Bγ and eEF1A. Although the mechanism of SidI interference with the activity of these elongation factors is unknown, SidI is able to inhibit *in vitro* translation in a fashion similar to the Lgts. Unlike the Lgts, interaction with eEF1A also induces a heat shock response through the activation of the heat shock transcriptional regulator, HSF1, which has been shown to be regulated by eEF1A, pointing to the specificity of SidI action (Shen et al 2009).

To understand the role of the translation elongation inhibitors during host cell challenge, a strain harboring deletion of each of the Lgts and SidI was constructed. To this strain, a deletion in the gene encoding SidL, which when ectopically expressed in

eukaryotic cells inhibits translation, was also added. Cells challenged with this strain, named Δ5, resulted in translation levels that were ~3-fold higher than seen during WT challenge at 2.5 hours post infection (hpi) (Fontana et al 2011). While this strain did not exhibit an intracellular replication defect in BMDMs, in the amoebal host *D. discoideum*, Δ5 displayed a ~10-fold growth defect (Fontana et al 2011). In macrophages challenged with Δ5, there was a significant decrease in the transcriptional induction of genes that are induced in response to the Icm/Dot T4SS, termed the effector triggered response (ETR), compared to WT. Among the transcripts that showed lowered expression were genes encoding cytokines, which could be partly explained by the limited activation of NF-κB relative to the WT strain. This was due to the continued translation of IκB in the presence of the Δ5 strain, resulting in a tempered response, due to its blocking of NF-κB activation (Fontana et al 2011). In contrast, the WT strain blocks IκB translation, which in turn is degraded, resulting in NF-κB activation. The inhibition of protein synthesis by these effectors also induces the activation of MAPK signaling, which plays a role in ETR (Fontana et al 2012). While there are dramatic differences in the levels of translation in cells challenged with WT or Δ5 at early time points during infection, as the infection progresses, cells challenged with the Δ5 strain begin to show low levels of translation that approach those observed in WT infected cells (Asrat et al 2014b). This is consistent with a second level of dampening host cell translation that is independent of the characterized *L. pneumophila* translation inhibitors.

In response to pathogenic *Legionella*, the host cell induces a response that acts to inhibit translation initiation (Ivanov & Roy 2013). This was observed when it was determined that factors in the mTOR pathway, including mTOR and its positive

regulators PI3K and Akt were ubiquitinated during host cell challenge. mTOR regulates Cap-dependent translation through the phosphorylation of 4E-BP1, which in its hyperphosphorylated state is unable to bind and inhibit the translation initiation factor eIF4E that is responsible for the recruitment of the 40S ribosomal subunit (Figure 1.1). Ubiquitination of mTOR and its positive regulators resulted in decreased levels of phosphorylation of Akt, mTOR, and the mTOR substrate 4E-BP1, relative to DotA$^-$ challenged, or LPS treated cells. The decreased phosphorylation of 4E-BP1 resulted in inhibition of Cap-dependent translation initiation in WT *L. pneumophila* challenged cells, which could be overcome through siRNA targeting 4E-BP1 (Ivanov & Roy 2013). These results point to a host mediated inhibition of translation initiation, through the ubiquitination of mTOR pathway factors in response to challenge with pathogenic *L. pneumophila,* as a host cell strategy that is totally independent of any known *L. pneumophila* IDTS.

Intriguingly, there are host proteins that are translated in spite of these powerful strategies to interfere with protein synthesis. Though the exact mechanism of overcoming the translation block is still unknown, patterns of proteins that are translated are becoming apparent. While transcripts that are strongly upregulated during infection are not always translated in the presence of protein synthesis inhibition (Shen et al 2009), there is a strong correlation between transcript abundance and protein translation. As transcripts encoding proinflammatory cytokines are upreglated to high abundance during challenge, these represent many of the translated proteins, indicating that this may be a mechanism that the host uses to induce a strong immune response while limiting other factors that may be beneficial to the pathogen (Ivanov & Roy 2013). In line with this

reasoning, MyD88$^{-/-}$ BMDMs, which show a decreased transcriptional response to *L. pneumophila*, also show little to no pro-IL-1β translation or secretion (Asrat et al 2014b). Confounding this, however, is that there is still strong ETR induction of *il1β* in MyD88$^{-/-}$ BMDMs that results in higher levels of transcripts than that seen for WT BMDMs to the DotA^{-} strain (Asrat et al 2014b). It is possible that, in addition to regulating cytokine transcript levels, TLR-mediated signaling may play additional roles in regulating translation by yet unknown mechanisms.

1.5 UNANSWERED QUESTIONS ADDRESSED BY THIS WORK

While much has been learned about the biology of how *L. pneumophila* manipulates the ER, there are still many unanswered questions in this field. As many pathogens utilize similar mechanisms to accomplish their goals, addressing these questions through study of *L. pneumophila* is broadly applicable to other systems. This study has addressed some of these questions to further our understanding of how *Legionella* interacts with the host cell ER.

Since the first IDTS was identified, the mechanism by which they manipulate the ER has been a constant question that has yielded important insights into host cell biology and bacterial pathogenesis (Nagai et al 2002). It is yet unknown if any single one of these effectors, that together function in the formation of the LCV, are essential for intracellular replication. Furthermore, while many of these effectors have been characterized for their manipulation of vesicle trafficking, a current question is how *L. pneumophila* interacts with ER tubules, and if any effector proteins play a role in this

function. Also, while mitochondria are observed to associate with the LCV during infection, what role this plays, if any, as well as what effectors are implicated in this, is largely unknown (Horwitz 1983a, Sun et al 2013). In this study we take steps to address these questions through study of the IDTS MavT.

While host cell UPR is activated by numerous pathogens and plays an important role in the induction of proinflammatory cytokines (Martinon et al 2010), it was unknown at the time these studies were initiated if *L. pneumophila* induces this response. It was also not known if host cell induction of the UPR is limiting for *L. pneumophila* intracellular replication. Furthermore, as *Legionella* manipulates many facets of the ER, if it also modulates specific pathways of the UPR was an unanswered question. More broadly, while some intracellular pathogens have been observed to inhibit the UPR, the mechanism by which they accomplish this was unknown (Mehlitz et al 2014). This thesis has provided answers for many of the question raised by the obvious presence of a UPR in response to pathogens.

Although IcmQ, a component of the Icm/Dot T4SS, has been shown to be required for *L. pneumophila* virulence, its function during host cell challenge is still relatively unknown (Dumenil et al 2004). Many of the signaling pathways leading to Icm/Dot complex formation are also unknown and it has been hypothesized that signal recognition by IcmQ may function in this role (Farelli et al 2013). In this study, I addressed if the recently characterized NAD^+ binding by this virulence factor was essential for intracellular replication. I further addressed the question of what levels of IcmQ are required for a productive infection.

1.6 THESIS SUMMARY

The goal of this thesis work was to further understand the interaction of *L. pneumophila* with the host cell endoplasmic reticulum. This was accomplished through studies analyzing the importance of the Icm/Dot T4SS and its substrates in manipulating the ER and signaling pathways emanating from it. In Chapter 2, MavT, an IDTS is identified and characterized for its ability to manipulate the ER as well as domain analysis of regions of the protein that may be responsible for accomplishing this. Chapter 3 describes studies on the manipulation of the host cell UPR by *Legionella* and the IDTS important in inhibition of this host response to pathogens. Finally, Chapter 4 describes work done as part of a collaborative project in which the role of NAD^+ binding by IcmQ, an Icm/Dot component, was assessed. This analysis also necessitated the development of tools that should serve in future studies on the requirements of different bacterial factors for intracellular replication. Together, these studies have helped to further our knowledge about the pathogenesis of *L. pneumophila* as well as to increase our understanding about the mechanisms by which the ER and its signaling pathways can be manipulated.

Chapter 2: Characterization of MavT, a J domain Icm/Dot translocated substrate

2.1 MATERIALS AND METHODS

2.1.1 Bacterial strains, culture, and genetic manipulation

Bacterial strains used in this study are described in (Table 2.1). *E. coli* were grown in Lysogeny Broth (LB) or on solid LB plates with antibiotic additions at the following concentrations: carbenicillin (Carb) (100 μg/ml), kanamycin (Kan) (50 μg/ml), or chloramphenicol (Cm) (25 μg/ml). *L. pneumophila* were grown in *N*-(2-acetamido)-2-aminoethanesulfonic acid (ACES) buffered yeast extract (AYE) broth or charcoal buffered yeast extract (CYE) solid medium with the following additives as appropriate: Kan (40 μg/ml), Cm (5 μg/ml), thymidine (Thy) (0.1 mg/ml), sucrose (5% wt/vol). *L. pneumophila* strains were struck out on CYE and incubated at 37^{o}C for 3-5 days to allow for colony formation. Colonies were patched onto new CYE plates and put at 37^{o}C for 1-2 days then; two-fold serial dilutions made in AYE were incubated overnight with rotation so that cultures in the desired physiological states were available the following day.

Molecular cloning was performed utilizing the *E. coli* strains and plasmids described in (Tables 2.1, 2.2). Oligonucleotides used for amplification of desired products are described in (Table 2.3) and include the underlined restriction sites used for molecular cloning.

For generation of in-frame deletions in *L. pneumophila*, a double-recombination strategy using the suicide vector pSR47S was employed. ~1000 bp fragments flanking the coding sequence were amplified from *L. pneumophila* genomic DNA by PCR and cloned into pSR47S using SacI, BamHI, and SalI restriction sites. This construct was transformed into *L. pneumophila* by electroporation and grown in AYE at 37^{o}C for four hours then plated on CYE + Kan, to select for the integration of pSR47S. After 4 days at 37^{o}C, colonies were restruck on CYE + Kan and grown for an additional 4 days then colonies were struck out on CYE + sucrose to counter select against the suicide plasmid. Deletion of the gene of interest in *L. pneumophila* was verified by PCR using adjacent primers or, in some cases, whole genome sequencing using HTML-PCR (Lazinski & Camilli 2013).

For incorporation of the *luxCDABE* operon into *L. pneumophila* strains, a single-recombination strategy was utilized. The vector pSR47-*aphC::lux* (a gift from Jörn Coers and Russel Vance) (Coers et al 2007) which, downstream of the *L. pneumophila aphC* promoter, encodes the *luxCDABE* operon from *Photorhabdus luminescens*. The *luxCDABE* operon was incorporated using tri-parental matings with the *E. coli* Tra^{+} helper strain RK600 and recombinants were selected for on medium containing Kan (Swanson & Isberg 1996).

Analysis of in vitro replication of *L. pneumophila* was performed in AYE broth. Overnight cultures were back diluted to an OD_{600} of 0.1 in 200 µl of fresh broth and six technical replicates for each strain were added to wells of a 96-well plate. Plates were incubated with shaking at 37^{o}C and OD_{600} readings were taken every 30 minutes for 24 hours using the Tecan Infinite 200 Pro.

Table 2.1: Bacterial strains

Strain	Genotype	Description	Reference
	Legionella pneumophila		
Lp02 (WT)	Philadelphia 1, *thyA rpsL hsdR*	wild type strain	(Berger & Isberg 1993)
Lp03 (DotA$^-$)	Lp02, *dotA03*	Icm/Dot translocation deficient	(Berger & Isberg 1993)
Lp02 Thy$^+$	Lp02, *thyA*$^+$	Thy+ wild type strain	(O'Connor et al 2011)
Δ*mavT*	Lp02, Δ*lpg0921*	Δ*mavT*	This study
Δ*mavT* Thy$^+$	Lp02, *thyA*$^+$, Δ*lpg0921*	Δ*mavT, Thy*+	This study
Lp02::lux	Lp02, *luxCDABE*	Luciferase expressing wild type strain	This study
Lp02Δ*mavT* ::lux	Lp02, *mavT, luxCDABE*	Luciferase expressing Δ*mavT* strain	This study
	Escherichia coli		
DH5α	*supE44 DlacU169* (F80lacZDM15) *hsdR17 recA1 endA1 gyrA96 thi-1 relA1*	Molecular cloning strain	
DH5α λpir	*endA1 glnV44 thi-1 recA1 relA1 gyrA96 deoR nupG* (*Φ80dlac ΔlacZ*) M15 (*ΔlacZYA-argF*)U169, *hsdR17*(*rK - mK +*), (*λpir*)	Molecular cloning strain	(Kolter et al 1978)
Rosetta^{TM}(DE3)pLysS	F- *ompT hsdS*B(rB- mB-) *gal dcm* (DE3) pRARE (CamR)	Protein expression strain	Millipore
WKG190	(MC4100 *araD139 ara714 cbpA*::*kan dnaJ*::Tn10-42)	Temperature sensitive *E. coli* for domain swap experiments	(Kelley & Georgopoulos 1997)
RK600	*recA56 pro-82 thi-1 hsdR17 supE44* pRK600	Tra+ helper strain	(Swanson & Isberg 1996)

Table 2.2: Plasmids

Plasmid	Genotype	Description	Reference
pJB2581 (pCyaA)	*cyaA*, cm^R	cyclase reporter vector	(Bardill et al 2005)
pCyaA-MavT	cyaA, mavT, CmR	CyaA-MavT expression vector	This study
pDTI101-MavT	pJB908 3xflag, mavT	3xFLAG-MavT expression vector	This study
pQE80L	6xHis, ColE1 ori, lacIq, ampR	N-terminal His_6-tagged protein expression vector	Qiagen
pQE80L-MavT J domain	pQE80L, *mavT (nt 1-375)*	His_6-MavT J domain expression vector	This study
pRJ-B	pQE30, *agtdnaJ*, *Bst*BI, amp^R	Agt DnaJ expression vector	(Nicoll et al 2007)
pRJ-B-MavT	pRJB, *mavT*	Agt DnaJ-MavT chimera expression vector	This study
pRJ-B-MavT H33Q	pRJB, *mavT* H70Q	Agt DnaJ-MavT H70Q chimera epression vector	This study
p3xFLAG-CMV-7.1	pBR322 ori, pCMV, *3xflag*, ampR	eukaryotic N-terminal 3xFLAG expression vector	Sigma
p3xFLAG-MavT	p3xFLAG-CMV-7.1, *mavT*	eukaryotic N-terminal 3xFLAG-MavT expression vector	This study
p3xFLAG-MavT J domain	p3xFLAG-CMV-7.1, *mavT (nt 1-375)*	eukaryotic N-terminal 3xFLAG-MavT J domain expression vector	This study
p3xFLAG-MavT C-terminus	p3xFLAG-CMV-7.1, *mavT (nt 822-1242)*	eukaryotic N-terminal 3xFLAG-MavT C-terminus expression vector	This study
p3xFLAG-MavT ΔJ domain	p3xFLAG-CMV-7.1, *mavT (nt 375-1242)*	eukaryotic N-terminal 3xFLAG-MavT ΔJ domain expression vector	This study

p3xFLAG-MavT ΔHydro	p3xFLAG-CMV-7.1, *mavT (nt 576-1242)*	eukaryotic N-terminal 3xFLAG-MavT Δhydrophobic expression vector	This study
pEGFP-C1	pUC ori, egfp, pCMV, kan^R	eukarotic N-terminal EGFP expression vector	Clontech
pEGFP-C1-MavT	pEGFP-C1, *mavT*	eukarotic N-terminal EGFP-MavT expression vector	This study
pEGFP-C1-MavT ΔHydro	pEGFP-C1, *mavT (nt 1-480, 822-1242)*	eukarotic N-terminal EGFP-MavT ΔHydro expression vector	This study
pEGFP-C1-MavT ΔJ domain	pEGFP-C1, *mavT (nt 1-375)*	eukarotic N-terminal EGFP-MavT ΔJ domain expression vector	This study
mCh-Sec61β	pAcGFP1-C1 Δ*gfp*, *mcherry*, *sec61*β, kan^R	eukaryotic mCh-Sec61β expression vector	(Zurek et al 2011)
pGW1-ATL1	pBR322 ori, pCMV, *ha-atl1*, amp^R	eukaryotic HA-ATL1 epxression vector	(Zhu et al 2003)
Myc-ATL K80A	pBR322 ori, pCMV, *myc-atl1* K80A, amp^R	eukaryotic Myc-ATL1 K80A expression vector	(Rismanchi et al 2008)
mito-BFP	pAcGFP1-N1 Δ*gfp*, *tagbfp*, *cox4 (nt 1-63)*, kan^R	eukaryotic BFP with mitochondrial targeting sequence	(Friedman et al 2011)
pJB3395	$thyA^+$, amp^R	*thyA* allelic exchange vector	(Merriam et al 1997)
pSR47-*ahpC::lux*	pSR47S, P*aphC*, *luxCDABE*	luciferase operon integration under the *ahpC* promoter	(Coers et al 2007)

Table 2.3: Oligonucleotides

	Name	Description	Sequence
1	AH5	*mavT* full length forward	AAACGCGGATCCATGACTATAGAAAGGGAATTAAAA
2	AH6	*mavT* full length reverse	AAACGCGTCGACTTAAGTTCCATTATAAACCACCAA
3	0921sac2	*mavT* deletion upstream forward	TGAGAGCTCCGAATTCTACTCGCTAATAACAAGG
4	0921bam12	*mavT* deletion upstream reverse	TATGGATCCAATTACTCCCTTAATAAACTTGACT
5	AH0921bam2	*mavT* deletion downstream forward	GGAGGATCCTAGCTGTTGCAAGTATCTCA
6	AH0921sal	*mavT* deletion downstream reverse	ATAGTCGACGGCTTTCGTTTGGCCTTCAT
7	AH6bamhi	*mavT* full length reverse	AAACGCGGATCCTTAAGTTCCATTATAAACCACCAA
8	0921jdomrev	*mavT* J domain forward	TAAATTCGAACTTGCTTTTGATATCTCC
9	0921jdomfwd	*mavT* J domain reverse	GGACGGATCCAATAATTGTTATAAATCCC
10	F0921JHQ	*mavT* H->Q quickchange forward	GATTAACTCTCTGCTTTCAGCCTGATCATGCTTCAGG
11	R0921JHQ	*mavT* H->Q quickchange reverse	CCTGAAGCATGATCAGGCTGAAAGCAGAGAGTTAATC
12	0921qRTR	*mavT* qPCR forward	AAATCGCAGAACCGATTTGT
13	0921qRTF	*mavT* qPCR reverse	CGCCTGCTTGAAATGACTTT

14	0921NoJF	*mavT* no J domain forward	CCTCGGATCCGATGATTTTAAACAATGGC
15	0921Ctermno hydroF	*mavT* no hydro forward	CCTCGGATCCGCAGAAGAATTGTTTGCTATC
16	SOE2large0921	*mavT* SOE no hydro	AGACTCTGATTTTTCCTTAGTCTCAAGAGAACCACTGGATTGTTCTAATAAATTAATTAA
17	SOE3large0921	*mavT* SOE no hydro	TTAATTAATTTATTAGAACAATCCAGTGGTTCTCCTGAGACTAAGGAAAAATCAGAGTCT
18	MavTCtermF	*mavT* C-term forward	AAACGCGGATCCTCTCCTGAGACTAAGGAAAAATCAGAG
19	JdomainRbam	*mavT* J domain reverse	TAAAGGATCCCTTGCTTTTGATATCTCC
20	JdomainRsal	*mavT* J domain reverse	TAAAGTCGACCTTGCTTTTGATATCTCC
21	16SF	16S rRNA qPCR forward	CTAAGGAGACTGCCGGTGAC
22	16SR	16S rRNA qPCR reverse	CGTAAGGGCCATGATGACTT

2.1.2 Eukaryotic cell culture and bacterial challenge

BMDMs were isolated from femurs of female mice and differentiated in medium containing 30% L-cell supernantent for 7 days (Asrat et al 2014b, Swanson & Isberg 1995), then frozen in aliquots at $5x10^6$ cells in 1 ml FBS that were thawed prior to use. BMDMs were plated in RPMI supplemented with 10% FBS and 1 mM L-glutamine at $1x10^5$ in 96-well plates 1 day prior to challenge. Cells were challenged at an MOI=0.05, centrifuged at 1,000 RPM then incubated at 37^{o}C for 2 hours. Wells were washed 3X with warm medium and infections were allowed to continue for 72 total hours with cell lysates plated on CYET at various time points for CFU analysis.

Dictyostelium discoideum spores, frozen in PBS at -80^{o}C, were plated on a lawn of *Klebsiella aerogenes* AM2515 plated on SM/5 agar medium and incubated at 21.5^{o}C. Fruiting bodies that arose from the bacterial lawn were used to culture *D. discoideum* axenically in HL-5 liquid medium (Sussman 1987) supplemented with penicillin and streptomycin (100 U/ml). Prior to challenge with *L. pneumophila*, cells were washed with PBS then resuspended in MB medium (Solomon et al 2000) and plated at $5x10^5$ cells/well and allowed to adhere for at least 2 hours at 37^{o}C prior to challenge.

Acanthamoeba castellanii was grown in peptone-yeast extract-glucose (PYG) medium at 25.5^{o}C. Prior to challenge by *L. pneumophila*, cells were resuspended in *A. castellanii* buffer (Moffat & Tompkins 1992) and plated at $5x10^5$ cells/well and allowed to adhere overnight. *A. castellanii* and *D. discoideum* were challenged with post-exponential *L. pneumophila* at an MOI=0.01and 0.05 respectively and after cell lysis with

saponin, intracellular replication was analyzed by plating on CYE and determining CFU counts.

U937 cells were cultured in RPMI supplemented with 1 mM glutamine and 10% FBS. Cells were differentiated by treatment with 10 ng/ml 12-tetradecanoyl phorbol 13-acetate (TPA) for 24-48 hours. Differentiated U937 cells were plated overnight in the absence of TPA prior to challenge. Cos7 and HEK293T cells were passaged in DMEM.

2.1.3 Protein expression and purification

For protein expression, coding regions of interest were cloned into the expression vector pQE80L (Qiagen), which incorporates an N-terminal 6xHis tag downstream of an isopropyl-β-D-thiogalactopyranoside (IPTG) inducible T5 promoter. Expression vectors were transformed into the Rosetta^{TM} (DE3) pLysS (Millipore), a BL21 derivative (Table 2.1). Overnight cultures were back diluted and then grown at 37^{o}C until an OD_{600} of 0.5 was reached. At this point, IPTG (1 mM) was added and cultures were put back at 37^{o}C for 2 additional hours to allow for protein expression. Cultures were then pelleted, resuspended in 20 ml lysis buffer (50 mM Tris pH 8.0, 200 mM NaCl, 10 mM imidazole) and lysed by French press and 200 µg/ml lysozyme. Lysates were pelleted at 25,000 x g for 40 minutes and the supernatant was incubated with 500 µl Ni-NTA agarose (Qiagen) overnight, washed 4 times with wash buffers of increasing imidazole concentration (50 mM Tris pH 8.0, 200 mM NaCl, imidazole 10 mM (2X), 50 mM (1X), 75 mM (1X)) then bound proteins were eluted with elution buffer (50 mM Tris pH 8.0, 200 mM NaCl, 250 mM imidazole). Buffer from elution fractions was exchanged into (50 mM Tris pH 8.0,

100 mM NaCl) by dialysis then proteins were further purified using a Mono Q 5/50 GL column (GE Healthcare Life Sciences) using a 20 column volume gradient from 100 mM NaCl to1 M NaCl, collecting 200 µl fractions.

2.1.4 Translocation of putative IDTS

The plasmid pJB2581 (pCyaA) (A generous gift from Joseph Vogel PhD, Washington University in St. Louis) allows for the cloning of the ORF encoding a putative IDTS fused to the 3′ end of the *cya* gene. The entire coding region of *mavT* was amplified to encode flanking *bamHI* and *salI* sites then cloned into pJB2581. This construct was then transformed into the WT *L. pneumophila* strain (Lp02) and the Icm/Dot deficient DotA- strain (Lp03). Overnight cultures were back diluted to an OD_{600}~2 and IPTG (100 µM) was added and cultures were allowed to grow until post-exponential phase was reached. Prior to host cell challenge, one OD_{600} of each culture was pelleted and lysed in 2X sample buffer. Expression of CyaA-IDTS fusions was analyzed by Western blot using rabbit anti CyaA (Santa Cruz) or rabbit serum specific to the *L. pneumophila* DotF protein, as a loading control.

Differentiated U937 cells were plated at ~$2.5x10^6$ cells/well in 24-well plates and challenged with post-exponential *L. pneumophila*, expressing the CyaA fusion constructs, at an MOI=1. Plates were spun down at 1000 RPM for 5 minutes then incubated at 37^oC for 1 hour. Wells were then washed 3X with Hank's balanced salt solution (HBSS) then lysed on ice for 10 minutes through the addition of 200 µl of lysis buffer (50 mM HCl, 0.1% Triton X-100). Lysates were boiled for 5 minutes, followed by neutralization with

12 µl of 0.5 M NaOH. This was then precipitated for 5 minutes on ice, by the addition of 400 µl of cold 95% EtOH then pelleted at 13,000 RPM 5 minutes at 4^{o}C. Collected supernatents were dried using a vacuum concentrator then resuspended in assay buffer. To analyze cyclase activity of the putative IDTS, cAMP concentration was determined in each sample using the Amersham Biotrak cAMP ELISA kit. cAMP levels were normalized to the level of CyaA-IDTS fusion expressed by post-exponential cultures and data were expressed as fmoles/well[fusion protein].

The plasmid DTI101 is a derivative of pJB908 that allows for the expression of an N-terminally FLAG-tagged protein by *L. pneumophila*. The entire *mavT* ORF was cloned into this plasmid and transformed into WT and DotA^{-} *Legionella*. Cultures were grown up overnight then induced for 4 hours with 1 mM IPTG. TPA treated U937 cells were plated in 6 well plates at 1.5x10^{7} cells/well. Cells were challenged with each 3xFLAG-MavT expressing strain at an MOI of 5, spun down at 1,000 RPM for 5 minutes then incubated at 37^{o}C for 1.5 hours. Cells were washed 3X with HBSS then lifted with trypsin and washed 1X with PBS. Cells were then pelleted for 5 minutes at 1,000 RPM and resuspended in 0.5% digitonin in PBS with protease inhibitor cocktail (Roche). This was incubated for 20 minutes at room temperature with rotation then pelleted at 10,000 RPM at 4^{o}C for 15 minutes. The supernatant was collected and the pellet was resuspended in 200 µl of 2% SDS. To each, 5X sample buffer was added and then boiled for 10 minutes. Fractions were separated by SDS-PAGE and immunoblot was performed using mouse monoclonal FLAG M2 (Sigma), rabbit serum raised against DotF, and rabbit polyclonal GAPDH (Santa Cruz).

2.1.5 Analysis of J domain activity

The *E. coli* MC4100 derivative WKG190 (OD259) (A kind gift from William Kelley, University Hospital and Medical School Geneva, Switzerland) (Table 2.1) contains disruptions of the genes encoding for two J domain proteins *dnaJ* and *cbpA*, resulting in a strain which is temperature sensitive for growth at 40^{o}C (Kelley & Georgopoulos 1997). The expression vector pRJ-B (Table 2.2) (A kind gift from Greg Blatch, Victoria University Melbourne, Australia) allows for IPTG regulated induction of N-terminally 6xHis tagged *Agrobacterium tumefaciens* DnaJ protein (Agt DnaJ), which rescues the growth of WKG190 at 40^{o}C. pRJ-B also contains BamHI and BstBI restriction sites which bound the AgtDnaJ J domain encoding sequence. The putative *mavT* J domain was amplified with oligonucleotides introducing BamHI and BstBI sites at each end and cloned into pRJ-B, replacing the *agt dnaJ* J domain. QuikChange site-directed mutagenesis (Agilent Technologies) was used to generate an H→Q mutation within the J domain invariant HPD motif, which is necessary for its function. Each of these constructs (pRJB, pRJB-MavT, pRJB-MavT H33Q, and pRJB containing a non-functional J domain (GL Blatch, unpublished) was transformed into WKG190 by electroporation. Strains were grown up overnight at 30^{o}C then back diluted 1:50 and grown at 30^{o}C until an OD_{600} ~2.0 was reached. 3 µl of 10-fold dilutions, ranging from 10^{0}-10^{6} were plated on LB plates containing IPTG and incubated overnight at 30^{o}C or 40^{o}C. To the remaining culture, IPTG (1 mM) was added and cultures were grown for 2 additional hours at 30^{o}C. One OD_{600} was taken from each culture, pelleted, and resuspended in 50 µl of 2X sample buffer. Expression of each construct was analyzed by immunoblot using rabbit polyclonal anti His (Sigma).

2.1.6 Identification of IDTS binding partners

For each construct to be analyzed (Figure 2.4B , Table 2.2), two 10 cm dishes of HEK293T cells were plated at $2.5x10^6$ and allowed to adhere overnight. Transfections were performed using lipofectamine 2000 (Invitrogen) and 24 μg DNA/ plate. Cells were incubated at 37°C for 24 hours to allow for expression of each construct. Plates were then washed 1X with PBS then lysed in 1 ml of cold lysis buffer (TBS pH 7.4, 1mM EDTA, 1% Trition X-100, protease inhibitor cocktail (Roche) for 10 minutes at 4°C. Lysates were collected by pipetting up and down and the lysates from two plates per construct were combined. Lysates were pelleted at 4°C for 10 minutes at 12,000 x g and the soluble fraction was taken. To this was added 20 μl of washed ANTI-FLAG M2 affinity gel (Sigma) and allowed to incubate with rotation overnight. Lysates were centrifuged at 4,000 RPM for 5 minutes and the supernatant was removed. Resin was washed 3X with lysis buffer and 3X with TBS for 30 minutes each. After the last wash, the resin was resuspended in 40 μl of 2X sample buffer. For identification of binding partners, lysates (0.5% total lysate, 0.5% unbound, and 30% of the lysate) were separated by SDS-PAGE and visualized by Commassie Blue staining. Putative binding partners were excised from the gel and analyzed by mass spectrometry at the Steen Laboratory at Boston Children's Hospital. For immunoblot analysis, 0.5% of the lysate and unbound and 25% of the bound fractions were separated by SDS-PAGE. After transfer to PVDF, proteins were detected with the following antibodies: mouse monoclonal FLAG M2 (Sigma), rabbit polyclonal Rho GDI α (Santa Cruz Biotechnology), mouse monoclonal Hsp70/Hsp72 (Enzo Life Sciences).

2.1.7 Immunofluorescence microscopy

For visualization of the expression and localization of MavT and its derivatives, the coding sequences of each were cloned into the expression vector pEGFP-C1, which incorporates an N-terminal EGFP downstream of a CMV promoter for expression in mammalian cells (Table 2.2). The mammalian expression vectors mCherry-Sec61β (Zurek et al 2011), mito-BFP (Friedman et al 2011), pGW1-ATL1 (Zhu et al 2003), and Myc-ATL1K80A (Rismanchi et al 2008) (Table 2.2) were also utilized to visualize protein localization of these factors for comparison to MavT. The African green monkey kidney fibroblast-like cell line, Cos7, was chosen for analysis of protein localization due to their large size and easily visualized cellular structures. Cos7 cells were plated at 2.5 $x10^4$ cells/well and allowed to adhere to coverslips overnight. Transfections were performed using Lipofectamine 2000 (Life Technologies) using 1 µl of reagent and 0.1-0.5 µg of DNA/ well. Transfections were allowed to proceed for 24 hours followed by 3 washes with PBS then fixed with 4% paraformaldehyde with 0.05% gluteraldehyde for 20 minutes at room temperature. For cells transfected with Myc- or HA- constructs, cells were permeabilized for 10 seconds at -20^{o}C with ice cold methanol, washed with PBS, blocked with 4% goat serum for 15 minutes at room temperature then probed with either rabbit polyclonal anti HA (1:100) (Santa Cruz), or rabbit polyclonal anti Myc (1:100) (Santa Cruz) for 1 hour at 37^{o}C. Slides were washed 3X with 4% goat serum then probed with goat anti rabbit IgG-AlexaFluor 594 (1:500) followed by washing 3X with 4% goat serum. All coverslips were mounted with SlowFade antifade reagent (Life Technologies) and visualized by immunofluorescence microscopy.

2.1.8 Immunoblotting and qRT-PCR

WT and Δ*mavT* strains were grown in AYE to an OD_{600} of 1, 2, and 4. Pelleted bacterial lysates were resuspended in 2X sample buffer or buffer RLT. Western blots of lysates separated by SDS-PAGE, then transferred to PVDF, was accomplished with rabbit serum against the purified MavT N-terminus (generated at the Pocono Rabbit Farm), or rabbit serum specific for DotF. RNA was isolated using the RNeasy kit (Qiagen), DNased with TURBO DNA-free (Life Technologies), followed by qRT-PCR using the one step RNA-to-C_t kit (Applied Biosystems) using oligonucleotides specific to *mavT* or 16S rRNA (Table 2.3).

2.2 RESULTS

2.2.1 Summary

This study was conducted to analyze the role of the predicted IDTS MavT during intracellular replication. MavT was first confirmed to be an IDTS by two independent methodologies, followed by the analysis of its in vitro expression. Bioinformatic studies revealed that MavT contained an N-terminal J domain, which was subsequently shown to be functional, and led to the identification of host binding partners. The activity of MavT in eukaryotic cells was also assayed by its ectopic expression and subsequent observation of its effect on cellular organelles. Finally, genetic approaches were taken to determine the requirement of this protein during intracellular replication in varying host cell environments. Study of MavT has led to a further understanding of the role of this

translocated substrate and the mechanisms by which it manipulates host cells during *L. pneumophila* challenge.

2.2.2 Rationale

Much of the understanding of the pathogenesis of *L. pneumophila* has come from the identification and study of IDTS that manipulate the host cell. Not only has this given insight into the pathogen, but it has also furthered the understanding of the cell biology of its host (Fontana et al 2011, Machner & Isberg 2007, Nagai et al 2002). Analysis of these IDTS has broad implications, as many of the mechanisms employed by these effectors also play roles in the pathogenesis of other intracellular pathogens (Creasey & Isberg 2012).

Prior to this study, a main focus of research had been to identify IDTS so they could be characterized in subsequent analyses. One study identified that multiple IDTS contained a C-terminal secretion signal, characterized by a glutamate rich stretch, termed an E block (Huang et al 2011). Using E block motifs from known IDTS, a bioinformatics analysis was undertaken to determine if other *L. pneumophila* ORFs, not known to be translocated, contained similar sequences. This resulted in the identification of 49 previously uncharacterized IDTS. Among these, some contained homology to domains of known function, as identified by BLAST analysis. Functional domains identified included those involved in ubiquitination, regulation of small GTPases, methyl transfer, and protein-protein interactions (Huang et al 2011). Identification of these functional

domains gave the first insight into the potential activity of these IDTS and what role they may play during *L. pneumophila* intracellular replication.

One ORF identified by bioinformatic analysis using the E block motif was *lpg0921*, which was subsequently given the name *mavT* (*more regions allowing vacuole colocalization T*). *mavT* was one of the ORFs which, as predicted by BLAST analysis, contained a putative domain of known function. The putative domain of function identified in *mavT* was a J domain, which is found in cochaperones and functions to activate cognate Hsp70 chaperones during protein folding. This was an unknown process of IDTS but was hypothesized to play a role in the folding of either host proteins or other IDTS that are translocated through the apparatus in an unfolded state (Amyot et al 2013).

Previous studies on the requirement of MavT during intracellular replication have given conflicting results. A TraSH selection experiment had predicted the requirement of MavT, but this was not confirmed in a subsequent Tn-Seq experiment (O'Connor et al 2012), (Foster, unpublished).

The presence of a domain of known function, as well as the possibility that MavT may be required for intracellular replication, pointed to the importance of further study of this IDTS. In this study, MavT was characterized by genetic and biochemical approaches to understand the role of this protein in *L. pneumophila* pathogenesis.

2.2.3 Translocation of MavT

Two independent methodologies were employed to verify that, as predicted by its C-terminal E block motif, MavT is a translocated substrate of the Icm/Dot T4SS. The first was to measure the enzymatic activity of a CyaA-MavT fusion protein, which is only active if translocated by the bacterium into host cells. The second method undertaken was a cellular fractionation experiment in which infected cells were solubilized with a detergent to separate bacteria from soluble cellular components.

Assessment of the ability of a protein to be translocated into host cells by *L. pneumophila* in an Icm/Dot dependent manner has been well studied using protein fusions to CyaA (Burstein et al 2009, Chen et al 2007). To utilize this assay to assess if MavT is an IDTS, *mavT* was fused to the 3′ end of *cyaA*, encoding a calmodulin-dependent adenylate cyclase (Sory & Cornelis 1994), which is active in eukaryotic cells expressing calmodulin. Expression of this fusion protein in Lp02 (WT) or the Icm/Dot deficient strain, Lp03 (DotA$^-$), prior to the challenge of U937 cells was induced by the addition of IPTG. U937 cells were challenged with each strain expressing the CyaA-MavT fusion, or CyaA alone (Figure 2.1A), for 1 hour and lysates were analyzed by ELISA for levels of cAMP, a readout for CyaA activity and protein translocation (Materials and Methods). cAMP levels were normalized to steady state levels of fusion or control protein harbored by each strain. Host cell challenge with the wild type strain expressing CyaA-MavT resulted in cAMP levels 21-fold higher than challenge with a strain expressing CyaA alone and 40-fold higher than challenge with DotA$^-$ expressing CyaA-MavT (Figure 2.1B). These results are consistent with those seen for other

translocated substrates of the Icm/Dot T4SS and identify MavT as one of the ~300 IDTS encoded by *L. pneumophila* (Burstein et al 2009, Huang et al 2011, Zhu et al 2011).

To verify through a second assay that MavT was a substrate of the Icm/Dot T4SS, the localization of MavT after challenge of host cells was assessed using cellular fractionation, a method that has been previously used to analyze the translocation of *L. pneumophila* proteins (Amyot et al 2013, Derre & Isberg 2005). 3xFLAG-MavT expression was induced in WT and DotA$^-$ strains by IPTG induction prior to challenge of U937 cells (Figure 2.1C). Cells were challenged for 1.5 hours with each strain in the presence of IPTG. Post challenge, cells were lysed in 0.5% digitonin, which does not lyse bacterial cells, and pelleted to separate the soluble fraction from insoluble fraction that contains the bacteria and unlysed cellular organelles. The pellet was resuspended in a volume equal to that of the soluble lysate and lysates were analyzed for the presence of FLAG-MavT, DotF (a *L. pneumophila* protein that is not translocated), and GAPDH (a soluble host cell protein) used to verify efficient cell lysis.

3xFLAG-MavT was observed in the soluble fraction of cells challenged with WT, but not DotA$^-$, confirming that MavT is a translocated substrate (Figure 2.1D). This is in contrast to DotF, which localized to only the insoluble fraction of digitonin lysed cells. GAPDH was found in the cytoplasmic fraction, consistent with efficient lysis of host cells. The expression levels of 3xFLAG-MavT in host cells were fairly similar when expressed by WT or DotA$^-$. As the levels of protein in the soluble and insoluble fraction of WT are equivalent, this indicates that if there had been protein in the soluble fraction of DotA$^-$ challenged cells, it would be detectable. These studies confirmed the previous

Figure 2.1 MavT is a translocated substrate of the Icm/Dot T4SS (A) Schematic of CyaA fusion constructs. (B) WT or DotA$^-$ (Icm/Dot deficient) strains harboring vectors that allow for the inducible expression of CyaA or CyaA-MavT, were used to challenge U937 cells at an MOI=1 for 1 hour, followed by the determination of levels of cAMP generated during each challenge (Materials and Methods). CyaA-MavT expressed by WT *L. pneumophila* shows a greater than 10-fold induction of cAMP in challenged cells, relative to the DotA$^-$ stain, or CyaA alone. (C) Similar levels of 3xFLAG-MavT are expressed by WT and DotA$^-$. Bacterial culture lysates were analyzed by immunoblot to determine levels of 3xFLAG-MavT and DotF, as a control. (D) WT or DotA$^-$ strains harboring 3xFLAG-MavT were used to challenge U937 cells at an MOI=5 for 1.5 hours. Post challenge, cells were solubilized with 0.5% digitonin and separated into soluble and insoluble fractions (Materials and Methods). Fractions were analyzed by immunoblot to determine the localization of 3xFLAG-MavT. Cells challenged with WT showed FLAG-MavT localized to the digitonin soluble fraction that was not seen in DotA$^-$, consistent with this being an Icm/Dot translocated substrate. DotF, a nontranslocated *L. pneumophila* control protein, localized to the insoluble fraction, while the control host cytoplasmic GAPDH protein is found in the soluble fraction. Data are representative of one (C), two (mean ±SEM) (B), or three (D) independent experiments.

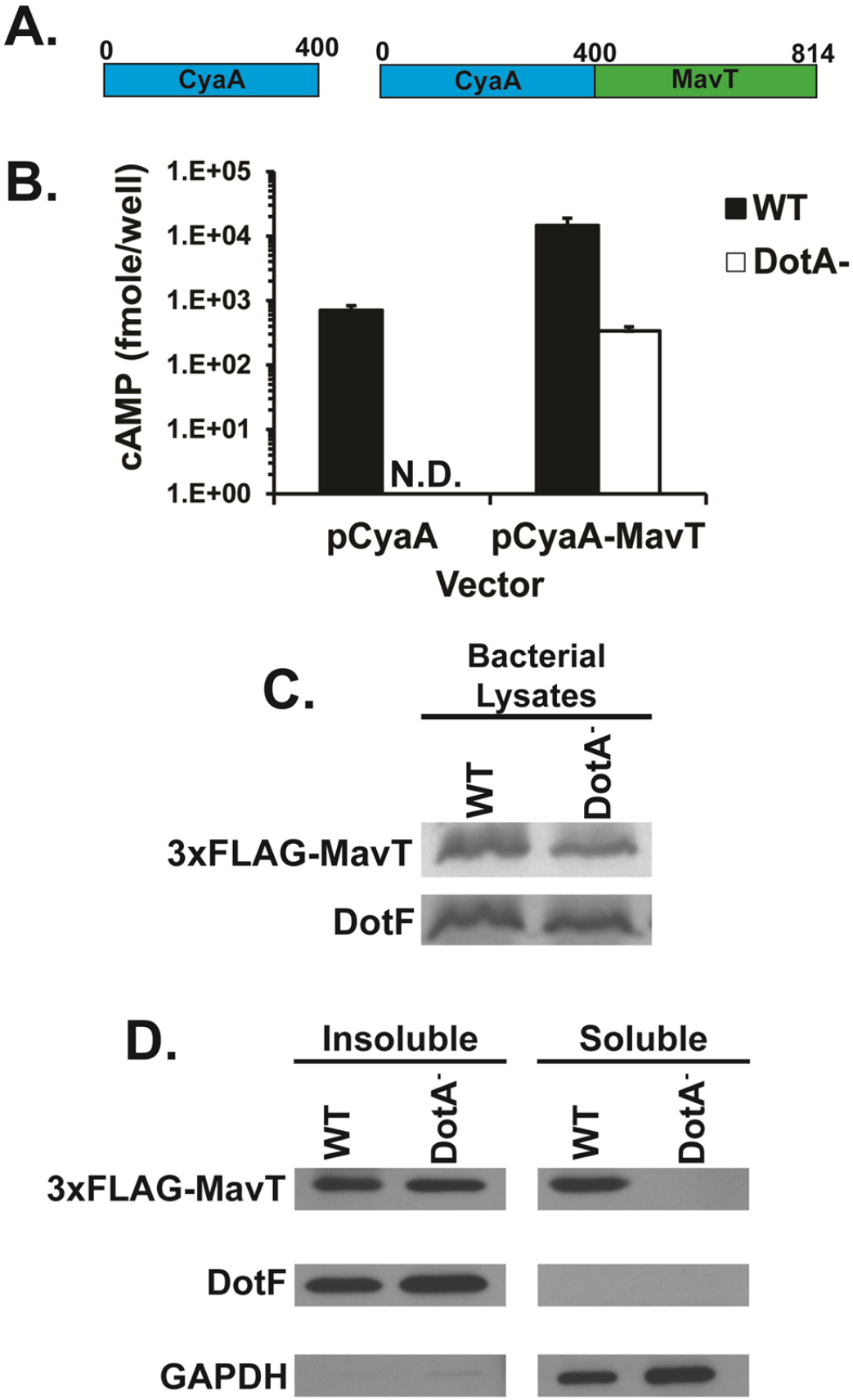
A.
0
400
CyaA
0
400
814
CyaA
MavT
B.
cAMP (fmole/well)
1.E+05
1.E+04
1.E+03
1.E+02
1.E+01
1.E+00
N.D.
WT
DotA-
pCyaA
pCyaA-MavT
Vector
C.
Bacterial Lysates
WT
DotA-
3xFLAG-MavT
DotF
D.
Insoluble
Soluble
WT
DotA-
WT
DotA-
3xFLAG-MavT
DotF
GAPDH

studies with CyaA-MavT, showing that MavT fusion proteins were translocated by the *L. pneumophila* Icm/Dot T4SS into challenged host cells.

2.2.4 Expression of MavT during in vitro growth

To begin to characterize MavT, transcript levels of this IDTS were assayed at varying times during in vitro replication in broth culture. The WT strain, was grown in AYE broth to an OD_{600} of approximately 1, 2, and 4 as representative time points of early exponential, mid-exponential, and post-exponential growth phases. RNA isolated from lysed cultures were analyzed for transcript levels by qRT-RTPCR using primers targeting *mavT* or 16S rRNA, as a control for equivalent total RNA levels. High levels of *mavT* transcription were observed in early- and mid-exponential cultures of *L. pneumophila* growth, relative to post exponential cultures (Figure 2.2A). No detectable levels of transcript were observed, at any growth phase, for a strain containing an in-frame deletion of *mavT* (Δ*mavT*) (data not shown), confirming the deletion of the ORF in this strain and the specificity of the primers targeting *mavT* transcript.

To further characterize the expression of this IDTS during broth growth, protein levels of MavT, when expressed from its native loci, were analyzed. This was accomplished using rabbit serum, which was generated against the expressed and purified soluble N-terminus of the protein (Materials and Methods). Early, late, and post exponential culture lysates (OD_{600}=1, 2, 4 respectively) from WT and Δ*mavT* stains were analyzed by immunoblot to detect MavT, and DotF as a control. Consistent with the transcript levels of *mavT*, MavT protein expression was observed in early- and mid-

Figure 2.2 MavT is expressed during exponential, but not post-exponential, growth phase in broth culture (A) *mavT* transcript is strongly upregulated at exponential phase, relative to post-exponential phase bacteria. qRT-PCR analysis of the *mavT* transcript at early-exponential, mid-exponential, and post- exponential phase, OD_{600} of 1, 2, and 4 respectively, during in vitro AYE broth culture growth. Plotted is the fold induction, relative to post-exponential cultures. (B) Expression of MavT in the WT and Δ*mavT* strains grown in vitro in AYE broth to an OD_{600} of 1, 2, and 4. MavT expression was analyzed in culture lysates using rabbit serum directed against the N-terminus of MavT (Materials and Methods). DotF protein levels from culture lysates were also determined by immunoblot as a control. MavT protein is detected at early- and mid-exponential phase, but is absent during post-exponential growth. Data are the mean of three independent experiments ±SEM (A) or representative from three independent experiments (B).

A.

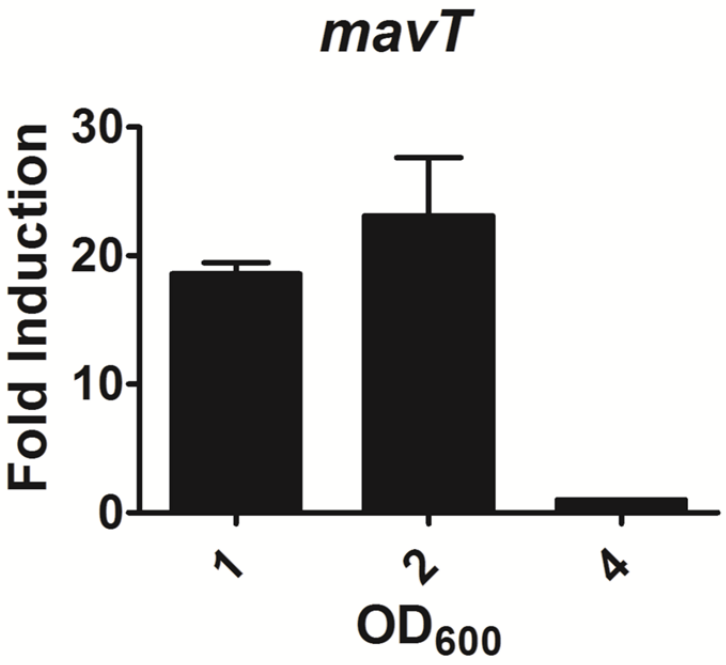
mavT
Fold Induction
30
20
10
0
1
2
4
OD600

B.

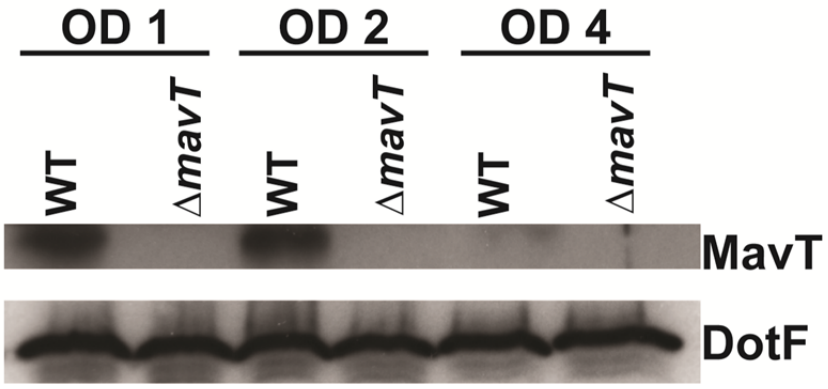
OD 1
OD 2
OD 4
WT
ΔmavT
WT
ΔmavT
WT
ΔmavT
MavT
DotF

exponential culture lysates, but little to no protein expression was observed in post-exponential culture lysates (Figure 2.2B).

2.2.5 MavT encodes a functional J domain

To begin to ascertain the role of MavT as an IDTS, a bioinformatic analysis was performed on the entire ORF. BLAST analysis of MavT revealed homology in the N-terminus of the protein to a functional domain known as a J domain, which is found in proteins encoded by both prokaryotic and eukaryotic species. Importantly, the putative J domain of MavT contained a His-Pro-Asp motif that is essential for the function of this domain in activating Hsp70 family chaperones (Figure 2.3A). To further verify the presence of this putative domain in MavT, the N-terminal region was analyzed by Phyre2 (Kelley & Sternberg 2009), which takes into account putative secondary structure. This analysis confirmed, to a high degree of confidence, that the N-terminal region of MavT contained an amino acid sequence, and secondary structure, consistent with a functional J domain.

The functional analysis of the MavT was undertaken using a domain swap experiment that has previously been used to verify the activity of J domains encoded by proteins of eukaryotic, prokaryotic, and viral origin (Kelley & Georgopoulos 1997, Nicoll et al 2007). The J domain encoding region was cloned into the expression vector pRJ-B, generating a fusion of the MavT J domain to the C-terminal region of the *Agrobacterium tumefaciens* DnaJ protein (Agt DnaJ), which has been shown to functionally complement the *E. coli* DnaJ protein (Nicoll et al 2007). This construct was transformed into the *dnaJ*

cbpA mutant *E. coli* strain WKG190 which, due to the lack of a functional soluble J domain containing protein, is unable to grow at high temperatures, when there is increased protein unfolding in the absence of DnaK (Hsp70) co-chaperone activity (Kelley & Georgopoulos 1997). A construct with an inactivating point mutation in the HPD motif of the MavT J domain (H→Q) (MavT H70Q) was also constructed to determine if the MavT J domain requires this motif for functionality, as has been seen with other J domain proteins (Kelley & Georgopoulos 1997, Nicoll et al 2007). Serial dilutions of each strain were plated on LB agar containing IPTG and plates were put o/n at either 30^{o}C or 40^{o}C for selection of temperature sensitivity. Strains expressing either Agt DnaJ or the MavT J domain- Agt DnaJ fusion were able to replicate at 40^{o}C (Figure 2.3B) as seen by colony formation up to dilutions of 10^{-5}, consistent with the ability of the MavT J domain to act as a functional J domain. Strains expressing the MavT-AgtDnaJ fusion containing the H→Q mutation, as well as a J domain from a type III *Agrobacterium* J domain protein that was previously shown not to complement the temperature sensitivity of WKG190 (Blatch, GL unpublished results), were able to grow at 30^{o}C, but no colonies were observed at dilutions of 10^{-2} or lower when incubated at 40^{o}C. Expression of each construct was verified by immunoblot detecting the N-terminal His-tag on each construct (Figure 2.3B). While expression levels varied, the low level expression of the WT MavT J domain fusion construct was sufficient to rescue the temperature sensitivity phenotype. These results confirmed that the MavT J domain functions in a manner similar to other known J domains.

Figure 2.3 MavT contains a functional N-terminal J domain (A) Alignment of the putative MavT J domain with the J domain of the human cochaperone Hsp40B12. Underlined and in blue are conserved helices 2 and 3. In red are highly conserved residues. (B) Domain swap experiment in which the J domain of MavT is fused to the coding region of *Agrobacterium* DnaJ (Agt DnaJ), lacking its native J domain, and expressed in the temperature sensitive *E. coli* strain WKG190 (*dnaJ cbpA*). Serial dilutions of cultures induced to express the chimeric DnaJ proteins were plated and grown overnight at 30^{o}C, or the restrictive temperature of 40^{o}C. Expression of each chimera was analyzed by immunoblot to detect the N-terminal His_6-tag. Chimeric AgtDnaJ containing the MavT J domain, but not one harboring an inactivating point mutation (H70Q), is able to rescue the temperature sensitivity of WKG190. Positive and negative controls harbor the native Agt DnaJ or a chimera containing a nonfunctional J domain respectively. Data are representative of three independent experiments.

A.

```
MavT      1 ERDFA---RFINQ-----QLL-ID-GPEKEKIVKN-YKRLTLCFHPD--HASGFSPEMVW
Hsp40B12 21 EQ-VAAVKR-VKQCKDYYEILGVSRGASDEDL-KKAYRRLALKFHPDKNHAPG-ATE---
               *   *   *   *       *    *   *   *  * ** * ****  ** *   *

MavT     48 LENNLSQSKNNGACFKILGLCYEKLIS-PEKFK--DSSLGDIKSK
Hsp40B12 74 -----------A-FKAIGTAYA-VLSNPEKRKQYDQ-FGDDKSQ
                     * **  *  *    * *** *  *   ** **
```

B.

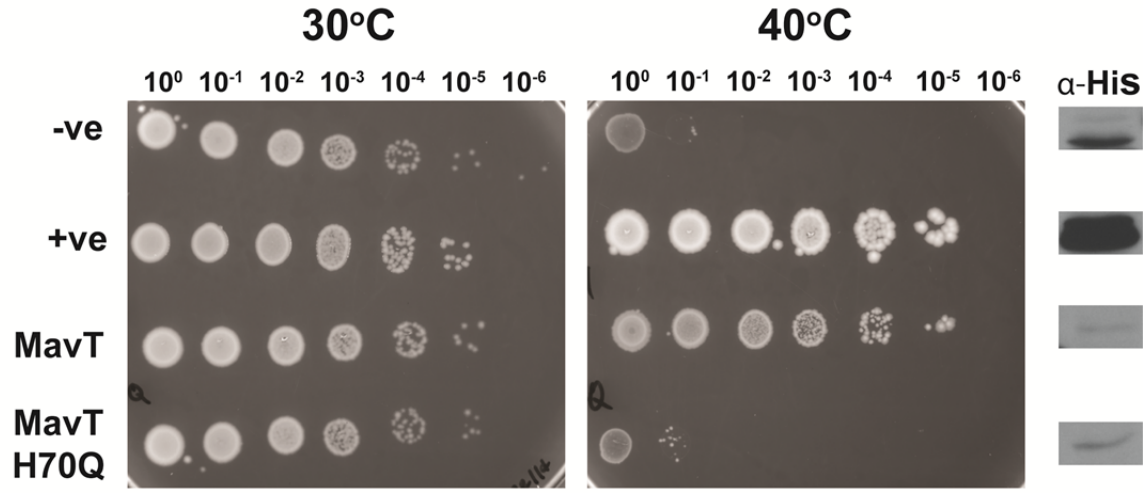

2.2.6 Analysis of mammalian MavT binding partners

The observation that MavT was an IDTS that contained a domain of known function led to the search for eukaryotic protein binding partners that MavT may act upon. To this end, an N-terminal 3xFLAG tagged MavT construct was ectopically expressed in HEK293T cells. Lysates, generated by incubation with TritonX-100 lysis buffer, were incubated with anti-FLAG resin to immunoprecipitate the 3xFLAG construct and any binding partners. Bound fractions from cells expressing either 3xFLAG alone, or 3xFLAG-MavT, were analyzed by Commassie brilliant blue staining after separation by SDS-PAGE. The ~50 kDa band observed in the bound fraction from cells expressing 3xFLAG-MavT is consistent with the size this construct, pointing to high levels of expression of the protein (Figure 2.4A). Also observed in this lane are 2-3 bands at approximately 70 kDa, and a faint band at ~90 kDa, which are not present in the bound fraction from cells expressing 3xFLAG. These bands are indicative of potential binding partners that specifically interact with 3xFLAG-MavT, relative to 3xFLAG alone.

To determine the identity of the ~70 kDa proteins that interacted specifically with MavT, mass spectrometry analysis was undertaken. The two bands observed in the bound fraction were excised from the gel and analyzed by mass spectrometry (Materials and Methods). This analysis revealed numerous peptides mapping to various members of the Hsp70 family (Table 2.4). These results are consistent with other J domain proteins, which have been shown to interact with their target Hsp70 proteins by immunoprecipitation (Campbell et al 1997, Sugito et al 1995).

Figure 2.4 MavT interacts with Hsp70 when ectopically expressed in mammalian cells (A) Comassie brilliant blue staining of immunoprecipitated fractions of soluble lysates from 3xFLAG construct expressing cells, separated by SDS-PAGE. HEK293T cells were transfected with mammalian expression vectors that encode 3xFLAG-MavT or 3xFLAG for 24 hours. Labeled is the ~50 kDa band corresponding to 3xFLAG-MavT and boxed are two groups of bands ~70 kDa and ~90 kDa that are unique to the bound fraction from 3xFLAG-MavT expressing cells (B) Schematic of 3xFLAG-MavT truncation constructs analyzed by co-immunoprecipitation experiments. (C) MavT truncation products containing the C-terminal region interact with Hsp70. Constructs immunoprecipiated by α-FLAG resin, after a 24 hour transfection, were analyzed by immunoblot to detect if each construct interacted with the ~70 kDa Hsp70. Data are a representative image (A) or representative from three independent experiments (C).

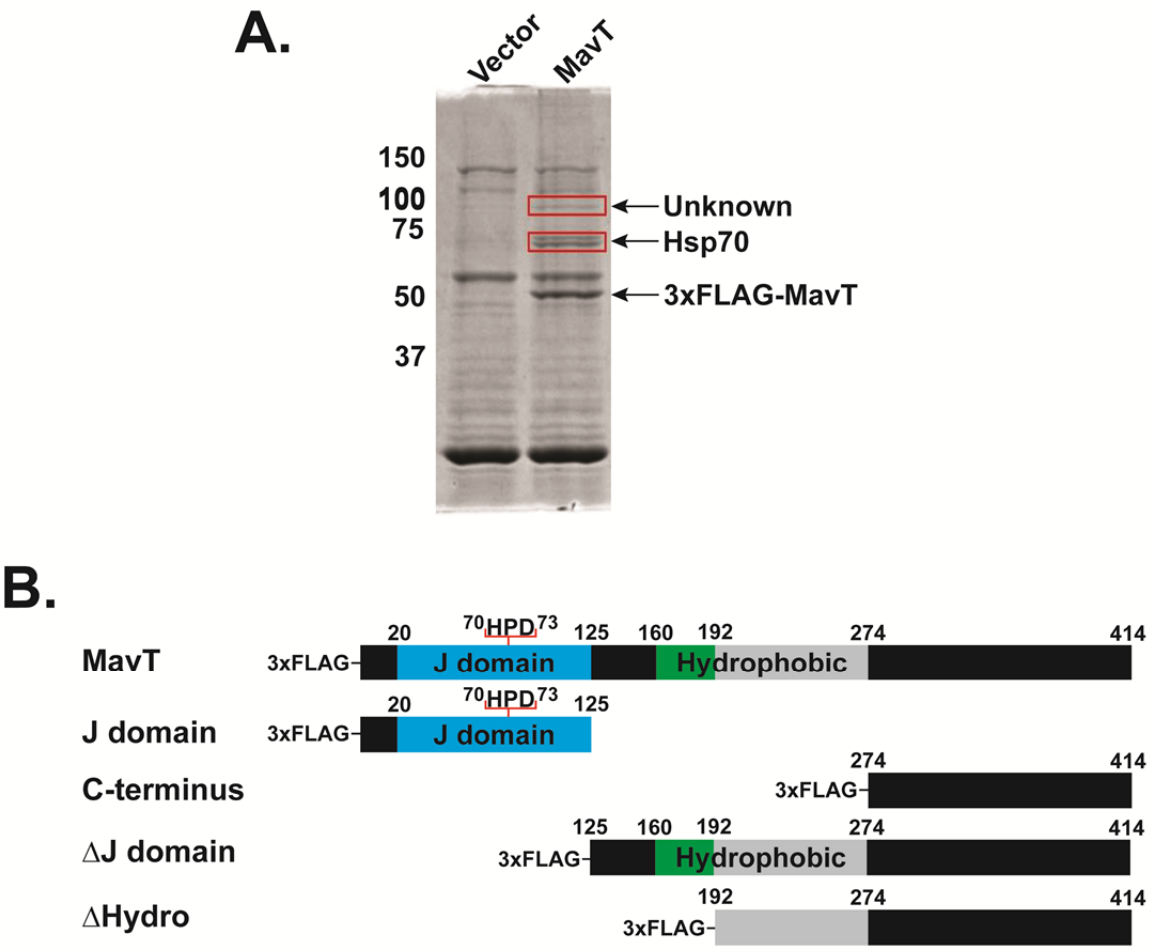
A.
Vector
MavT
150
100
75
50
37
Unknown
Hsp70
3xFLAG-MavT
B.
MavT
3xFLAG
20
70HPD73
125
160
192
274
414
J domain
C-terminus
ΔJ domain
ΔHydro
J domain
Hydrophobic
C.
FLAG
MavT
J domain
C-terminus
ΔJ domain
ΔHydro
Input
Unbound
Bound
Hsp70
FLAG
RhoGDI

Table 2.4: Binding partners of MavT identified by mass spectrometry

Description	Mass (Da)	Mapped Peptides
HSPA1A;HSPA1B Heat shock 70 kDa protein 1	70337	214
HSPA8 Isoform 1 of Heat shock cognate 71 kDa protein	71125	192
HSPA1L Heat shock 70 kDa protein 1L	70774	101
HSPA6 Heat shock 70 kDa protein 6	71484	82
HSPA2 Heat shock-related 70 kDa protein 2	70305	73
HSPA9 Stress-70 protein, mitochondrial precursor	73965	19
PRMT5 protein arginine methyltransferase 5 isoform b	71947	10

Studies of other J domain proteins have shown that the J domain is necessary and sufficient for the interaction with Hsp70 family proteins (Campbell et al 1997). To determine if this was the case for MavT, we generated constructs of the MavT protein lacking its J domain or the J domain alone, each with an N-terminal 3xFLAG tag (Figure 2.4B). These fusions were ectopically expressed in HEK293T cells, followed by immunoprecipitation with FLAG-resin. Lysates, as well as bound and unbound fractions, were analyzed by immunoblot using an antibody specific to Hsp70. Consistent with the mass spectrometry results, we observed that Hsp70 interacted with full length 3xFLAG-MavT, but not with 3xFLAG alone (Figure 2.4C). Surprisingly, we did not observe any interaction of Hsp70 with the 3xFLAG-MavT J domain construct. This may point to an alternative mechanism by which MavT interacts with Hsp70, relative to other known J domain proteins. Consistent with this idea, 3xFLAG-MavTΔJ domain was able to bind to Hsp70 pointing to an alternative region of the protein that is responsible for the interaction (Figure 2.4 C).

Further mutational analysis was undertaken to identify the region of MavT that specifically interacts with Hsp70. Two 3xFLAG tagged constructs were generated, one containing only the C-terminal 140 amino acids of MavT and the other with a deletion of the N-terminal 192 amino acids, which includes a hydrophobic stretch predicted to form a transmembrane helix (TMHMM Server v. 2.0) (Figure 2.4B). Other studies on Hsp70 binding have shown that hydrophobic stretches are the targets of Hsp70 interaction on client proteins (Fourie et al 1994). When these constructs were expressed in HEK293T cells, followed by immunoprecipitation, Hsp70 was observed to bind both of these

constructs (Figure 2.4C). These results demonstrate that the C-terminal hydrophilic region of MavT is sufficient for binding of MavT to Hsp70.

2.2.7 MavT localization and manipulation of ER structure

To further understand the role of MavT as an IDTS, its localization was assessed when expressed in mammalian cells. To this end, an N-terminal EGFP fusion to MavT was expressed in Cos7 cells, an African green monkey kidney fibroblast-like cell line which, because of their large size, allows for optimal visualization of cellular organelles. After 24 hours of transfection, EGFP-MavT was observed to localize to a perinuclear space with elongated tubules extending to the periphery of the cell (Figure 2.5A, 2nd from top, far left panel). This is in contrast to EGFP alone that localizes throughout the cell (Fig 2.5A, top panel, far left).

The localization of EGFP-MavT to a perinuclear space is consistent with many other IDTS that show ER localization when ectopically expressed in mammalian cells. To determine if MavT localized to the ER, Cos7 cells were co-transfected with mCh-Sec61β, a component of the Sec61 translocon that localizes throughout the ER, and either pEGFP or pEGFP-MavT. When mCh-Sec61β was co-expressed in cells expressing EGFP, Sec61β localized to the perinuclear ER sheets, as well as to the ER tubules which extend to the cell periphery and showed an extensive network formed by three-way junctions (Figure 2.5A, top, middle panel). These results are consistent with Sec61β localization when expressed in the absence of EGFP cotransfection (data not shown). When mCh-Sec61β was co-expressed in EGFP-MavT expressing cells, a strikingly

different morphology was observed. In these cells, Sec61β co-localized with MavT at the perinuclear space and also in the elongated tubules that extend towards the cell plasma membrane (Figure 2.5A 2nd from top, middle panel). These tubules lacked the extensive network that results from three-way junctions, observed in ER tubules, and is consistent with MavT manipulating ER tubule structure by interfering with the formation of three-way junctions.

Domain analysis of MavT was undertaken to determine which regions of the protein are required for Sec61β colocalization and manipulation of ER structure. The following constructs, containing an N-terminal EGFP tag, were generated to analyze their localization: EGFP-MavT ΔJ domain and EGFP-MavT Δhydro, which is encoded by a construct with a deletion of the entire central hydrophobic region (Figure 2.5 A). Each construct was co-transfected, along with mCh-Sec61β, into Cos7 cells. EGFP-MavT ΔJ domain showed similar manipulation of the ER as observed with EGFP-MavT, with perinuclear localization and elongation of tubules, while EGFP-MavT Δhydro was diffusely localized throughout the cell, similar to what was observed for EGFP alone (Figure 2.5A bottom two panels, far left). Manipulation of ER structure corresponded to the ability of MavT to localize to the ER as EGFP-MavTΔJ domain induced altered tubular localization of mCh-Sec61β while EGFP-MavT Δhydro did not appear to alter Sec61β localization (Figure 2.5A bottom two panels, middle). It is likely that the central hydrophobic region, predicted to have at least one membrane spanning helix (TMHMM Server v. 2.0), is responsible for the ER localization of MavT, as it is absent in this, and another construct (EGFP-MavT C-terminus) that doesn't co-localize with mCh-Sec61β (data not shown). Or, this construct may be misfolded resulting in its mislocalization.

Figure 2.5 MavT colocalizes with ER markers but manipulates ER structure (A) MavT colocalizes with the ER resident translocon subunit Sec61β, which is dependent on a central MavT hydrophobic region. Cos7 cells were transfected for 24 hours with the indicated fluorescent protein fusion constructs. Co-transfected cells were visualized by fluorescence microscopy to determine the localization of each construct. Presented is also a schematic of MavT truncation EGFP fusion proteins. (B) MavT manipulation of ER structure resembles that of a dominant-negative ATl1. Cos7 cells transfected with constructs that express Myc-ATL1 or HA-ATL1 K80A for 24 hours were analyzed by immunofluorescence microscopy. (C) MavT manipulation of ER structure overcomes the co-expression of ATL1 and co-localizes with ATL1 K80A. Co-transfected Cos7 cells were visualized by immunofluorescence microscopy 24 hours post transfection.

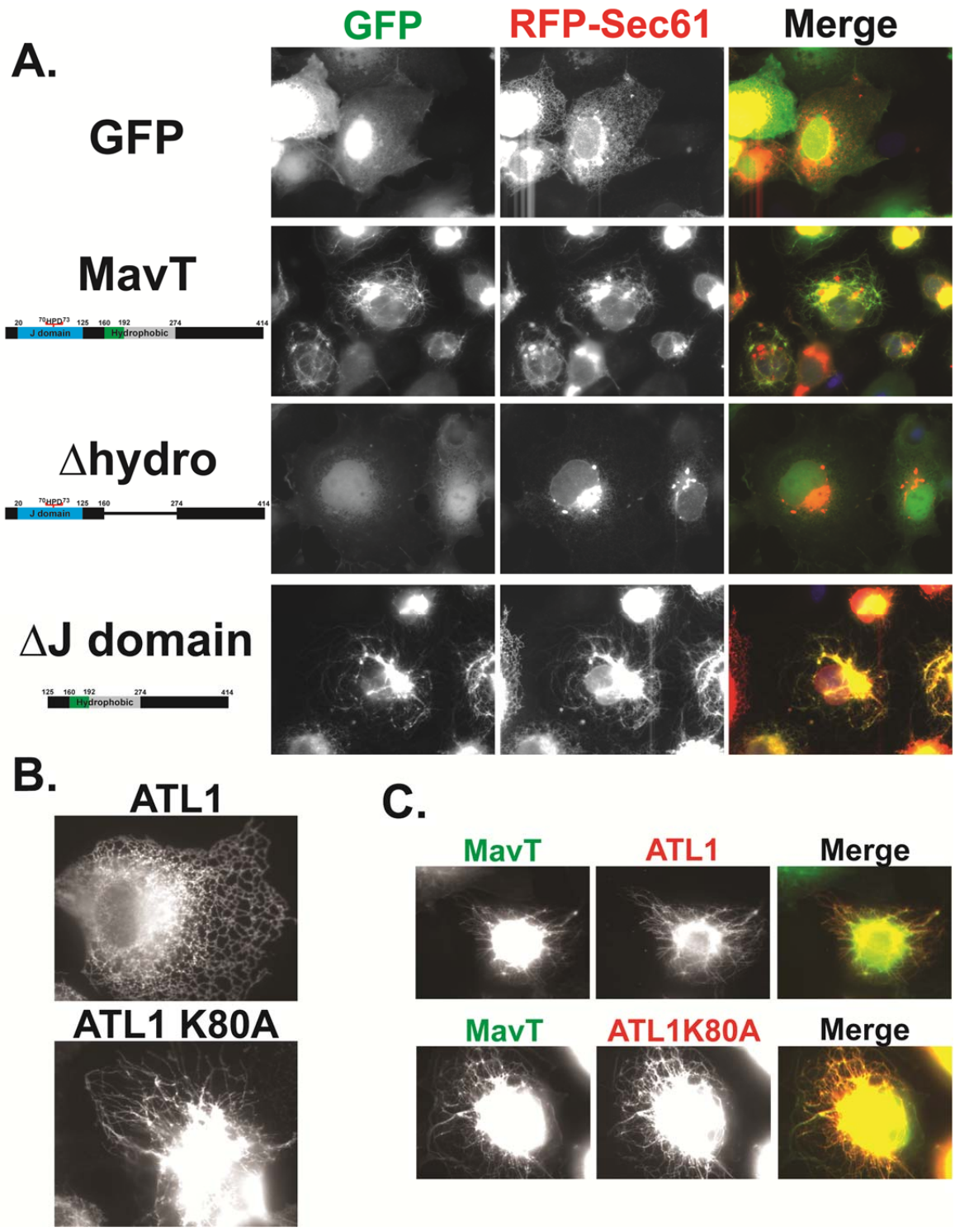
A.
GFP
RFP-Sec61
Merge
GFP
MavT
20 70HPD73 125 160 192 274 414
J domain
Hydrophobic
ΔHydro
20 70HPD73 125 160 274 414
J domain
ΔJ domain
125 160 192 274 414
Hydrophobic
B.
ATL1
ATL1 K80A
C.
MavT
ATL1
Merge
MavT
ATL1K80A
Merge

Three-way junctions of ER tubules are formed by fusogens of the dynamin-like GTPase family of atlastins (Hu et al 2009, Rismanchi et al 2008). Mutations in atlastin, resulting in a dominant negative form of the protein, result in elongated ER tubule morphology (Rismanchi et al 2008), similar to what was seen when MavT was overexpressed. To determine if the observed tubular ER morphologies were a similar phenotype, Myc-Atlastin 1 (ATL1) or HA-Atlastin 1 K80A (a dominant negative construct) were co-expressed with EGFP-MavT. Cells expressing Myc-ATL1 showed ER localization to the perinucular space as well as tubules having clear three-way junctions, consistent with normal ER morphology, while co-expression of HA-ATL1 K80A resulted in the previously observed elongated tubule phenotype, which lacks three-way junctions (Figure 2.5B). When HA-ATL1 K80A was co-expressed in cells expressing EGFP-MavT, there was strong co-localization of the two proteins, consistent with a similar ER morphology phenotype resulting from the expression of these proteins (Figure 2.5C, bottom panel). In cells co-expressing Myc-ATL1 and EGFP-MavT, ATL1 localized to elongated tubules lacking three-way junctions, similar to what is seen for the dominant negative construct (Figure 2.5C, top panel). These results are consistent with MavT expression overcoming the activity of ATL1 to limit the formation of ER tubule three-way junctions. Importantly, this phenotype was observed even in cells strongly expressing ATL1, indicating that it is unlikely that the activity of MavT is to induce the turnover of the ATL1 protein. Rather, MavT appears to interfere with ATL1 activity, by either blocking the supply of an important component of three-way junctions, directly blocking ATL1 mediated membrane fusion, or breaking down three-way junctions previously formed by ATL1.

2.2.8 Mitochondrial fission induced by MavT

The observed effect of MavT on ER morphology prompted the search for additional phenotypes associated with its expression in mammalian cells. One of the proposed functions of ER tubules in cellular physiology is the fission of mitochondria (Friedman et al 2011, Korobova et al 2013). Mitochondrial fission is accomplished by the action of Drp1, another dynamin-family protein, which localizes to sites of mitochondrial constriction by ER tubules (Bleazard et al 1999, Labrousse et al 1999).

Because of the localization to, and alteration of ER tubules by MavT, as well as its ability to overcome the activity of overexpressed ATL1, a dynamin-family GTPase, we analyzed the effect of expressing MavT on mitochondrial morphology. Cos7 cells were co-transfected with mito-BFP, which encodes the cytochrome C oxidase subunit IV mitochondrial targeting signal tagged with BFP, and either pEGFP or pEGFP-MavT. In cells co-transfected with pEGFP and mito-BFP, mitochondria showed normal elongated morphology (Figure 2.6A, top panel). Notably, in Cos7 cells co-transfected with mito-BFP and pEGFP-MavT, an altered mitochondrial morphology was observed. In these cells, shortened spherical mitochondria were observed adjacent to the perinuclear space (Figure 2.6A, 2nd from top panel). These results are consistent with MavT expression inducing mitochondrial fission or, alternatively, blocking fusion.

To assess the domains of MavT required for the mitochondrial fragmentation phenotype, as well as to determine if there was a correlation between the manipulation of ER tubules and the induction of mitochondrial fission, we analyzed mitochondrial morphology in cells expressing MavT domain deletion constructs. In cells co-expressing

Figure 2.6 MavT induces mitochondrial fragmentation (A) Cells expressing MavT constructs that manipulate ER structure also induce mitochondrial fragmentation. Cos7 cells were transfected for 24 hours with eukaryotic expression vectors to express EGFP-MavT constructs, and mito-BFP, were visualized by fluorescence microscopy. (B) Dominant-negative ATL1 does not induce mitochondrial fragmentation. Co-transfected Cos7 cells were visualized by immunofluorescence microscopy to visualize the effect of expression of Myc-ATL1 or HA-ATL1 K80A on mitochondrial structure, as analyzed by mito-BFP localization.

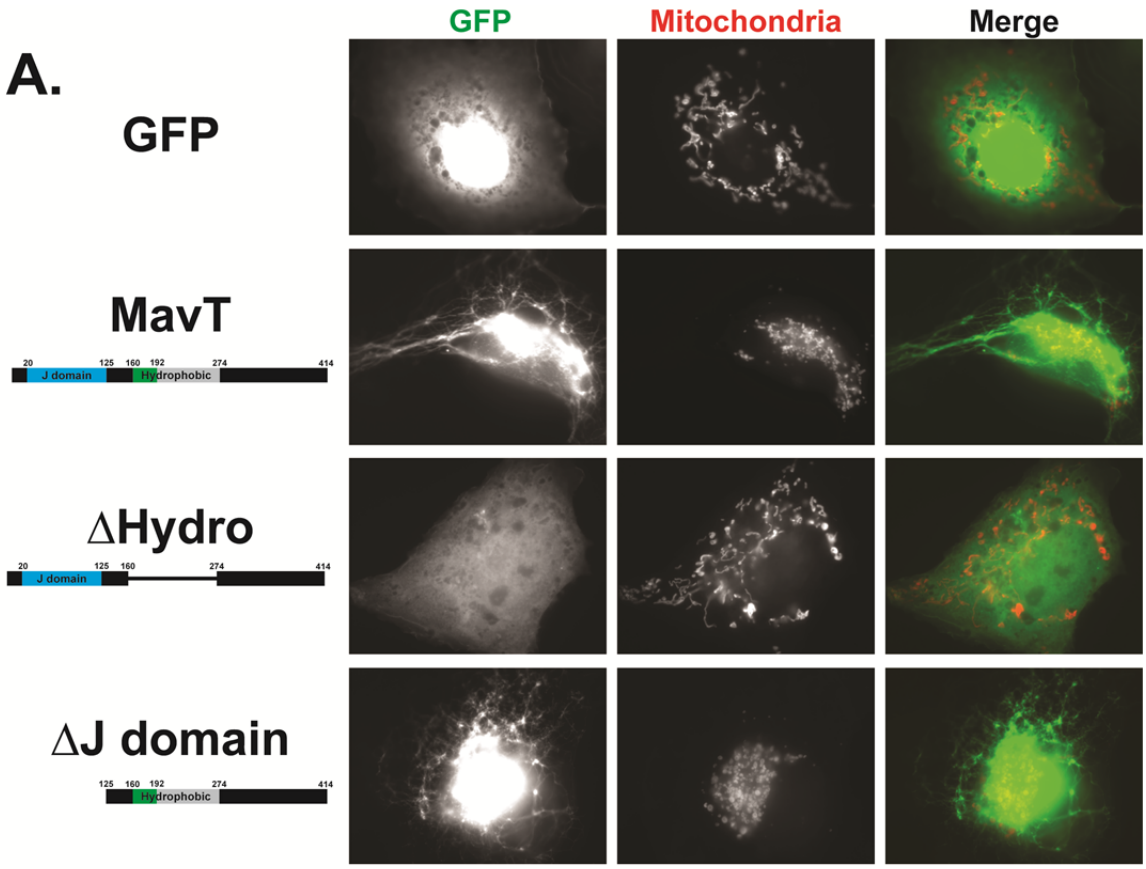
A.
GFP
Mitochondria
Merge
GFP
MavT
20
125
160
192
274
414
J domain
Hydrophobic
ΔHydro
20
125
160
274
414
J domain
ΔJ domain
125
160
192
274
414
Hydrophobic

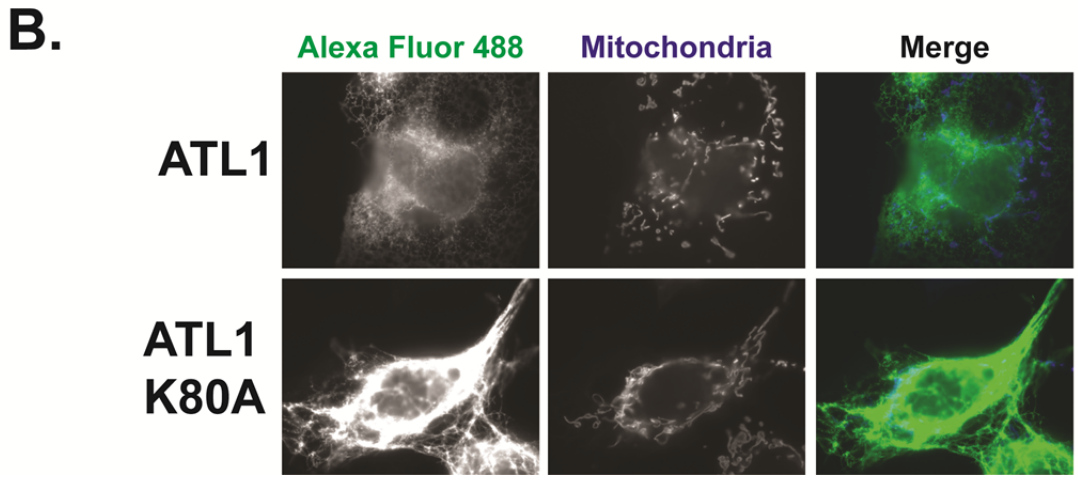
B.
Alexa Fluor 488
Mitochondria
Merge
ATL1
ATL1
K80A

pEGFP-MavT-ΔJ domain and mito-BFP, there was a similar mitochondrial fragmentation phenotype to that seen when the full length MavT was expressed (Figure 2.6A, bottom panel). In cells expressing the other MavT constructs (EGFP-MavT-J domain, EGFP-MavT-C-terminus, EGFP-MavT-Δhydrophobic region), there was no evidence of an induced mitochondrial fragmentation (Figure 2.6A, data not shown). These data show a connection between the ER localization and manipulation of the ER by each construct and the observed mitochondrial fragmentation phenotype, providing a potential link between the activities of MavT on host cell organelles.

It was previously observed that there was a similar ER manipulation phenotype induced by the expression of MavT and ATL1 K80A (Figure 2.5C). To determine if ER manipulation by this mechanism also induced mitochondrial fragmentation, Cos7 cells were cotransfected with constructs expressing mito-BFP and either Myc-ATL1 or HA-ATL1 K80A, and observed by immunofluorescence microscopy. Myc-ATL1 expression did not have any noticeable effect on mitochondrial appearance (Figure 2.6B upper panel). HA-ATL1 K80A also showed no effect on mitochondria, in contrast to what was observed for MavT (Figure 2.6B bottom panel). These results indicate that although MavT and ATL1 K80A induce a similar aberrant ER morphology phenotype, the induction of mitochondrial fission appears to be unique to MavT and may point to a separate function of the protein.

2.2.9 Replication of *Legionella pneumophila* lacking MavT

Attempts to further understand the role of MavT in the manipulation of host cells were undertaken through a genetic approach using the Δ*mavT* strain. This strain was analyzed for growth, relative to the WT parental strain, in broth culture and during intracellular replication in mammalian and amoebal hosts.

To analyze the ability of Δ*mavT* to replicate in vitro, the WT and Δ*mavT* strains were grown in AYE broth and replication was measured by analysis of the OD_{600} over a 24 hour period. It was observed that WT and Δ*mavT* have similar growth kinetics, and reached a similar OD_{600} during a 24 hour period of growth (Figure 2.7A). This is similar to other known translocated substrates that, as they function to manipulate the host during intracellular growth, are not required for replication in broth culture (O'Connor et al 2011).

Intracellular replication of *L. pneumophila* in BMDMs isolated from A/J mice serves as a model system for intracellular replication in mammalian macrophages. To determine if Δ*mavT* is able to replicate efficiently within host cells, A/J BMDMs were challenged with WT and Δ*mavT* and intracellular replication was assayed by plating for CFUs at 2, 24, 48, and 72 hours post challenge. At each time point, similar levels of replication were seen for WT and Δ*mavT* (Figure 2.7B). These data provide evidence that MavT is not required for efficient intracellular replication in BMDMs.

In the environment, *Legionella* replicates within numerous amoebal hosts (Fields 1996, Rowbotham 1980). Multiple amoebal systems have been used to analyze the replication of *L. pneumophila* mutants that, at times, reveal intracellular replication

Figure 2.7 Strains lacking *mavT* replicate to WT levels in broth culture and within host cells (A) Replication of WT and Δ*mavT* in AYE broth, as measured by change in OD_{600} over a 24 hour period (Materials and Methods). (B) Growth curve to analyze intracellular replication of WT and Δ*mavT* in A/J BMDMs. Cells were challenged at an MOI=0.05 and intracellular replication was measured by CFU counts at time points throughout a 72 hour time period. (C, D) Analysis of intracellular replication of the WT and Δ*mavT* strains within the amoebal hosts *D. discoideum* and *A. castellanii*. Challenges were performed at an MOI=0.05 or 0.01 respectively and intracellular replication was determined by plating for CFUs from cell lysates at various time points during a 72 hour challenge. Data are the mean ±SEM from three independent experiments (A-C) or a single experiment (D).

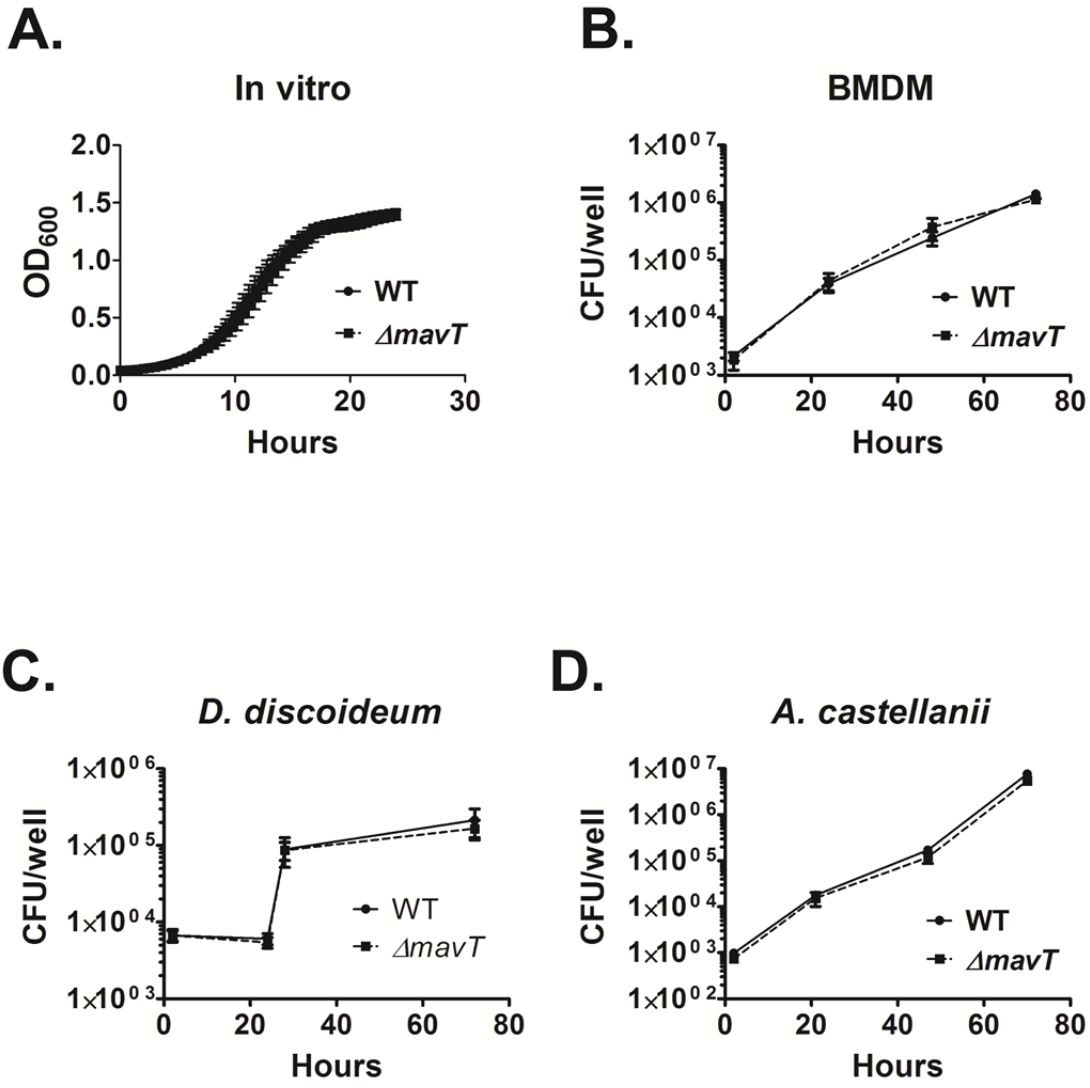
A.
In vitro
OD600
2.0
1.5
1.0
0.5
0.0
0
10
20
30
Hours
WT
ΔmavT
B.
BMDM
CFU/well
1×10^7
1×10^6
1×10^5
1×10^4
1×10^3
0
20
40
60
80
Hours
WT
ΔmavT
C.
D. discoideum
CFU/well
1×10^6
1×10^5
1×10^4
1×10^3
0
20
40
60
80
Hours
WT
ΔmavT
D.
A. castellanii
CFU/well
1×10^7
1×10^6
1×10^5
1×10^4
1×10^3
1×10^2
0
20
40
60
80
Hours
WT
ΔmavT

phenotypes that were not observed in BMDMs (Bardill et al 2005, Fontana et al 2011, O'Connor et al 2011). The ability of Δ*mavT* to replicate in two amoebal species: *Dictyostelium discoideum* and *Acanthamoeba castellanii* was assayed. Each of these amoebal species was challenged with WT and Δ*mavT* for 72 hours with intracellular replication measured by CFU counts, as was performed for BMDMs. Levels of intracellular replication by Δ*mavT* were consistent with those of WT in both *D. discoideum* and *A. castellanii* at each time points analyzed (Figure 2.7C, D). Similar to what was observed in BMDMs, the absence of MavT does not seem to adversely affect the ability of *Legionella* to replicate within a host in these model systems.

2.2.10 Analysis of Δ*mavT* intracellular replication by a long-term competition assay

The absence of an observed intracellular replication phenotype of Δ*mavT* in mammalian and amoebal hosts led to the possibility that the intracellular growth assays used in the laboratory were not sensitive enough to detect minor variances in intracellular replication. To address this possibility, 36 day intracellular growth competitions were performed in A/J BMDMs. The following competitions were performed: WT vs. WT::lux, WT vs. Δ*mavT*::lux, and Δ*mavT* vs. WT::lux (Figure 2.8A). Insertion of the *luxCDABE* operon into these strains allowed for differentiation of CFUs in each competition by visualization after plating. Cells were challenged at a MOI of 0.025 for each strain and at 3 days post challenge host cell lysates were used to initiate a secondary challenge. At varying time points, cellular lysates were also plated to enumerate the CFU from each strain, which could be differentiated by luciferase expression. Lysates were also frozen down so that they could be further analyzed if necessary.

Figure 2.8 Strains harboring an in-frame deletion of *mavT* exhibit an intracellular growth advantage during long-term competition assays (A) Schematic of long term growth competition. Three competitions were performed: WT vs. WT::lux, WT vs. Δ*mavT*::lux, and Δ*mavT* vs. WT::lux. Cultures were mixed at a 1:1 ratio and used to challenge A/J BMDMs at a total MOI of 0.05. Three days post infection, cells were lysed and either plated to determine CFUs, or used to challenge a second plate. This was repeated for 36 days total. (B) Ratio of luciferase expressing over not expressing CFUs in each competition, at varying time points after infection. The presence of the *luxCDABE* operon results in a competitive defect, as seen in the WT only competition. This defect is potentiated when WT::lux is competed against Δ*mavT*, indicating that the absence of *mavT* results in a growth advantage. This is consistent with the results of the WT vs. Δ*mavT*::lux competition in which, even when containing the lux operon, Δ*mavT*::lux is able to outcompete WT. Data are from three independent lineages for each competition that were from the same initial broth culture mixture ±SEM.

A.

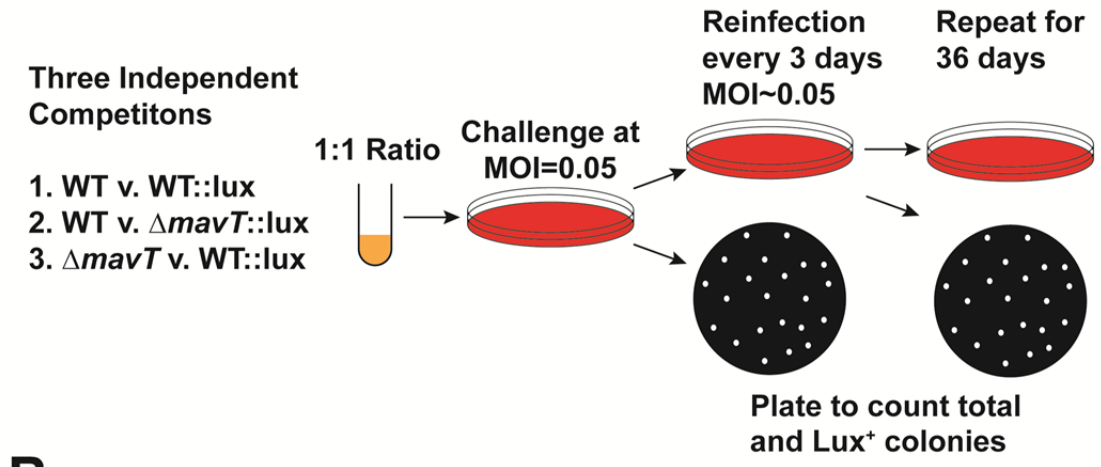
Three Independent Competitons
1. WT v. WT::lux
2. WT v. ΔmavT::lux
3. ΔmavT v. WT::lux
1:1 Ratio
Challenge at MOI=0.05
Reinfection every 3 days MOI~0.05
Repeat for 36 days
Plate to count total and Lux+ colonies

B.

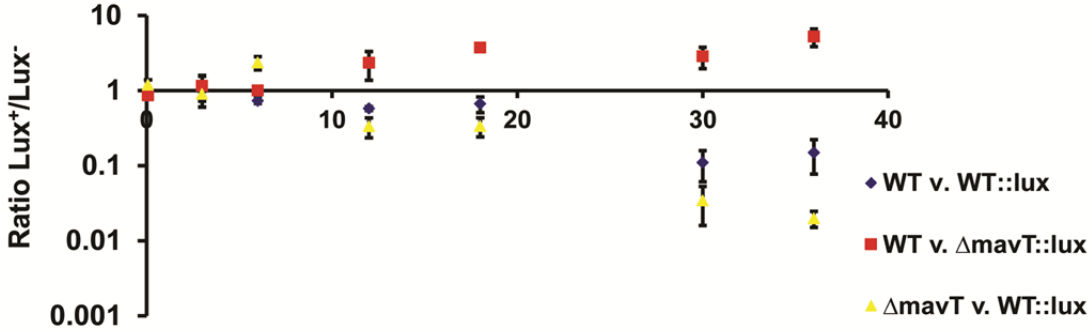
Ratio Lux+/Lux-
10
1
0.1
0.01
0.001
0
10
20
30
40
WT v. WT::lux
WT v. ΔmavT::lux
ΔmavT v. WT::lux

A 36 day long-term competition allowed for the differentiation of the competitive indices of each strain when competed against each other. This revealed slight intracellular growth phenotypes that were not observed in three day intracellular growth assays that were measured by CFU counts. At ~12 days post initial challenge, differences in competitive indices began to be revealed. At this time point, the insertion of the luciferase operon begins to show an adverse effect on intracellular replication as WT::lux is outcompeted by WT (Figure 2.8B). This also occurs in the WT::lux vs. Δ*mavT* competition, but to a greater extent. A differing trend is seen in the WT vs. Δ*mavT*::lux competition in which, at 12 days post initial challenge, Δ*mavT*::lux is outcompeting WT, despite the presence of the lux operon. These trends for each competition continue out to 36 days post infection, consistent with small differences in intracellular replication rates that were are observable only by a long-term growth experiment.

The combined data from each of these three competitions show that the absence of *mavT* results in an intracellular growth advantage of Δ*mavT*, in comparison to the WT strain in mouse macrophages. This is shown in both Δ*mavT* vs. WT::lux, where WT::lux is outcompeted to a greater extent than seen in the WT vs. WT::lux, and to an even greater extent in the WT vs. Δ*mavT*::lux where Δ*mavT*::lux outcompetes WT, even when encoding the luciferase operon. As no replication enhancement of Δ*mavT* was observed in vitro broth culture (Figure 2.7A), it is likely that the replication phenotype observed for Δ*mavT* is only present during intracellular growth.

It remained a possibility that the competitive advantage of Δ*mavT* might be due to a second site mutation that was acquired during the 36 day competition. While performing each competition in three independent biological replicates, all of which

showed a similar phenotypic pattern, would make this unlikely, it is possible that the absence of MavT could result in a second site mutation. To determine if this was the case, one clone of Δ*mavT* and Δ*mavT*::lux was selected from both the initial input cultures used for challenge at day 0 and from the population recovered after the 36 day competition assay. Whole genome sequencing was performed by homopolymer tail-mediated ligation PCR (HTML-PCR) (Lazinski & Camilli 2013) using the Illumina HiSeq. Sequencing resulted in ~3,000,000 50 bp reads for each strain, resulting in ~45 fold coverage of the *L. pneumophila* Philadelphia 1 genome. Analysis was performed using the Geneious software package. Single nucleotide polymorphism (SNP) analysis revealed that there were no SNPs that were acquired during the long-term growth competition. This is consistent with the enhanced intracellular growth phenotype of Δ*mavT* being due to the absence of this IDTS, rather than a second site mutation. This argues that the presence of this protein, and high conservation through known *L. pneumophila* isolates, is due to selection in environmental hosts other than those assayed in this work.

Chapter 3: Manipulation of the unfolded protein response by *Legionella pneumophila*

The following chapter contains text and figures from a manuscript submitted for publication currently under review. Experimental work was performed by the author.

3.1 MATERIALS AND METHODS

3.1.1 Bacterial culture and media

L. pneumophila strains used in this study are described in (Table 3.1). Strains were propagated as described in Chapter 2.1.1. Plasmids used in this study are described in (Table 3.2). The Δ5 strain and plasmids pLgt3 and pLgt3* were kind gifts from Zhao-Qing Luo PhD (Purdue University West Lafayette, Indiana). Strains harboring the pGFP Cm^R plasmid, encoding an IPTG inducible GFP*mut3* (O'Connor et al 2012), were cultured on BCYE containing 5 μg/ml Cm and 0.1 mg/ml thymidine, with the addition of 1 mM IPTG during growth in broth.

3.1.2 Eukaryotic cell culture

BMDMs and U937 cells were grown as described in Chapter 2.1.2. HeLa cells were passaged in DMEM supplemented with 10% FBS while WT and PERK $^{-/-}$ mouse embryonic fibroblasts (MEFs) (A kind gift from David Ron, University of Cambridge) were cultured in DMEM supplemented with 10% FBS, 2 mM L-glutamine, 55μM β-mercaptoethanol, and 1X nonessential amino acid mix.

Table 3.1: Bacterial strains

Strain	Genotype	Description	Reference
Lp02 (WT)	Philadelphia 1, *thyA rpsL hsdR*	wild type strain	(Berger & Isberg 1993)
Lp03 (DotA$^-$)	Lp02, *dotA03*	Icm/Dot translocation deficient	(Berger & Isberg 1993)
Δ5	Lp02, *lgt1-3, sidI, sidL*	Lacking 5 IDTS that inhibit translation	(Fontana et al 2011)
Δ5 Thy$^+$	Δ*5, thyA*$^+$	Thy+ Δ5 strain	(Fontana et al 2011)

Table 3.2: Plasmids

Plasmid	Genotype	Description	Reference
pEC101	pMMB207Δ267 (*mobA*$^-$), *gfp-mut3*, cm^R	GFP expression plasmid	(O'Connor et al 2012)
pJB908	RSF1010 ori, *td*Δ*I*, Δ*oriT*, *thyA*$^+$, amp^R, p*tac*	in trans complementation empty vector	(Sexton et al 2004)
pLgt3	pJB908:FLAG-*lgt3*, p*sidF*	Lgt3 complementation vector	(Fontana et al 2011)
pLgt3*	pJB908:FLAG-*lgt3**, p*sidF*	Lgt3* complementation vector	(Fontana et al 2011)

3.1.3 Immunofluorescence microscopy

To determine intracellular replication, BMDMs isolated from A/J mice were plated on glass coverslips at a density of $2x10^5$/well in 24-well plates. Prior to challenge, medium was replaced with RPMI, 200 μg/ml thymidine, and either DMSO, 500 nM Tp (Sigma), or Tm 1 μg/ml (Sigma). Cells were challenged at MOI = 0.5 with post-exponential bacteria, and plates were centrifuged at 1,000 RPM for 5 minutes. The incubation was allowed to proceed for 1 hour at 37°C, washed 3 times with warm media and then continued for an additional 13 additional hours. Coverslips were washed 3 times with PBS, fixed with 4% paraformaldehyde for 20 minutes at room temperature, and washed three times with PBS. After blocking with 4% goat serum, extracellular *Legionella* were detected by anti-*L. pneumophila* rat serum (1:5000) and goat anti-rat IgG-AlexaFluor 594 (1:500). Cells were permeabilized with 0.1% Triton X-100 for 10 mins, probed with anti-*L. pneumophila* rabbit serum (1:5000) for 1 hour, followed by detection with goat anti-rabbit IgG-AlexaFlour 488 (1:500). The number of bacteria per cell was determined for 100 cells/coverslip by immunofluorescence microscopy.

For the detection of eIF2α~P in infected cells, A/J BMDMs were plated at $4x10^5$ cells/well on glass coverslips. Cells were challenged for 2 hours at an MOI=1.0 and treated as above, with the addition of staining for eIF2α~P (Cell Signaling Technology) followed by detection with goat anti-rabbit IgG-AlexaFlour 488 (1:500).

3.1.4 Analysis of XBP1 splicing by RT-PCR

U937 cells ($8x10^5$-$1x10^6$) were challenged at described MOI, and plates were centrifuged for 5 minutes at 1,000 RPM then incubated at 37°C for 2 hours. Cells were washed 3X with warm media and replaced with RPMI containing the initial chemicals and allowed to incubate further. AJ BMDMs ($4x10^5$) were challenged at an MOI of 3, centrifuged 5 minutes at 1,000 RPM then incubated at 37°C for 1 hour. Medium was replaced and allowed to incubate for 6 additional hours. At the time of analysis, cells were washed 3X with HBSS then lysed in buffer RLT. For sorted cell experiments, 6 wells of U937 cells, plated at $2x10^6$ were challenged with *L pneumophila* at the indicated MOI for 2 hours at 37°C then treated as above for unsorted samples for the remainder of the challenge. Prior to sorting, cells were washed with HBSS then lifted with trypsin, washed with HBSS, and resuspended in PBS + 1mM EDTA. $1.5x10^6$ cells were collected on the BD Influx sorter at the Tufts University Flow Cytometry Core. Sorted cells were pelleted and resuspended in buffer RLT.

RNA isolation from buffer RLT lysates was performed using the RNeasy kit (Qiagen), then treated with TURBO DNA-free (Life Technologies). cDNA was generated with SuperScript III (Invitrogen) using oligo dT and 100-750ng RNA as the template. *XBP1* and *GAPDH* were amplified using human specific primer sets while mouse transcripts were amplified with *Xbp1* and *Gapdh* oligonucleotides described in (Table 3.3). Products were analyzed by separation on 2.5% agarose gels and imaged with the Gel Logic 100 Imaging System (Kodak). Quantification of XBP1 splicing was performed using Fiji software to determine the mean pixel intensity for spliced and unspliced

Table 3.3: Oligonucleotides

	Name	Description	Sequence
25	hXBP1F	human *XBP1* forward	TTACGAGAGAAAACTATGGCC
26	hXBP1R	human *XBP1* reverse	GGGTCCAAGTTGTCCAGAATGC
27	hGAPDHF	human *GAPDH* forward	TTGCCATCAATGACCCCTTCA
28	hGAPDHR	human *GAPDH* reverse	CGCCCCACTTGATTTTGGA
29	mXbp1F	mouse *Xbp1* forward	GAACCAGGAGTTAAGAACACG
30	mXbp1R	mouse *Xbp1* reverse	AGGCAACAGTGTCAGAGTCC
31	mGapdhF	mouse *Gapdh* forward	AGGCCGGTGCTGAGTATGTC
32	mGapdhR	mouse *Gapdh* reverse	TGCCTGCTTCACCACCTTCT
33	splicedmXbp1F	mouse spliced *Xbp1* forward	TGCTGAGTCCGCAGCAGGTG
34	splicedmXbp1R	mouse spliced *Xbp1* reverse	ACTAGCAGACTTGGGGAAG
35	m18SF	mouse 18S rRNA forward	CGCCGCTAGAGGTGAAATTCT
36	m18SR	mouse 18S rRNA reverse	GCTTTCGTAAACGGTTCTTCA
37	hERdj4F	human *ERdj4* forward	AAAATAAGAGCCCGGATGCT
38	hERdj4R	human *ERdj4* reverse	CGCTTCTTGGATCCAGTGTT
39	hGFAT1F	human *GFAT1* forward	GGACAGCACAACCTGCCTTT
40	hGFAT1R	human *GFAT1* reerse	CAGCACTTGCATCAGAAGCAA
41	hp58^{IPK}F	human p58^{IPK} forward	CTCAGTTTCATGCTGCCGTA
42	hp58^{IPK}R	human p58^{IPK} reverse	TTGCTGCAGTGAAGTCCATC
43	h18SF	human 18S forward	CGCCGCTAGAGGTGAAATTCT

44	h18SR	human 18S reverse	CATTCTTGGCAAATGCTTTCG
45	mIl6F	mouse *Il6* forward	GAGGATACCACTCCCAACAGACC
46	mIl6R	mouse *Il6* reverse	AAGTGCATCATCGTTGTTCATACA
47	mTNFαF	mouse *Tnf*α forward	GCACCACCATCAAGGACTCAA
48	mTNFαR	mouse *Tnf*α reverse	GCTTAAGTGACCTCGGAGCT
49	mGapdhF	mouse *Gapdh* forward	TGTGTCCGTCGTGGATCTGA
50	mGAPDHR	mouse *Gapdh* reverse	CCTGCTTCACCACCTTCTTGAT

products, as well as the hybrid product, which was accounted for as ½ spliced and ½ unspliced product.

3.1.5 Immunoblotting

U937 cells were challenged for four hours, as for XBP1 splicing analysis. Post challenge, cells were washed 3X with HBSS then lysed with 2X Laemmli sample buffer, followed by boiling the lysates for 10 mins. SDS-PAGE was performed, followed by transfer to PVDF. Protein detection was performed with antibodies to XBP1s (BioLegend) (1:1000) or α-Tubulin (Sigma) (1:10,000).

Detection of eIF2α~P levels was performed in MEFs or HeLa cells. HeLa cells were plated at $2x10^5$/well and after allowing to adhere overnight, were challenged at an MOI=5 for 1 hour then media was replaced with Tm (5 μg/ml) and challenge was allowed to continue for 6 additional hours. After adhering overnight, MEFs plated at $4x10^5$/well were challenged at an MOI=5 for 2 hours then Tp (500 nM) was added for 4 additional hours. Cells were lysed in 2X sample buffer containing the phosphatase inhibitors sodium orthovanadate (1 mM) and sodium fluoride (10 mM). Protein levels were detected by immunoblot using anti eIF2α~P and anti eIF2α (Cell Signaling Technology).

3.1.6 Quantitative RT-PCR

For qRT-PCR analysis of Xbp1 splicing, wild type and Myd88$^{-/-}$ C57BL/6 BMDMs, plated at 4x10^5-8x10^5, were treated with Tp, heat killed *L. pneumophila* (HKLp), heat killed *Escherichia coli* (HKEc), or heat killed *Yersinia pseudotuberculosis* (HKYpt) (performed by heating at 60^{o}C for 1 hour) at an effective MOI = 100. Plates were centrifuged at 1,000 RPM for 5 mins then incubated at 37^{o}C for 6 hours. Cells were washed 3 times with PBS then lysed with buffer RLT. RNA was isolated as in RT-PCR procedure. Xbp1 splicing was then detected (van Schadewijk et al 2012), but with the following modifications. Transcripts were measured using the one step RNA-to-C$_t$ kit (Applied Biosystems) using mouse spliced Xbp1 primer pair and normalized to 18S ribosomal RNA using oligonucleotides described in (Table 3.3).

For detection of transcripts regulated by XBP1s, RNA isolated from sorted experiments, described above, was analyzed by qRT-PCR using the one step RNA-to-C$_t$ kit (Applied Biosystems). The following primer pairs were utilized: human *ERDJ4*, human *GFAT1*, human *p58^{IPK}*, and human 18S ribosomal RNA, described in (Table 3.3)

For detection of cytokine transcripts during conditions of UPR induction in the presence of *L. pneumophila* derived PAMPs, AJ BMDMs were plated at 8x10^5 cells. Wells were either uninfected, or treated with HKLp at an effective MOI of 30. Plates were spun down at 1,000 RPM then incubated at 37^{o}C for 6 hours. Wells were washed 3X in PBS, lysed in buffer RLT and RNA preparation and qRT-PCR were performed as described above. The following primer pairs were used for detection of transcripts: mouse *Il6*, mouse *Tnfα*, and mouse *Gapdh*, described in (Table 3.3)

3.1.7 Translation, labeling and quantification

In order to measure host cell translation, U937 cells were challenged with WT-GFP and the Δ5-GFP strain at an MOI = 1 for 9 hours. The medium was replaced with RPMI lacking methionine (Invitrogen) and cells were incubated for 1 hour at 37^{o}C. The medium was replaced with fresh methionine-free medium containing 50μM L-azidohomoalanine (AHA) (Invitrogen), and cells were incubated for an additional hour at 37^{o}C. Cells were washed with HBSS, lifted with trypsin, washed with PBS, fixed with 4% paraformaldehyde for 20 mins at RT then washed 3X with PBS and stored at 4^{o}C. Cells were blocked with 1% BSA for 30 mins at RT then incubated for 1-3 hours at 37^{o}C in 1% BSA with 100μM APC-phosphine. Washing was performed with 0.5% Tween-20, followed by 2 washes with PBS. Flow cytometry analysis was performed on 20,000 cells in a live cell gate using the BD FACSCalibur.

Adaptation of the SUnSET immunofluorescence microscopy protocol was also used to determine levels of translation (Schmidt et al 2009). AJ BMDMs plated at 2x10^{5} were challenged at an MOI = 0.5, centrifuged at 1,000 RPM for 5 mins, and then incubated at 37^{o}C for 1 hour. Cells were washed 3X with warm media then incubated at 37^{o}C for 9 additional hours. Medium was replaced with RPMI containing puromycin (Sigma) at 1 μg/ml for 1 additional hour. Cells were fixed and stained, as for intracellular replication, with the addition of anti-puromycin (12D10, Millipore) at 1:200 to detect incorporation of puromycin into ribosomes.

3.2 RESULTS

3.2.1 Summary

In this study, the interaction of *L. pneumophila* with pathways of the host UPR was analyzed. As it was previously shown that TLR recognition of PAMPs induces the IRE1 branch of the UPR, we first analyzed if *Legionella* derived PAMPs could induce this response. The ability of *Legionella* to inhibit pathways of the UPR was also determined through study of pathway activation by pharmacological treatment during bacterial challenge. Furthermore, chemical inducers of ER stress were utilized to determine the consequences of activation of UPR pathways on intracellular replication during host cell challenge. IDTS that inhibit host translation elongation where further analyzed for their role in the inhibition of XBP1 splicing. To verify that the translation elongation inhibition mediated by these IDTS was directly responsible for the inhibition of IRE1 pathway activation, chemical inhibitors of translation were analyzed for their ability to inhibit XBP1 splicing. These studies provide the mechanistic basis by which an intracellular bacterial pathogen is able to limit the induction of a UPR pathway.

3.2.2 Rationale

While there is a large body of evidence showing that *Legionella* manipulates the ER during intracellular replication, little is known about how the cell responds to these perturbations. Other bacterial pathogens that replicate within a similar intracellular niche have been shown to activate pathways of the UPR, indicating that this may be a cellular response to the pathogen (de Jong et al 2013, Smith et al 2013). Since the IRE1 pathway

of the UPR is activated in response to TLR agonists, and induces proinflammatory signaling, its activation could play a role in the host's ability to respond to, and clear the pathogen (Martinon et al 2010).

The ability of *Legionella* to replicate within a eukaryotic cell is dependent on its interaction with the host through translocated effectors of its Icm/Dot T4SS. These virulence factors manipulate multiple facets of host cell biology to the benefit of the bacterium. A subset of IDTS encoded by *L. pneumophila* functions to inhibit host cell translation elongation during infection (Belyi et al 2006, Fontana et al 2011). In addition to the bacterially mediated inhibition of translation, the host also acts to inhibit translation initiation through downregulation of mTOR pathways (Ivanov & Roy 2013).

Prior to this study, little was known about the interaction of *Legionella* with pathways of the UPR, even though much was known about the interaction of this pathogen with the host ER. As translation and its regulation are intricately linked with pathways of the UPR (Harding et al 1999, Yamamoto et al 2011), it was hypothesized that bacterial manipulation of the translation machinery may further manipulate pathways of the evolutionarily conserved IRE1 UPR pathway. In this study, the ability of *L. pneumophila* to inhibit the IRE1 pathway through IDTS that inhibit the host cell translation elongation was analyzed.

3.2.3 *Legionella pneumophila* inhibits activation of the IRE1α branch of the unfolded protein response

It has been previously shown that TLR detection of PAMPs activates IRE1α to induce the cytosolic splicing of mRNA encoding the transcription factor Xbp1s (Martinon et al 2010, Qiu et al 2013). To determine if *L. pneumophila*-derived PAMPs induced Xbp1 splicing, BMDMs from WT and Myd88$^{-/-}$ mice were treated with heat-killed *L. pneumophila* (HKLp) (Figure 3.1A). Cells were also treated with the TLR stimulators heat-killed *E. coli* (HKEc) and *Y. pseudotuberculosis* (HKYpt) (Akira & Takeda 2004) to induce Xbp1 splicing, and thapsigargin (Tp) to induce ER stress due to depletion of luminal ER calcium stores. RNA isolated from challenged cells was analyzed by qRT-PCR to detect splicing of Xbp1, and splicing was compared to untreated controls. HKLp induced levels of Xbp1 splicing in WT macrophages that were similar to those observed in response to the other heat-killed organisms (Figure 3.1A). In contrast, no splicing could be observed in the Myd88$^{-/-}$ macrophages, consistent with this response being driven by TLR detection of *L. pneumophila* (Figure 3.1A). While levels of Xbp1 splicing were low relative to those seen during Tp treatment, they are consistent with that of previous reports showing PRR-mediated XBP1 splicing (Martinon et al 2010, Qiu et al 2013)

It was next tested if *L. pneumophila*-derived PAMPs could induce the IRE1α branch of the UPR during host cell challenge with live bacteria. BMDMs were challenged with the wild type strain, Lp02 (WT), or the Icm/Dot deficient strain, Lp03 (DotA^{-}), to assess if there was a specific response to IDTS. In addition, Tp was added 1 hour post challenge to determine how an ER stress-inducing reagent affects UPR in the

Figure 3.1 *L. pneumophila* inhibits chemically induced XBP1 splicing (A) PAMPs derived from *Legionella pneumophila* induce Xbp1 splicing in a Myd88-dependent manner. WT and *Myd88*$^{-/-}$ C57BL/6 BMDMs were incubated with heat killed *L. pneumophila* (HKLp), *Escherichia coli* (HKEc), or *Yersinia pseudotuberculosis* (HKYpt) at an effective MOI = 100, or treated with thapsigargin (Tp) (500 nM), for 6 hours. Total RNA isolated from lysates was used to measure levels of Xbp1s transcript by qRT-PCR (Materials and Methods). (B) *L. pneumophila* is able to inhibit Tp induced Xbp1 splicing in an Icm/Dot dependent manner. A/J BMDMs were challenged with Lp02 (WT) or Lp03 (DotA$^-$) at an MOI = 3 for 7 hours, with the addition of Tp (500 nM), as indicated, 1 hour post challenge. cDNA generated from total RNA lysates was used to analyze Xbp1 splicing by semi-quantitative RT-PCR (Materials and Methods). (C) Chemical induction of the IRE1α pathway is also limited in a human macrophage-like cell line. U937 cells, treated with Tp (500 nM), or DMSO as a vehicle control, were challenged with WT or DotA$^-$ at an MOI = 5 for 6 hours. XBP1 splicing was determined as in (B). (D) Similar results were seen in cells treated with tunicamycin (Tm) (1μg/ml) to induce ER stress. (E) Induction of XBP1s protein is also limited by WT challenge. Total lysates from challenged U937 cells were probed with antibodies specific to the product of spliced XBP1 transcript (XBP1s), or α-Tubulin as a loading control. Data are mean $\pm$ SEM of three independent experiments (A), or representative of three independent experiments (C, D, E), or a representative experiment (B). Statistical analysis performed using unpaired t test with Welch's correction where appropriate * $p<0.05$, ** $p<0.01$, *** $p<0.001$.

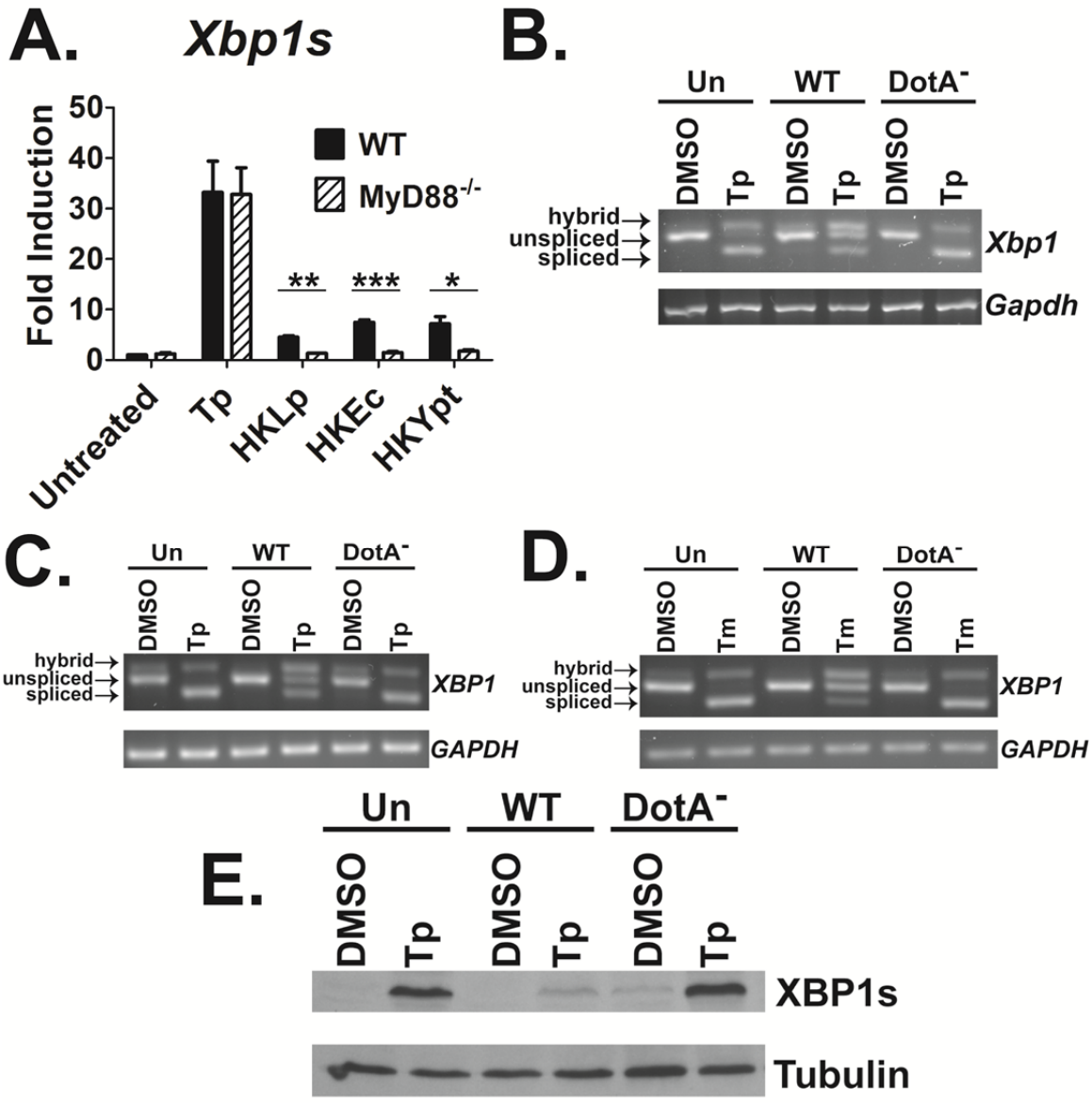
A.
Xbp1s
Fold Induction
50
40
30
20
10
0
WT
MyD88-/-
**
***
*
Untreated
Tp
HKLp
HKEc
HKYpt
B.
Un
WT
DotA-
DMSO
Tp
hybrid
unspliced
spliced
Xbp1
Gapdh
C.
XBP1
GAPDH
D.
Tm
E.
XBP1s
Tubulin

presence of *L. pneumophila* infection. Xbp1 splicing was then analyzed by semi-quantitative RT-PCR analysis (Materials and Methods). In this system, the spliced product is presented as a band that electrophretically migrates faster than the unspliced product. In addition, a spliced/unspliced hybrid presents as the slowest migrating form, as noted in previous work (Shang & Lehrman 2004)**.** In the DMSO treated cells there was little evidence for the induction of Xbp1 splicing due to *L. pneumophila* challenge (Figure 3.1B). Tp alone resulted in almost complete loss of the unspliced Xbp1 transcript (Figure 3.1B; Un, Tp). In contrast, infection of cells with *L. pneumophila* WT resulted in clear retention of the unspliced form (WT, Tp). Blockage of Xbp1 splicing required the Icm/Dot system, as the DotA$^-$ strain showed no blockage (DotA$^-$, Tp). The blockage of splicing observed in the WT infection was not complete; likely due to uninfected bystander cells undergoing Tp induced Xbp1 splicing.

Even at these low levels of infectivity, cytotoxicity of the primary macrophages could be observed. A macrophage-like cell line, which showed lower levels of cytotoxicity, was instead used to eliminate the possibility that the UPR blockage was due to cell death. Phorbol ester-differentiated U937 cells were challenged with WT, or DotA$^-$. As seen with BMDMs, WT inhibited Tp induced XBP1 splicing, which was not observed for the DotA$^-$ strain (Figure 3.1C; WT, Tp vs DotA$^-$, Tp). Furthermore, in the absence of Tp, XBP1 splicing was undetectable in cells challenged with WT, with a clear reduction in levels of the hybrid band, compared to challenge of macrophages with the DotA$^-$ strain, or uninfected cells (Figure 3.1C; WT, DMSO vs DotA$^-$, DMSO). Similar results were seen in cells challenged in the presence of tunicamycin (Tm), which induces ER stress by inhibiting N-linked glycosylation, consistent with the inhibition of XBP1 splicing being

independent of the inducing agent (Figure 3.1D). Finally, consistent with the WT ability to inhibit XBP1 splicing, XBP1s protein levels were reduced in cells challenged with WT when treated with Tp, relative to the uninfected or DotA$^-$ challenged populations (Figure 3.1E). These results indicate that *L. pneumophila* infection suppresses pharmacologically induced XBP1 splicing.

3.2.4 Inhibition of XBP1 splicing is dependent on five translocated substrates, which limit host translation elongation

Previous studies have shown that chemical translation elongation inhibitors, such as cycloheximide (CHX), can block pharmacological induction of the UPR (Yamamoto et al 2011). *Legionella* has been shown to target host translation elongation through IDTS that inhibit the activity of the eukaryotic elongation factors eEF1A and eEF1Bγ (Belyi et al 2006, Shen et al 2009). A strain lacking these IDTS (Lgt1-3 and SidI), as well as an additional IDTS (SidL), named Δ5, displays a decreased ability to inhibit host protein translation (Asrat et al 2014b, Fontana et al 2011). We therefore hypothesized that the ability of *L. pneumophila* to limit the induction of XBP1 splicing is dependent on these elongation inhibitors. To test this model, we challenged cells with *L. pneumophila*-GFP, and U937 cells harboring bacteria were sorted from uninfected cells to specifically analyze XBP1 splicing in the population harboring bacteria. In the absence of uninfected bystanders, RNA isolated from cells challenged with WT showed an almost complete inhibition of Tp-induced XBP1 splicing, in contrast to cells challenged with Δ5 or DotA$^-$ (Figure 3.2A, B). This was further verified to be dependent on the activity of these IDTS, as complementation of Δ5 by the IDTS Lgt3, but not a mutant Lgt3 that harbors a

Figure 3.2 Inhibition of XBP1 splicing is dependent on T4SS substrates that inhibit host translation elongation (A) Inhibition of XBP1 splicing is largely dependent on host translation elongation inhibitors. U937 cells were challenged with GFP expressing WT, DotA$^-$, or Δ5 at an MOI = 2 for 4 hours in the presence or absence of 100 nM Tp. Populations having associated bacteria were obtained through sorting by flow cytometry and lysates were used to determine XBP1 splicing (Materials and Methods). (B) Quantitation of XBP1 splicing from (A). (C, D) Expression of Lgt3, but not a catalytically inactive mutant (Lgt3*), limits Tp induced XBP1 splicing and XBP1s protein expression. Tp (100 nM), or DMSO, treated U937 cells were challenged with the indicated strains at an MOI = 2 for 4 hours. XBP1 splicing and XBP1s protein levels were determined from total cell lysates (Materials and Methods). Data are representative from at least 3 independent experiments (A, C, D), or the mean $\pm$ SEM of three independent experiments (B). Statistical analysis performed using unpaired t test ** $p<0.01$, *** $p<0.001$.

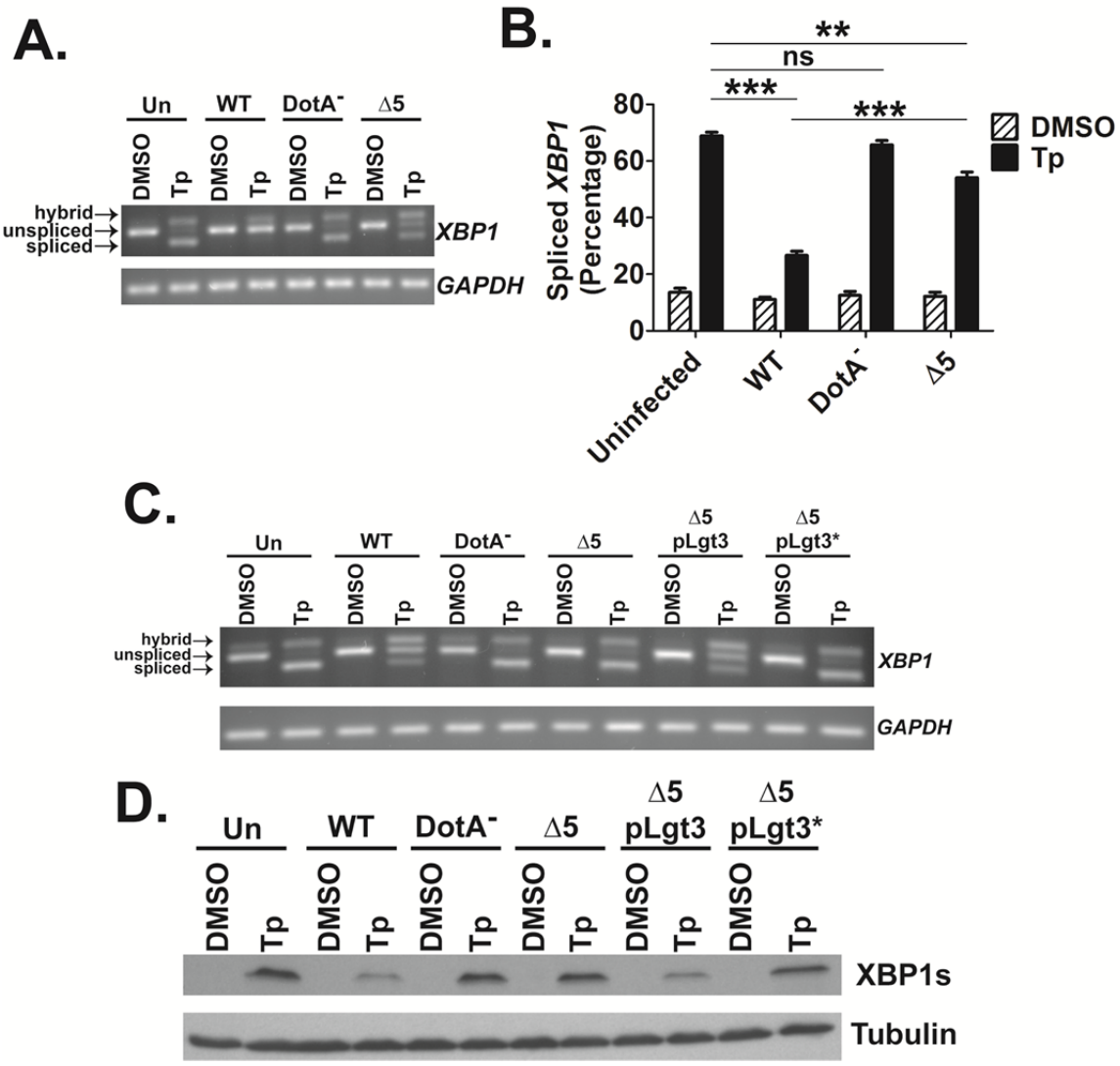
A.
Un
WT
DotA-
Δ5
DMSO
Tp
hybrid
unspliced
spliced
XBP1
GAPDH
B.
**
ns
***
***
Spliced XBP1 (Percentage)
80
60
40
20
0
DMSO
Tp
Uninfected
WT
DotA-
Δ5
C.
Un
WT
DotA-
Δ5
Δ5 pLgt3
Δ5 pLgt3*
DMSO
Tp
hybrid
unspliced
spliced
XBP1
GAPDH
D.
Un
WT
DotA-
Δ5
Δ5 pLgt3
Δ5 pLgt3*
DMSO
Tp
XBP1s
Tubulin

catalytically inactive point mutation (Lgt3*), limited XBP1 splicing in a population of cells challenged by these strains (Figure 3.2C). When levels of XBP1s protein were analyzed by Western blotting, a similar dependence on the translation elongation inhibitors was seen (Figure. 3.2D). Furthermore, it was dependent on the biochemical activity of Lgt3 in complementation experiments (Figure 3.2D). These results show that bacterial inhibitors of host translation elongation block IRE1 signaling at both XBP1 splicing and downstream XBP1s protein expression.

3.2.5 Induction of transcripts regulated by XBP1s is limited by *L. pneumophila* challenge

Transcription of a subset of genes has been shown to be specifically upregulated by XBP1s in response to ER stress (Lee et al 2003, Wang et al 2014). To determine if *L. pneumophila* challenge attenuates signaling downstream from XBP1s induction, Tp-treated cells were challenged with *L. pneumophila*-GFP strains, RNA was isolated from the infected (GFP^+) population, and analyzed by qRT-PCR. The XBP1s-regulated transcripts analyzed, *ERdj4*, *GFAT1*, and $p58^{IPK}$, all exhibited reduced Tp-dependent induction in cells challenged with WT, relative to uninfected cells, or cells challenged with either $DotA^-$ or the Δ5 strain (Figure 3.3A-C). The effect was most profound for *ERdj4*, which showed 80% lower induction in the presence of WT, compared to the $DotA^-$ strain (Figure 3.3A). The extreme attenuation of the response was also dependent on the translocated protein synthesis inhibitors as the Δ5 strain showed a higher induction than the WT strain (Figure 3.3A). This indicated the importance of inhibition of

Figure 3.3 *L. pneumophila* blocks transcription of genes controlled by XBP1s U937 cells were challenged with noted GFP-harboring strains at an MOI = 2 for four hours, treated with either Tp (100 nM), or DMSO, and sorted into infected and uninfected populations by flow cytometry. RNA isolated from GFP positive populations was used to measure transcriptional expression of genes regulated by XBP1s by qRT-PCR. Shown is the fold enhancement, in the infected populations, resulting from Tp treatment. (A) *ERdj4*, (B) *GFAT1*, and (C) $p58^{IPK}$. Expression is relative to 18S ribosomal RNA. Data are the mean $\pm$ SEM of three independent experiments. Statistical analysis performed using unpaired t test ** $p<0.01$, *** $p<0.001$.

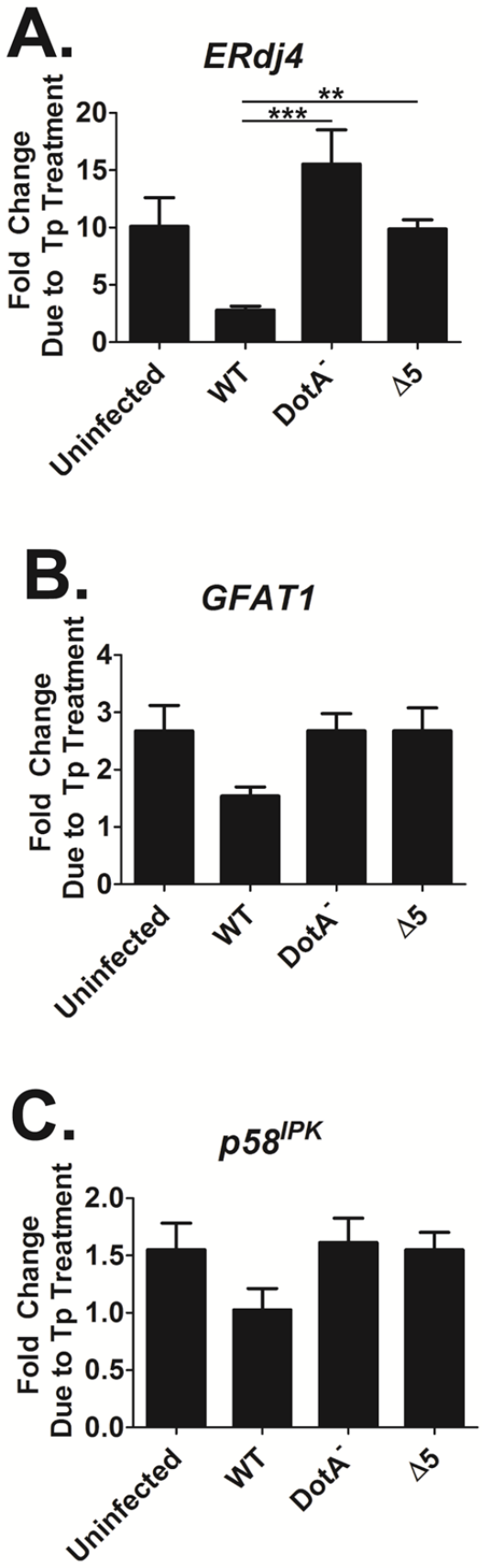
A.
ERdj4
Fold Change Due to Tp Treatment
20
15
10
5
0
**
***
Uninfected
WT
DotA-
Δ5
B.
GFAT1
Fold Change Due to Tp Treatment
4
3
2
1
0
Uninfected
WT
DotA-
Δ5
C.
p58IPK
Fold Change Due to Tp Treatment
2.0
1.5
1.0
0.5
0.0
Uninfected
WT
DotA-
Δ5

translation elongation in limiting the response and is consistent with the limited inhibition of Tp induced XBP1 splicing by Δ5 (Figure 3.2A, B).

3.2.6 Induction of UPR does not limit *L. pneumophila* intracellular replication

Activation of the UPR through the IRE1α pathway has been implicated in enhanced expression of proinflammatory cytokines (Fontana et al 2011, Martinon et al 2010, Qiu et al 2013). This enhanced induction occurs under conditions of activation of PRRs by PAMPs. To determine if detection of *L. pneumophila*-derived PAMPs, during activation of the UPR, enhanced the expression of cytokines, BMDMs were treated with HKLp, in the presence or absence of Tp. RNA isolated from stimulated macrophages showed markedly increased transcription of both *Tnf-α* and *Il-6* in cells treated with both HKLp and Tp, relative to HKLp alone (Figure 3.4A, B).

The enhanced cytokine transcription under conditions of PRR engagement by *L. pneumophila*, in cells undergoing UPR, would likely create an environment limiting for intracellular replication of the bacterium. This has been seen for other intracellular pathogens, such as *Listeria monocytogenes* (Pillich et al 2012). It is possible that the ability of wild type *L. pneumophila* to inhibit XBP1 splicing may limit the cells ability to respond in this manner. To assess this, BMDMs were challenged with either WT or the Δ5 strain, which is defective for inhibiting XBP1 splicing (Figure 3.4C, D). Challenged cells were analyzed by immunofluorescence microscopy to determine bacterial replication by counting the number of bacteria/vacuole. In cells treated with either Tp or Tm, both strains were able to replicate at similar levels. Thus, *L. pneumophila* was

Figure 3.4 *Legionella* replicates in presence of an induced UPR (A, B) The UPR synergizes with *L. pneumophila* PAMPS to induce transcription of proinflammatory cytokines. A/J BMDMs were treated with Tp (500 nM), HKLp (effective MOI of 20), or both HKLp and Tp, for 6 hours. RNA isolated from total lysates was analyzed for transcription of *Il-6* or *Tnf-α* by qRT-PCR. Expression is plotted relative to *Gapdh* transcript levels. (C, D) *Legionella* replicates in presence of an induced UPR. A/J BMDMs, treated with Tp (500 nM), Tm (1 μg/ml), or DMSO were challenged with bacteria for 14 hours at an MOI = 0.5. Infected macrophages were fixed and probed with anti-*L. pneumophila* (Materials and Methods). The number of bacteria/ vacuole was determined for 100 cells for each of three replicates. Plotted is the percentage of vacuoles with the indicated number of bacteria. Data are the mean $\pm$ SEM of three independent experiments. Statistical analysis performed using unpaired t test with Welch's correction where appropriate * $p<0.05$, ** $p<0.01$.

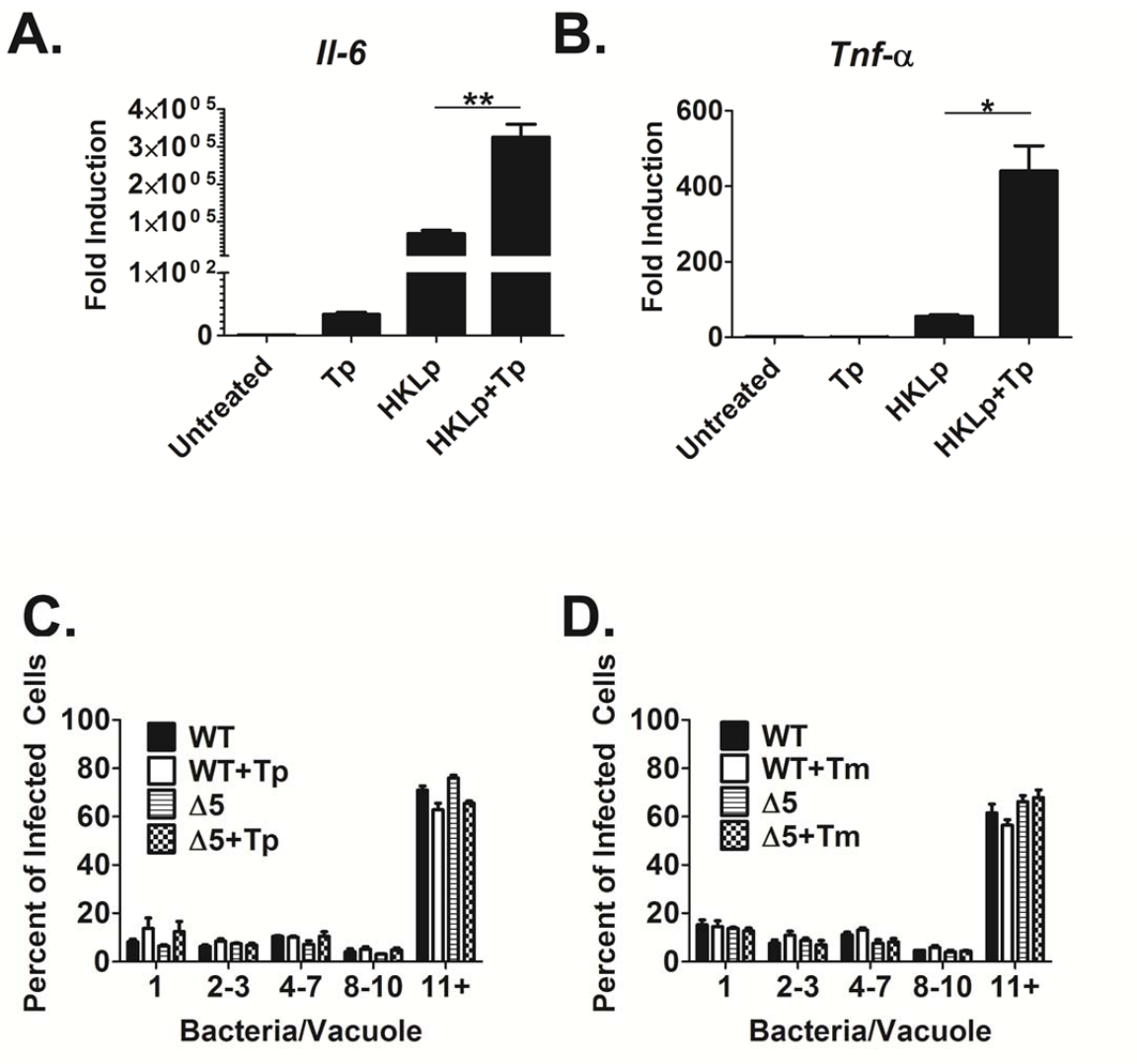
A.
Il-6
Fold Induction
4×10^05
3×10^05
2×10^05
1×10^05
1×10^02
0
**
Untreated
Tp
HKLp
HKLp+Tp
B.
Tnf-α
Fold Induction
600
400
200
0
*
Untreated
Tp
HKLp
HKLp+Tp
C.
Percent of Infected Cells
100
80
60
40
20
0
WT
WT+Tp
Δ5
Δ5+Tp
1
2-3
4-7
8-10
11+
Bacteria/Vacuole
D.
Percent of Infected Cells
100
80
60
40
20
0
WT
WT+Tm
Δ5
Δ5+Tm
1
2-3
4-7
8-10
11+
Bacteria/Vacuole

markedly resilient in the presence of UPR inducers, as BMDMs treated with either Tp or Tm caused little or no decrease in intracellular replication (Figure 3.4C, D).

3.2.7 The mechanism of translation inhibition is critical for blocking XBP1 splicing

It has been previously shown that protein synthesis in host cells challenged by WT *L. pneumophila* are ~95% below that of uninfected cells while Δ5 strain challenged cells are still ~80% below that of uninfected cells, at an early time point post challenge (Fontana et al 2011). Furthermore, as infection progresses, levels of translation in Δ5 infected cells continue to decrease, relative to earlier time points (Asrat et al 2014b). Much of this translation inhibition in the Δ5 strain can be explained by the observation that the host cell shuts down translation initiation in response to the pathogen (Ivanov & Roy 2013).

Based on these previous results, we hypothesized that the ability of Δ5 to replicate during conditions of an induced UPR could be explained by inhibition of XBP1 splicing at late time points during host cell challenge, as a consequence of protein synthesis inhibition by the host. To analyze this issue further, we measured host protein synthesis at late time points. At 10 hpi, host cells were incubated with the amino acid analog L-azidohomoalanine (AHA) for 1 hr, and levels of incorporation into nascent polypeptides were determined by flow analysis after fluorescent labeling of the incorporated analog (Materials and Methods). Cells harboring either WT or Δ5 showed label incorporation that was indistinguishable from background controls, indicating translation was inhibited

in host cells at late time points after challenge by both strains (Figure 3.5A). We verified this using an adaptation of the SUnSET protocol (Schmidt et al 2009), in which translation is analyzed by the incorporation of puromycin into translating ribosomes. When infected cells, treated with puromycin at 10 hpi, were observed microscopically after 1 additional hour of infection, there was some detectable puromycin incorporation into translating ribosomes in Δ5 infected cells that was distinguishable from the WT infection, but the levels of incorporation were much lower than that seen in neighboring uninfected bystander cells, again indicating that translation was inhibited at late time points, even in response to the Δ5 strain (Figure 3.5B).

Given the significant shutdown of host protein synthesis in response to the Δ5 strain at 10-11 hpi, we determined if this could interfere with the UPR, by analyzing XBP1 splicing. In U937 cells challenged with GFP-*L. pneumophila* and treated with Tp for 2 hours at 9 hpi, there was no evidence that the Δ5 strain could limit XBP1 splicing in the sorted infected population (Figure 3.5C, D), even though there was little host translation at this time point (Fig. 5A, B). In fact, at 11 hpi, the Δ5 strain induced XBP1 splicing in the absence of Tp treatment, as visualized by a hybrid band and faint spliced band (Figure 3.5C, D). Evidence for UPR was not observed in untreated WT challenged cells, consistent with the ability of this strain to limit the response that was observed in Δ5 challenged cells. Also consistent with early time points, the Δ5 strain harboring Lgt3 was sufficient to inhibit XBP1 splicing (Figure 3.5E). It is notable that, in contrast to earlier time points (Figure 3.2C), the strain bearing the plasmid-borne Lgt3 showed enhanced inhibition of Tp induced XBP1 splicing relative to that observed with the WT

Figure 3.5 The mechanism of translation inhibition is critical for blocking XBP1 splicing (A) Δ5 inhibits protein synthesis at late time points during infection. U937 cells were challenged with GFP-*L. pneumophila*, to analyze infected cells, at an MOI = 1 for 10 hr., then incubated with the methionine analog, L-azidohomoalanine (AHA, 100μM) for 1 hour. Fixed cells were analyzed for levels of translation by detection of AHA incorporation into nascent peptides using DyLight 650-phosphine and flow cytometry (Materials and Methods). (B) Low levels of translation are observed at late timepoints during challenge with the Δ5 strain when analyzed by puromycin incorporation into translating ribosomes. A/J BMDMs were challenged with bacteria at an MOI = 0.5 for 10 hours then treated with puromycin (1 μg/ml) for 1 additional hour. Cells were fixed and permeablized, then stained with antibodies specific to *L. pneumophila* or puromycin, to measure translation (Materials and Methods). Scale bar: 10 μm. (C) At late time points, the Δ5 strain induces XBP1 splicing and is unable to inhibit chemically induced XBP1 splicing. U937 cells were challenged with bacteria at an MOI of 1 for 9 hours then cells were treated with either DMSO or Tp (100nM) for 2 hours. Cells were sorted by GFP (for the infected populations), and lysates from each population were used to isolate RNA (Materials and Methods). (D) Quantitation of XBP1 splicing from (C). (E) Expression of Lgt3 limits chemically induced XBP1 splicing at late time points. U937 cells were challenged with each strain at an MOI = 1 for 11 hours and treated with DMSO or Tp (100nM) at 9 hours post challenge. RNA isolated from the total cell population was analyzed for XBP1 splicing (Materials and Methods). Data are representative of three independent experiments (A-C, E), or the mean $\pm$ SEM of three independent experiments (D). Statistical analysis performed using unpaired t test * $p<0.05$, *** $p<0.001$

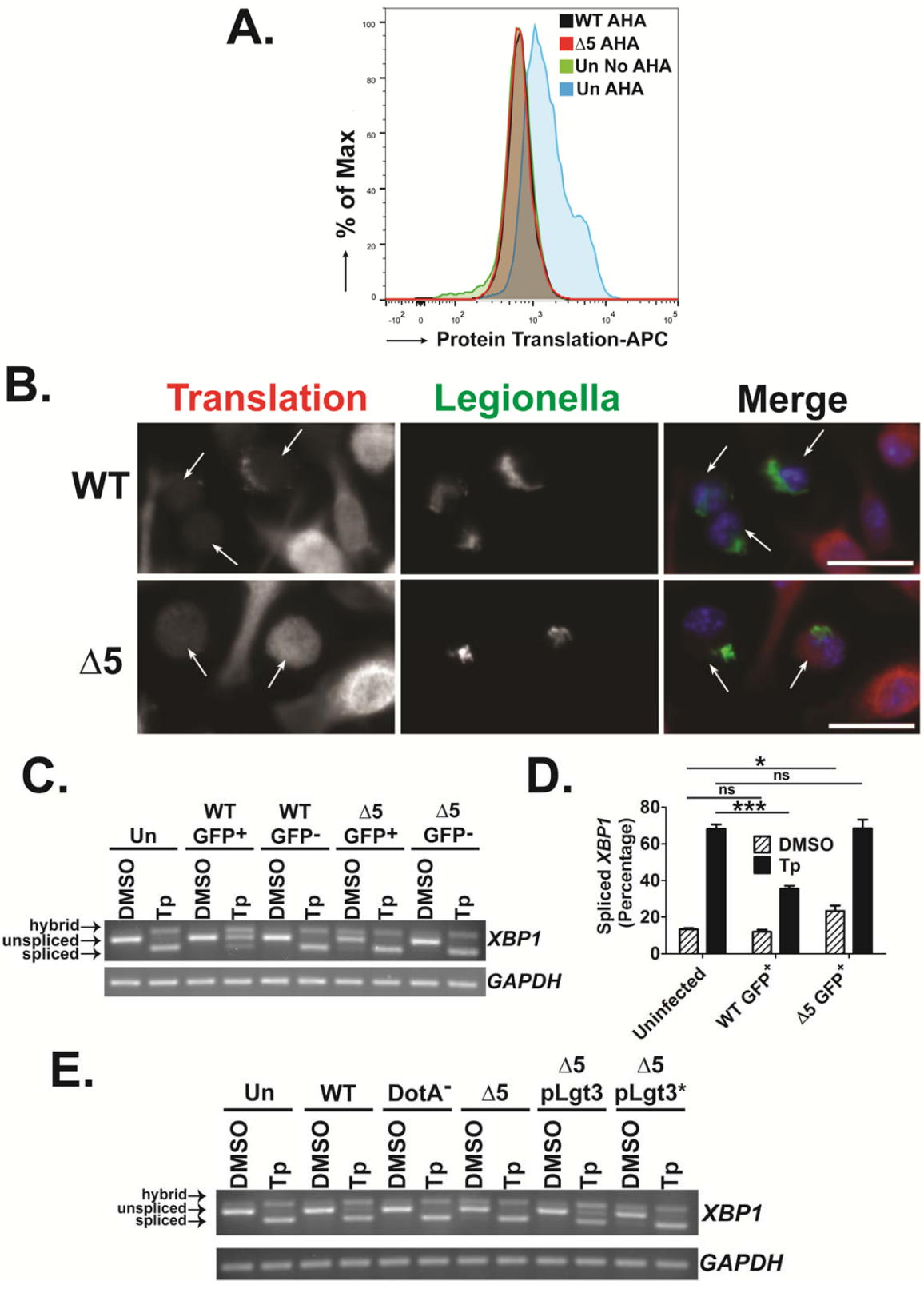
A.
WT AHA
Δ5 AHA
Un No AHA
Un AHA
% of Max
Protein Translation-APC
B.
Translation
Legionella
Merge
WT
Δ5
C.
Un
WT GFP+
WT GFP-
Δ5 GFP+
Δ5 GFP-
DMSO
Tp
hybrid
unspliced
spliced
XBP1
GAPDH
D.
Spliced XBP1 (Percentage)
DMSO
Tp
ns
ns
***
*
Uninfected
WT GFP+
Δ5 GFP+
E.
Un
WT
DotA-
Δ5
Δ5 pLgt3
Δ5 pLgt3*
DMSO
Tp
hybrid
unspliced
spliced
XBP1
GAPDH

strain. Also, at 11 hours post challenge, sorted, WT-challenged cells treated with Tp showed clear evidence of a fully spliced XBP1 message (Figure 3.5C, D).

The presence of spliced message after WT challenge was surprising, given that at earlier time points there was no evidence for this level of XBP1 splicing in WT challenged cells treated with Tp (Figure 3.2A, B) and there was little evidence of host translation occurring in the presence of the WT strain (Figure 3.5A, B). The ability to block XBP1 splicing appears to decay over time in spite of the lack of host protein synthesis. In contrast, interference of XBP1 splicing can be maintained at late time points by expression of an unregulated translation elongation inhibitor (Lgt3) harbored on a plasmid. Therefore, blocking of elongation may be specifically required for limiting the XBP1 arm of the UPR.

3.2.8 Pharmacological inhibition of translation elongation limits both chemically and bacterially induced XBP1 splicing

That a bacterial effector specifically targets translation elongation, and not initiation, to limit XBP1 splicing, indicates elongation blockage may be required to disrupt this arm of the UPR. To determine if we could rescue inhibition of XBP1 splicing in U937 cells challenged with the Δ5 strain, we treated cells with the elongation inhibitor CHX throughout a 4 hour challenge with this strain. Incubation of the Δ5 strain simultaneously with CHX resulted in the inhibition of Tp-induced XBP1 splicing, with greatly reduced amounts of the fully spliced form (Figure 3.6A), consistent with an elongation block being required for blockage of XBP1 splicing. In contrast, treatment

Figure 3.6 Inhibition of translation elongation inhibits chemical and PRR mediated XBP1 splicing (A) U937 cells were challenged with Δ5 at an MOI = 2 for 4 hours in the presence of Tp (100 nM), CHX (2 μg/ml), or Tp+CHX. CHX inhibits Tp-induced XBP1 splicing in uninfected cells and those challenged with the Δ5 strain. (B) Challenge of U937 cells by Δ5 at an MOI = 2 for 4 hours with the addition of Tp (100 nM), rapamycin (100 nM), or rapamycin+Tp. Rapamycin treatment does not inhibit Tp mediated XBP1 splicing. (C) CHX limits XBP1 splicing induced by *L. pneumophila*. U937 cells treated with HKLp or HKEc at an effective MOI = 100, challenged with DotA$^-$ at an MOI = 20, or Δ5 at an MOI = 2, all for 11 hours, were treated with CHX (2 μg/ml) throughout the experiment. Data are representative of two (B) or three (A, C) independent experiments.

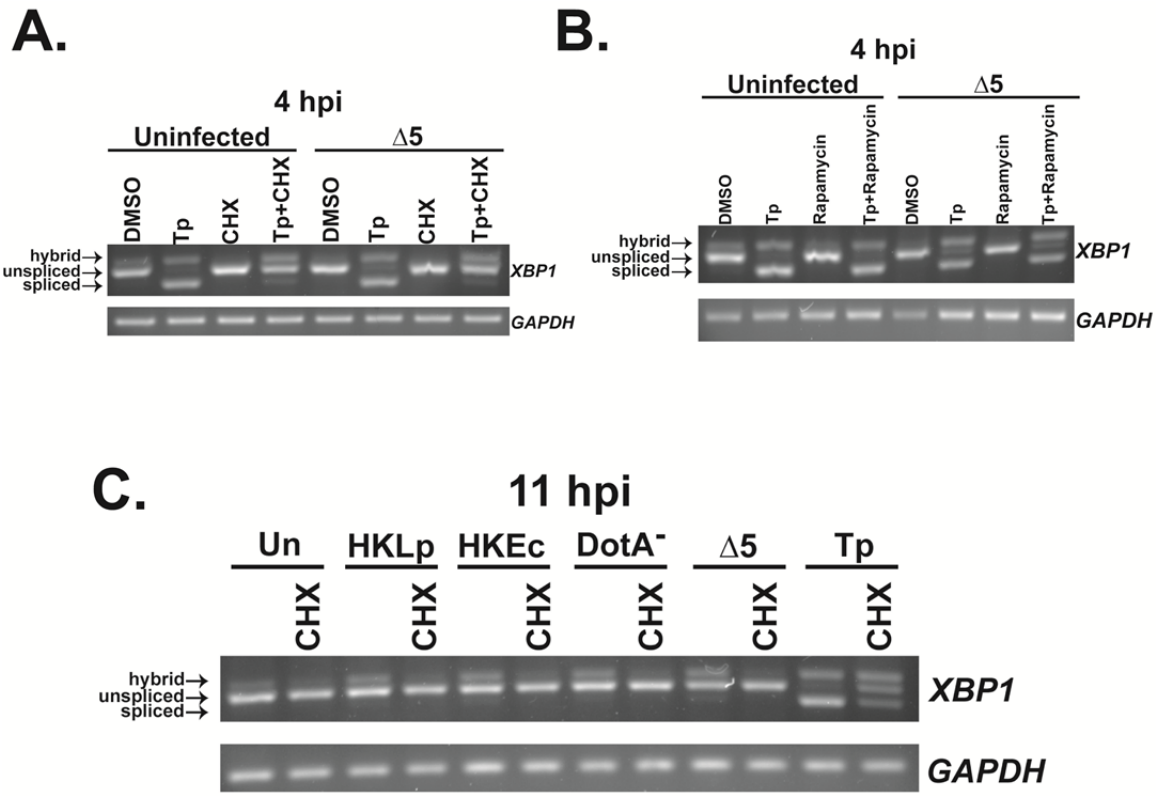
A.
4 hpi
Uninfected
Δ5
DMSO
Tp
CHX
Tp+CHX
DMSO
Tp
CHX
Tp+CHX
hybrid
unspliced
spliced
XBP1
GAPDH
B.
4 hpi
Uninfected
Δ5
DMSO
Tp
Rapamycin
Tp+Rapamycin
DMSO
Tp
Rapamycin
Tp+Rapamycin
hybrid
unspliced
spliced
XBP1
GAPDH
C.
11 hpi
Un
HKLp
HKEc
DotA-
Δ5
Tp
CHX
CHX
CHX
CHX
CHX
CHX
hybrid
unspliced
spliced
XBP1
GAPDH

with rapamycin, which interferes with translation initiation, did not result in the inhibition of Tp-induced XBP1 splicing, either in the presence or absence of the Δ5 strain (Figure 3.6B). Therefore, either the mechanism of translation inhibition plays a critical role in blocking XBP1 splicing, or the high efficiency of CHX translation inhibition, relative to rapamycin (data not shown), is responsible for the block.

While CHX had previously been shown to inhibit chemically induced XBP1 splicing (Yamamoto et al 2011) (Figure 3.6A), it was unknown what effect inhibition of host translation elongation would have on PAMP-induced XBP1 splicing. To determine this, we challenged U937 cells with HKLp, HKEc, DotA$^-$, or the Δ5 strain, for 11 hours, a time point at which Δ5 strain induces XBP1 splicing (Figure 3.5C, D), and determined the effect of CHX treatment. In the absence of CHX, each of these conditions induced XBP1 splicing, as can be seen by the hybrid band. In contrast, CHX completely inhibited XBP1 splicing in all cases (Figure 3.6C). This result is consistent with the lack of induction of XBP1 splicing by WT at 11 hours post challenge, relative to Δ5 challenged cells (Figure 3.5C, D), and shows that inhibition of translation elongation blocks XBP1 splicing induced by varying signals.

3.2.9 Analysis of other UPR pathways during infection

While it was observed that *L. pneumophila* was able to inhibit the IRE1 pathway of the UPR, it was unknown what the effect of *L. pneumophila* challenge would be on ER stress mediated induction of other UPR pathways. To analyze this, induction of the PERK pathway was assayed by determining the levels of eIF2α phosphorylation, which

is induced following activation of the PERK kinase domain (Figure 1.3). This results in the inhibition of translation initiation within the cell. HeLa cells were challenged with WT, DotA$^-$, or Δ5 *L. pneumophila* strains and treated with Tm to induce ER stress. Total cell lysates, analyzed by immunoblot, showed that, unlike what was observed for XBP1 splicing during infection, the WT strain did not inhibit Tm induced eIF2α~P (Figure 3.7A WT Tm). Also surprisingly, WT, but not DotA$^-$ or Δ5, induced eIF2α~P in the absence of Tm treatment (Figure 3.7A), indicating that the WT strain, specifically through the activity of the five translocated translation elongation inhibitors, was inducing this cellular response. Similar results were seen in untreated cells when eIF2α~P levels were analyzed in infected HeLa cells (data not shown), or BMDMs (Figure 3.7 B), by immunoflurorecence microscopy. In cells challenged with the WT strain, there are high levels of eIF2α~P observed in the perinuclear space, which is not seen in cells challenged with DotA$^-$ or Δ5, although the levels seen in Δ5 harboring cells are slightly higher than that observed in DotA$^-$ infected cells.

There are four kinases that induce eIF2α~P in response to varying stimuli: PKR, PERK, HRI, and GCN2 (Raven & Koromilas 2008). To determine if the eIF2α~P observed during challenge was due to PERK activation, WT and PERK$^{-/-}$ MEFs were challenged with the WT and DotA$^-$ *L. pneumophila* strains. In WT MEFs, similar to what was observed in HeLa cells, WT *L. pneumophila*, but not DotA$^-$, induced eIF2α~P in the absence of chemically induced ER stress (Figure 3.7C). In PERK$^{-/-}$ MEFs, the WT strain induced eIF2α~P to levels higher than that seen in either the uninfected or DotA- challenged cells. While eIF2α~P levels are lower than that seen in WT MEFs, this is at least partially due to decreased cell numbers that are observed in slower growing PERK$^{-/-}$

Figure 3.7 *L. pneumophila* induces eIF2α~P but this is independent of PERK activation (A) *L. pneumophila* is does not inhibit chemically induced eIF2α phosphorylation and induces it in the absence of a pharmacological induction of ER stress. HeLa cells were challenged with the indicated strains at an MOI=5 for 1 hour then treated with Tm (2 μg/ml) for 6 additional hours. Lysates were analyzed for eIF2α~P levels by immunoblot. (B) The WT strain induces eIF2α~P specifically in infected cells. BMDMs challenged for 2 hours with WT, DotA$^-$, and Δ5 then analyzed for the levels of eIF2α~P by immunofluorescence microscopy. (C) *L. pneumophila* induction of eIF2α~P does not require PERK signaling. WT and PERK$^{-/-}$ mouse embryonic fibroblasts (MEFs) were challenged with the indicated strains for 2 hours then treated with Tp (500 nM) for 4 additional hours. eIF2α~P levels were determined by immunoblot. Data are a representative image (A, B) or an independent experiment (C).

A.

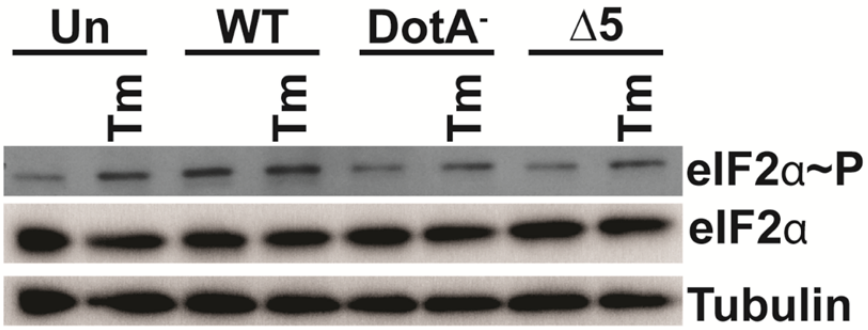
Un
WT
DotA-
Δ5
Tm
Tm
Tm
Tm
eIF2α~P
eIF2α
Tubulin

B.

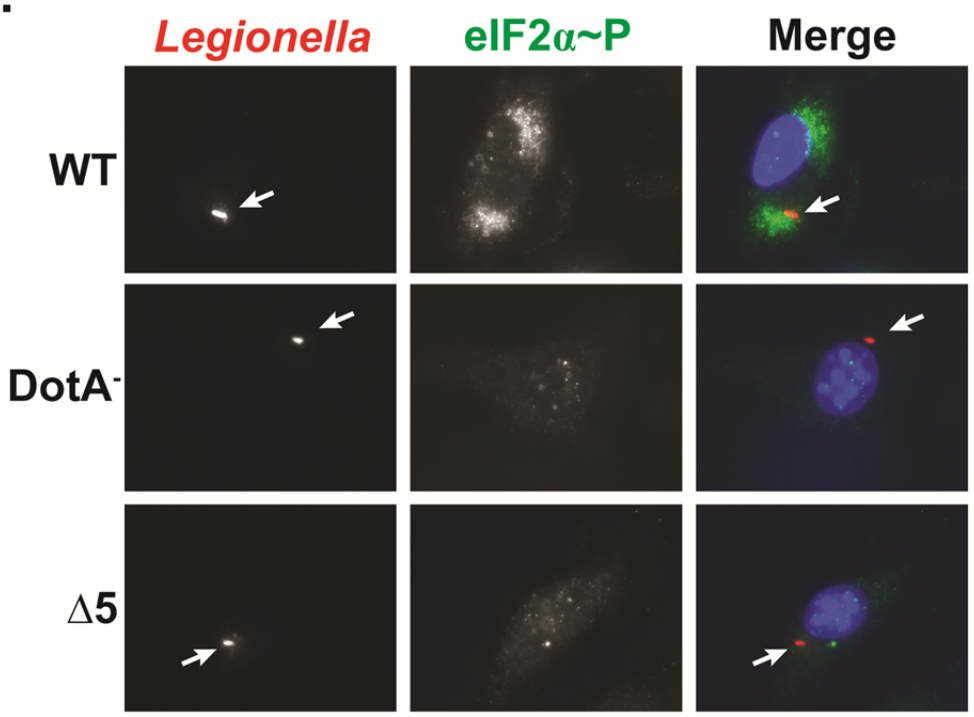
Legionella
eIF2α~P
Merge
WT
DotA-
Δ5

C.

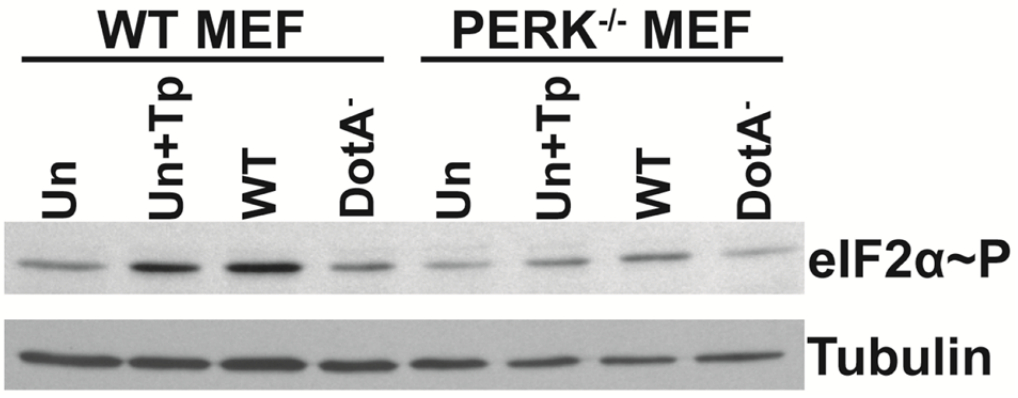
WT MEF
PERK-/- MEF
Un
Un+Tp
WT
DotA-
Un
Un+Tp
WT
DotA-
eIF2α~P
Tubulin

cells, which can be seen by lower Tubulin levels. It is notable that there was also a low level of eIF2α~P in Tp treated PERK$^{-/-}$ cells that is likely due to activation of other eIF2α kinases (Ron Lab communication). These results are consistent with *L. pneumophila* inducing eIF2α~P by a mechanism that is at least partially independent of PERK and points to another kinase playing a role in this cellular response.

Chapter 4: Analysis of an IcmQ mutant deficient in NAD^+ binding

Sections in this chapter were adapted, with permission, from:

Farelli JD, Gumbart JC, Akey IV, Hempstead A, Amyot W, et al. 2013. IcmQ in the Type 4b secretion system contains an NAD+ binding domain. *Structure* 21: 1361-73

4.1 MATERIALS AND METHODS

4.1.1 Plasmid constructions

Plasmids used in this study are described in (Table 4.2). PCR was used to amplify *icmQ* from genomic DNA from Lp01 and Lp01 (*icmQ* D151A) using *Sac*I and *Sal*I tails on the primers (Table 4.3). PCR products were then digested with *Sac*I and *Sal*I, ligated into similarly digested pKB9 (no transcription terminator plasmid), pKB25 (single transcription terminator plasmid), and pKB26 (double transcription terminator plasmid). Plasmids chosen for their IcmQ expression levels were digested with *Apa*I and *Sal*I, and the fragments containing P_{tac}, *rrnB* T1 transcriptional terminators upstream regions and *icmQ* coding sequence were ligated into *Apa*I and *SalI* digested pMMB207Δ267 to generate pIcmQ and pIcmQD151A.

4.1.2 Bacterial growth and cell culture

L. pneumophila strains used in this study are described in (Table 4.1) and were propagated as described in Chapter 2.1.1. To induce IcmQ expression in *L. pneumophila* strains, IPTG was added to a concentration of 1 mM.

Table 4.1: Bacterial strains

Strain	Genotype	Description	Reference
Lp02 (WT)	Philadelphia 1, *thyA rpsL hsdR*	wild type strain	(Berger & Isberg 1993)
GD59	*thyA*, *hsdR*, *rpsL*, *icmQ*	Δ*icmQ*	(Dumenil & Isberg 2001)
Lp01	Philadelphia 1, *rpsL hsdR*	Lp02 progenitor	(Berger & Isberg 1993)
Lp01 *icmQ*(D151A)	Philadelphia 1, *rpsL hsdR, icmQ*(D151A)	IcmQ NAD+ binding mutant	(Farelli et al 2013)

Table 4.2: Plasmids

Plasmid	Genotype	Description	Reference
pKB9	pKB7 , *td*Δ*I, dotA*	DotA expression	(Roy et al 1998)
pKB25	pKB7 , *td*Δ*I*, rrnB T1 transcriptional terminator, *dotA*	Regulated DotA expression	(Roy et al 1998)
pKB26	pKB7 , *td*Δ*I*, rrnB T1 transcriptional terminator (2X), *dotA*	Regulated DotA expression	(Roy et al 1998)
pMMB207Δ267	pMMB207 *mobA*-	cm^R in trans complementation empty vector	(Creasey & Isberg 2012)
pKB26IcmQ	pKB26 *dotA- icmQ*	Regulated IcmQ expression	(Farelli et al 2013)
pKB25IcmQD151A	pKB25 *dotA- icmQ* D151A	Regulated IcmQ D151A expression	(Farelli et al 2013)
pIcmQ	pMMB207Δ267 *rrnB* T1 transcriptional terminator (2X) *icmQ*	Regulated IcmQ expression	(Farelli et al 2013)
pIcmQD151A	pMMB207Δ267 *rrnB* T1 transcritpional terminator *icmQ* D151A	Regulated IcmQ D151A expression	(Farelli et al 2013)

Table 4.3: Oligonucleotides

	Name	Description	Sequence
23	IcmQF	*icmQ* forward	GGGAGCTCTCCCCTAATTCTTGGTTCCCATAAGT
24	IcmQR	*icmQ* reverse	GGGTCGACAACGGCCTATGCATTTTT

Culture of BMDMs and analysis of *L. pneumophila* intracellular replication was performed as described in Chapter 3.1.3. IPTG was added to a concentration of 1 mM during host cell challenge to induce the expression of IcmQ.

4.2 RESULTS

4.2.1 Summary

In this study, the role of NAD^+ binding by the Icm/Dot component IcmQ was analyzed. Initial assays were performed to develop a system that allowed for the equivalent expression of IcmQ and the NAD^+ binding deficient mutant IcmQ(D151A) (Farelli et al 2013). The Δ*icmQ* strains, expressing equivalent levels of the wild type or NAD^+ binding mutant of IcmQ, were then analyzed for their ability to replicate within host cells. This work shows that *L. pneumophila* is able to replicate when expressing only low levels of IcmQ, but also that IcmQ(D151A) is able to support a productive host cell challenge in the absence of binding of NAD^+ by IcmQ.

4.2.2 Rationale

While IcmQ, a component of the Icm/Dot T4SS, is necessary for intracellular replication (Coers et al 2000), little is known about its function. Biochemical studies of the protein revealed that it binds to NAD^+ with high affinity through a scorpion motif (Farelli et al 2013). Furthermore, it has been reported that nicotinic acid, the precursor of NAD^+, plays an important role in inducing the virulence of *L. pneumophila* (Edwards et al 2013). This indicated that NAD^+ may act on IcmQ to regulate its activity and modulate

bacterial virulence. Interestingly, an IcmQ mutant (D151A) that is deficient in NAD^+ binding was relatively unstable when expressed in *L. pneumophila* (Farelli et al 2013), making study of the contribution of NAD^+ binding to bacterial virulence difficult.

4.2.3 Construction of a vector allowing for regulated expression of IcmQ

Previously, constructs had been generated to allow for the regulated expression of *dotA*, an *icm*/*dot* gene required for intracellular replication (Roy et al 1998). These vectors, named pKB9 and pKB25-pKB28 contained 0, 1, 2, 3, or 4 *rrnB* T1 transcriptional terminators (Brosius et al 1981) respectively, upstream of *dotA*. The *dotA* coding sequence in each of these vectors was replaced with that of *icmQ* or *icmQ*(D151A) and these vectors were transformed into the Δ*icmQ* strain. IcmQ expression was analyzed by immunoblot of lysates from post-exponential cultures (Figure 4.1A). Similar levels of IcmQ expression were observed for pKB26IcmQ (two terminators) and pKB25IcmQD151A (one terminator) and these were chosen for further study. Due to issues of these plasmids inducing host cell death due plasmid transfer into the host, the region including Ptac, *rrnB* T1 transcriptional terminators, and *icmQ* was cloned into pMMB207Δ267, which is $mobA^-$, to generate pIcmQ and pIcmQD151A (Figure 4.1B). Expression from these vectors by Δ*icmQ* showed similar levels of IcmQ and IcmQ(D151A), with levels that were approximately 5-10% of that seen for IcmQ expressed by WT (Figure 4.1C).

Figure 4.1 The *IcmQ* (D151A) mutation has no effect on intracellular replication for cells showing matched expression levels of mutant and wild type IcmQ (A) Expression of IcmQ and IcmQ(D151A) from plasmids containing 0, 1, or 2 copies of the *rrnB* T1 transcriptional terminator (pKB9, pKB25, pKB26, respectively) Western blot analysis was performed with anti-IcmQ (Dumenil & Isberg 2001)on whole cell extracts fractionated on 12.5% gels from post-exponential cultures of *L. pneumophila.* (B) Plasmid maps are shown of constructs used to express equivalent low levels of IcmQ and IcmQ (D151A) from the P*tac* promoter. The number of copies of the *rrnB* T1 transcriptional terminator are indicated by black stem loop structures. The double terminator structure used to express wild type protein was necessary to reduce steady state levels to be equivalent to the D151A mutant. (C) Artificial terminators allow identical levels of steady state IcmQ to be obtained in the two constructions as analyzed by Western blot from post-exponential cultures. (D) Efficient replication vacuole formation was observed for *L. pneumophila* having low level expression of IcmQ and the IcmQ (D151A) mutant. Quantitative data for the number of bacteria/vacuole in A/J bone marrow derived macrophages is shown for cells challenged 14 hours with each strain. Data are the mean ± SD of three independent experiments performed in triplicate.

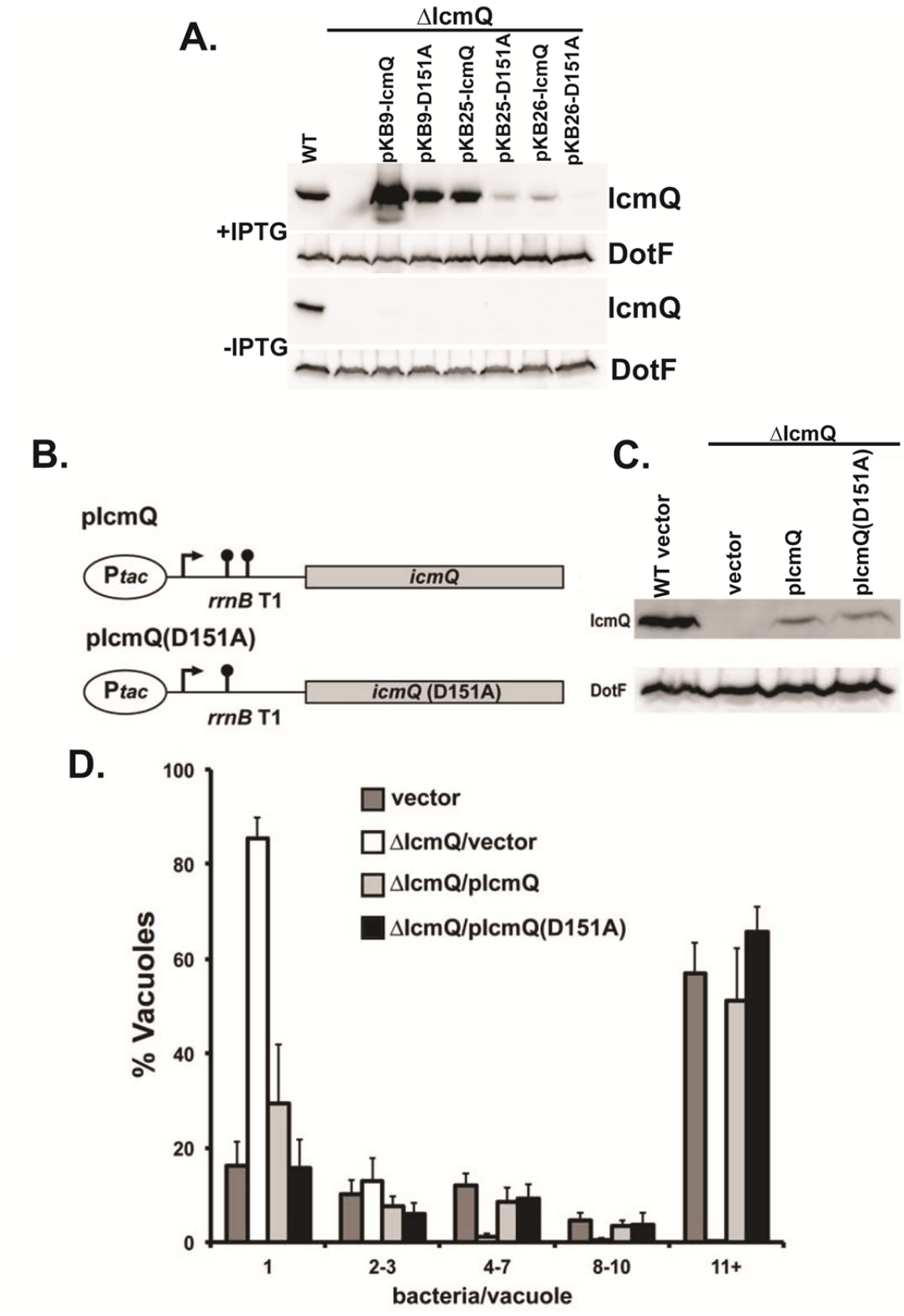
A.
ΔlcmQ
WT
pKB9-lcmQ
pKB9-D151A
pKB25-lcmQ
pKB25-D151A
pKB26-lcmQ
pKB26-D151A
+IPTG
-IPTG
lcmQ
DotF
lcmQ
DotF
B.
plcmQ
Ptac
rrnB T1
icmQ
plcmQ(D151A)
Ptac
rrnB T1
icmQ (D151A)
C.
ΔlcmQ
WT vector
vector
plcmQ
plcmQ(D151A)
lcmQ
DotF
D.
vector
ΔlcmQ/vector
ΔlcmQ/plcmQ
ΔlcmQ/plcmQ(D151A)
% Vacuoles
100
80
60
40
20
0
1
2-3
4-7
8-10
11+
bacteria/vacuole

4.2.4 Analysis of the intracellular replication of Δ*icmQ* expressing equivalent levels of IcmQ or IcmQ(D151A)

The ability of these strains to replicate within BMDMs was analyzed by determining the number of bacteria/vacuole 14 hours post challenge. Δ*icmQ* harboring pIcmQ or pIcmQ(D151A) was able to replicate to levels similar to that of the wild type strain, rescuing the intracellular growth defect of Δ*icmQ* (Figure 4.1D). These results are consistent with levels of IcmQ only ~5-10% of wild type being all that is necessary for replication of *Legionella* in BMDMs. Also, the ability of IcmQ to bind to NAD^+ does not appear to be required for intracellular replication, as IcmQ(D151A) is able to complement the intracellular replication of Δ*icmQ*, if not allow for growth at a slight advantage, when expressed at levels equivalent to wild type IcmQ.

Chapter 5: Discussion and future directions

The following chapter contains text and a figure from a manuscript submitted for publication that is currently under review.

5.1 CHARACTERIZATION OF MAVT AS AN IDTS

5.1.1 Discussion

There are currently ~300 different *L. pneumophila* IDTS that have been identified and experimentally verified by at least one assay (Huang et al 2011, Zhu et al 2011). While the Icm/Dot T4SS is necessary for intracellular replication, the absence of only two IDTS results in the inability of the bacterium to replicate within a host cell (Laguna et al 2006) (Isaac et al submitted), despite many playing roles in functions that are necessary for the bacterium. Characterization of IDTS has given great insight into the pathogenesis of *L. pneumophila* as well as a further understanding of the cell biology of the eukaryotic hosts that it infects (Derre & Isberg 2005, Machner & Isberg 2006, Mukherjee et al 2011).

MavT was initially identified as a substrate of the Icm/Dot T4SS due to the presence of a C-terminal secretion signal, termed an E block motif (Huang et al 2011). Subsequently, full-length MavT, as well as the C-terminal E block containing region, were shown to be translocated in an Icm/Dot dependent manner (Huang et al 2011). While the C-terminal region of MavT alone was translocated (Huang et al 2011), there was an enhancement in the levels of translocation of the full length protein, pointing to other regions of the effector protein that, as has been seen for other IDTS (Jeong et al 2015), are important for translocation.

In this study, we observed that there was no intracellular defect for strains harboring an in-frame deletion of *mavT*, in any host cell type tested. This clarifies previous conflicting reports in which mutants harboring Tn insertions in *mavT* had shown either defective or wild type levels of intracellular replication, within a population of Tn mutants (O'Connor et al 2012) (Foster, unpublished). It is possible that differences in the experimental approach were responsible for the conflicting results, but this study has clarified the requirement of MavT during intracellular replication.

To determine if there might be a minor intracellular defect of the *mavT* mutant, that was not observable during a three day host cell challenge, a long-term competition assay was performed. Surprisingly, this experiment revealed that, during many rounds of intracellular replication in BMDMs, the Δ*mavT* stain was able to outcompete the WT strain. As *mavT* is highly conserved among *Legionella* spp., it appears to be under high levels of selective pressure. Thus, the most likely explanation is that MavT may be required for replication within an alternative host that has not been analyzed. If this model is correct, strains lacking MavT would be unable to replicate to high levels in this host, but in BMDMs, where MavT does not appear to be required, the cost of production of this protein limits bacterial replication. It is likely that replication is only limited during intracellular growth since we did not observe an in vitro growth defect for the Δ*mavT* strain (Figure 2.7A). It is probable that this alternative host would be an environmental host, such as an amoebal host, although we did not observe an intracellular defect of the Δ*mavT* strain in the amoebal species *D. discoideum* or *A. castellanii* (Figure 2.7C, D). In this alternate host, specific manipulation of ER tubules, mitochondria, and/or the Hsp70 chaperone machinery may be required to promote intracellular replication.

While the requirement of MavT within an environmental host is the most likely explanation for its increased replication in BMDMs, there are other potential alternatives. One possibility is that BMDMs may generate a response to this foreign bacterial protein, which may act to limit the bacterium, and in its absence, the bacterium is able to replicate unrestricted. Alternatively, this protein may act to slow replication of the bacterium, which may play an important role in the environment to prevent overgrowth that may not be maintainable in certain habitats.

We identified that MavT contained a functional J domain in its N-terminal region that acted in a similar manner to other known J domains, as mutation of a critical residue within the HPD tripeptide motif inhibited its activity. *E. coli* encodes three J domain proteins that are able to function as Hsp70 cochaperones: DnaJ, DjlA, and CbpA (Genevaux et al 2001), which are also found in *L. pneumophila*. Research has shown that *Legionella* DjlA plays a role in the virulence of the pathogen. In *Legionella dumoffii*, a Tn insertion mutation in *djlA* resulted in a strain that was defective for intracellular replication in macrophage and amoebal cell lines (Ohnishi et al 2004). In *L. pneumophila*, a mutation in *djlA* rescued the Δ*dotL* lethality phenotype that is believed to be due to the production of a toxic subcomplex, indicating that DjlA may play a role in the assembly of the Icm/Dot T4SS (Vincent et al 2006a). Our characterization of MavT has identified an additional *L. pneumophila* J domain protein that, similar to DjlA, may play a role during intracellular replication.

The utilization of J domain effector proteins may be a common virulence mechanism as a J domain translocated effector protein has also been identified in the plant pathogen *Pseudomonas syringae* pv. *maculicola*. This effector, named Hopl1, is

secreted by the T3SS, and contains a C-terminal J domain (Jelenska et al 2007). Similar to MavT, this effector binds to Hsp70 and the J domain shows activity in domain swap experiments (Jelenska et al 2010, Jelenska et al 2007). In eight different plant models of infection, strains lacking Hopl1 show a significant replication defect compared to the wild type strain (Jelenska et al 2010). When expressed in plant cells, Hopl1 localizes to chloroplasts where it induces remodeling of thylakoid structures. As a result, salicylic acid signaling, which initiates from the chloroplasts and is involved in defense against pathogens, is disrupted (Jelenska et al 2007). While the mechanisms of action of MavT and Hopl1 may be very different, it is intriguing that they both induce the reorganization of large membrane bound organelles within the host.

The manipulation of ER structures, especially three-way junctions between tubules, in cells expressing MavT, may point to the role of this effector during intracellular replication. The altered ER morphology, visualized by the localization of Sec61β, that is induced by MavT expression, is reminiscent of what is seen during expression of a dominant negative form of ATL1(ATL1 K80A). Furthermore, expression of WT ATL1, in cells also expressing MavT, does not rescue the altered ER morphology and dramatic decrease in three-way junctions. These results point to MavT either directly inhibiting the activity of ATL1, or indirectly preventing ATL1 from functioning in the formation of three-way junctions. We observed that the ability of MavT to disrupt ER morphology was dependent on an internal hydrophobic region that is responsible for the localization of MavT to the ER, while the N-terminal J domain was largely dispensable for this activity. It is possible that MavT may function to recruit an Hsp70 family member to the ER, through the action of the C-terminal Hsp70 binding domain, where Hsp70 may

act on an ER localized factor to manipulate ER structure. This would be reminiscent of Hopl1, which induces the localization of cytosolic Hsp70 to chloroplasts (Jelenska et al 2010). Alternatively, MavT itself may be acting on ATL1 to limit its ability to induce three-junction formation. This could either be through direct binding of MavT to ATL1, or alternatively that the overexpression of this protein along ER tubules prevents the accumulation of ATL1 at sites destined for three-way junction formation.

In addition to the manipulation of ER structure, when expressed in eukaryotic cells, MavT induced the fragmentation of mitochondria. This phenotype corresponded to the ER manipulation phenotype as only MavT constructs that localized to the ER also showed the induction of mitochondrial fragmentation. This is in contrast to ATL1 K80A which, although it induced a similar ER phenotype, did not appear to induce mitochondrial fragmentation. This may point to the mechanism by which MavT inhibits the formation of three-way junctions occurring through a mechanism independent of the activity of atlastins. Alternatively, the inhibition of three-way junctions may be a byproduct of the activity of MavT on mitochondrial division, a process that takes place along ER tubules.

Fission of mitochondria is accomplished by the dynamin-related GTPase named Drp1 (Bleazard et al 1999, Labrousse et al 1999). Drp1binds to the preconstruction site on mitochondria and oligomerizes to form a spiral around the organelle (Friedman et al 2011, Ingerman et al 2005). Through GTP hydrolysis, the ring constricts, resulting in downstream fission by a yet unknown mechanism (Mears et al 2011). Studies have found that the preconstruction site is marked by ER tubules that wrap around a mitochondrion prior to division (Friedman et al 2011). It has also been shown that an ER localized

formin protein, which is involved in the nucleation and elongation of actin, named INF2-ER, plays a critical role in mitochondrial fission, as its depletion results in elongated mitochondria (Korobova et al 2013). The current model for mitochondrial division at sites of interaction with ER tubules is that at these sites, INF2-ER is activated, resulting in the production of actin filaments. This is followed by the recruitment of myosin, resulting in an actomyosin network surrounding the mitochondrion. Through the activity of myosin, this network constricts, resulting in the preconstruction of mitochondria, which is followed by recruitment of Drp1 by its interaction with actin and receptors on mitochondria (Hatch et al 2014).

There are several potential roles that MavT may play in the induction of mitochondrial fission at ER tubules. One possibility is that MavT may interact with either a factor on mitochondria or Drp1, bringing them in close contact at ER tubule sites to facilitate division. Alternatively, MavT may serve to activate INF2-ER, resulting in overactivation of this factor and driving high levels of actin nucleation and polymerization. It is possible that these mechanisms would be dependent on the localization of Hsp70 to the site of fission as only MavT constructs that colocalize with the ER and bind Hsp70 induce the mitochondrial fission phenotype.

5.1.2 Future directions

While genetic studies have not yet elucidated a role for MavT during intracellular replication, there are several possible activities that would be consistent with our findings using cell biological and biochemical techniques. These include the presence of an N-terminal J domain, a region that binds Hsp70, the manipulation of ER structure, and the

induction of mitochondrial fission. Further research into these observations could yield greater insight into the role of this IDTS during intracellular replication.

As MavT both binds to Hsp70 family members, and contains a functional J domain, it is possible that it may play a role in protein folding within the host. In this role, the C-terminal region of the protein could recruit Hsp70, where its chaperone activity could be activated by the J domain. The proteins targeted for folding by MavT could be either host proteins, that the bacterium relies on during intracellular growth, or alternatively IDTS, after their translocation into the host. As IDTS are translocated in an unfolded state, it is likely that they rely on bacterial or host chaperones for refolding (Amyot et al 2013) of which, MavT may play a role in activating or recruiting. Additional binding studies could be performed to determine if there are factors, in addition to Hsp70, that interact with MavT. This could be performed in both bacterial and eukaryotic lysates to identify either *Legionella* or host binding partners. Additionally, these experiments could be performed with purified MavT, rather than previous experiments in which ectopically expressed proteins were used to identify binding partners through co-immunoprecipitation.

The observation that MavT induces changes in ER morphology shows that MavT may have a direct activity that plays a role in the biogenesis of the LCV. As many IDTS are involved in the recruitment of ER membrane to the LCV, the localization of MavT to the ER may point to its role in this process as well. Other IDTS that are involved in vesicle trafficking appear to be functionally redundant with one another and, as such, this may explain the lack of phenotype for the Δ*mavT* strain. For some IDTS involved in vesicle trafficking, the depletion of a host factor involved in a potentially alternative

pathway of ER membrane recruitment results in an intracellular growth defect (O'Connor et al 2012). Interestingly, in a TraSH selection performed under conditions of depletion of host factors involved in vesicle trafficking, insertions in *mavT* resulted in an enhanced intracellular replication defect, relative to untreated cells (O'Connor et al 2012). Similar experiments could be performed with the in-frame *mavT* deletion strain to determine if during challenge under host cell factor depletion, by methods such as RNAi knockdown or CRISPR-Cas9 mediated knock out (Ran et al 2013), an intracellular growth defect is revealed.

While the role of mitochondria during the intracellular replication is still unclear (Sun et al 2013), their recruitment is one of the characteristics that defines the LCV (Horwitz 1983a). It is possible that MavT may play a role in this recruitment, or act on them in such a way that is beneficial to the bacterium. While MavT induced the fragmentation of mitochondria when expressed in mammalian cells, this could be a product of overexpression, and the activity during infection may be instead to recruit mitochondria to the ER-derived membrane of the LCV. Alternatively, as other effectors have been shown to target the mitochondria (Degtyar et al 2009), MavT may act in conjunction with them to alter mitochondrial function by a yet unknown mechanism. Lastly, as many signaling pathways initiate from the mitochondria, mitochondrial fission, induced by MavT, may alter this signaling, although high levels of mitochondrial fission have not been observed during host cell challenge.

Analysis of the host factors necessary for MavT induced mitochondrial fission may begin to show the mechanism by which it occurs. While Drp1 has been shown to play an important role in mitochondrial fission, Drp1-null MEFs are viable, arguing that

low levels of fission occur in its absence (Loson et al 2013). To determine if MavT induced mitochondrial fission is a Drp1 dependent process, MavT could be expressed in cells either knocked down for *Drp1* or expressing a dominant negative Drp1 construct. If MavT is able to induce fission in the absence of a functional Drp1, it would indicate that MavT plays a direct mechanistic role in mitochondrial fission.

It was observed that constructs of MavT that were recruited to the ER and bound Hsp70 were sufficient for the manipulation of the ER and induction of mitochondrial fission, while a construct that bound Hsp70, but was not recruited to the ER, did not (Figure 2.5A). Currently, a MavT construct that is recruited to the ER, but does not bind to Hsp70 has not been made. It is possible that a deletion of the C-terminus, the region that is sufficient for Hsp70 binding, may show this phenotype. This could help to determine if Hsp70 binding, or only recruitment to the ER, is necessary to induce both ER manipulation and mitochondrial fission. Additionally, the phenotypes of ER localization and manipulation are consistent across each MavT construct. If a mutant could be discovered that showed only one of these phenotypes, it may point to the mechanism by which MavT acts.

5.2 MANIPULATION OF THE HOST CELL UNFOLDED PROTEIN RESPONSE BY *LEGIONELLA PNEUMOPHILA*

5.2.1 Discussion

This study showed that *Legionella* is able to inhibit the activation of the IRE1α branch of the UPR. Inhibition is dependent on the Icm/Dot T4SS, and specifically five IDTS that interfere with host translation elongation. In the absence of these translocated

proteins, *Legionella* induces XBP1 splicing at late time points, even in the absence of a chemically-induced UPR. This is consistent with bacterial-mediated inhibition of host translation elongation blocking XBP1 splicing that results from pathogen detection.

Interference with the host cell UPR during the intracellular replication of bacterial pathogens is an emerging theme in bacterial pathogenesis, as documented previously with viral pathogens (Pavio et al 2003, Tardif et al 2004). A recent report demonstrates that the chlamydial organism *Simkania negevensis*, replicates in a vacuole that is closely associated with the ER and mitochondria (Mehlitz et al 2014), similar to *L. pneumophila*. Interestingly, this pathogen does not induce an ER stress response, and furthermore, is able to inhibit chemically induced activation of UPR pathways, including that of IRE1α (Mehlitz et al 2014). While the mechanism by which *S. negevensis* limits UPR pathways is unknown, it is possible that it may employ an analogous mechanism for limiting UPR through bacterially mediated inhibition of host translation.

Recent studies on the inhibition of host protein translation during *Legionella* challenge have revealed that at least two mechanisms are at play, one mediated by the bacterium, and the other by the host cell (Belyi et al 2006, Fontana et al 2011, Ivanov & Roy 2013). The bacterial-mediated inhibition of translation most notably involves inactivation of elongation factors eEF1A and eEF1Bγ (Belyi et al 2006, Fontana et al 2011, Shen et al 2009). The host response to pathogenic *Legionella* results in the ubiquitination of positive regulators of mTOR, limiting its activity and causing the inhibition of translation initiation (Ivanov & Roy 2013). In a previous study, it was observed that as infection progresses, cells challenged by the Δ5 strain show low levels of protein translation, in spite of the lack of translation elongation inhibitors in this strain

(Asrat et al 2014b). Consistent with that observation, this study showed that levels of protein translation at 11 hours post infection are low after challenge with either the WT or Δ5 strains. Based on these data, it is likely that during the first few hours after infection there is limited global translation in the host cell due to bacterial inhibition of host translation elongation. As the infection proceeds, a second layer of inhibition of protein synthesis occurs as a consequence of host-promoted self-inhibition of translation initiation. It is likely that the bacterial inhibition of elongation is necessary to inhibit XBP1 splicing, as at 9-11 hpi, treatment with Tp strongly induces XBP1 splicing in cells challenged with the Δ5 strain, even though there is little host protein synthesis. Furthermore, the ability of WT *L. pneumophila* to inhibit Tp-induced XBP1 splicing at these later time points appears impaired relative to the more robust inhibition observed just a few hours prior. Expression of Lgt3 harbored on a plasmid reverses this effect at late time points, allowing more robust blockage of Tp-induced XBP1 splicing than observed in WT. This supports the model that the activity of the bacterially-derived elongation inhibitors translocated shortly after formation of the *L. pneumophila* replication vacuole are the primary down-modulators of UPR, while host-mediated translation initiation inhibition is ineffective at interfering with this response.

The ability of CHX to inhibit PAMP-induced XBP1 splicing was surprising, as the mechanism of XBP1 splicing in response to microbial ligands has not been shown to occur via direct induction of luminal ER protein misfolding (Qiu et al 2013). This would be consistent with a model in which microbial ligands, through TLR signaling, cause TRAF6-dependent ubiquitination of IRE1α, allowing for the maintenance of low levels of IRE1α phosphorylation resulting from physiological, or Nox2 mediated, levels of

protein misfolding in the ER (Martinon et al 2010). When translation elongation is blocked, due to CHX treatment, microbial ligands cannot induce XBP1 splicing because there is no misfolding-driven IRE1α phosphorylation in the cell. The ability of wild type *Legionella* to inhibit host protein translation elongation may limit luminal ER protein folding to levels that are insufficient to induce IRE1α phosphorylation (Figure 5.1).

Here, it was observed that *Legionella* was able to replicate to high levels in cells pharmacologically induced to undergo UPR, despite the strong transcriptional upregulation of proinflammatory cytokines under conditions of *L. pneumophila*-derived PAMPs and chemically induced ER stress. Other studies have found that the effects of UPR on intracellular replication is dependent on the pathogen, as chemical induction of the UPR inhibits *Listeria* replication, while induction of the IRE1 pathway supports intracellular replication of *Brucella* (Pillich et al 2012, Qin et al 2008, Smith et al 2013). It is possible that UPR pathways may play a role in limiting *L. pneumophila* replication in their environmental host, amoeba, as the IRE1 branch has been shown to play important roles in the innate immune response in other lower eukaryotes (Richardson et al 2010). Consistent with this hypothesis, the UPR-inducing Δ5 strain is defective for intracellular replication in *D. discoideum* (Fontana et al 2011). *L. pneumophila* antagonism of the UPR likely provides a selective advantage for the bacterium during growth in environmental hosts to counteract this evolutionarily ancient anti-microbial response (Moreno et al 2012, Richardson et al 2010).

Provided by this study is the first mechanism by which a bacterial pathogen inhibits the induction of the IRE1α branch of the UPR. As this response to PRR engagement induces downstream innate immune signaling, and a number of other

Figure 5.1 Model for inhibition of TLR induced XBP1 splicing by inhibition of translation elongation TLR detection of PAMPs induces XBP1 splicing through TRAF6 mediated ubiquitination of IRE1. This inhibits the activity of the phosphatase PP2A, resulting in prolonged IRE1 phosphorylation (Qiu et al 2013). Phosphorylation of IRE1 is likely induced by physiological levels of protein misfolding or TRAF6 mediated induction of Nox2 mediated protein unfolding (Martinon et al 2010). Inhibition of the translation of luminal ER bound proteins by either WT *Legionella* or CHX inhibits low levels of IRE1 phosphorylation resulting in the lack of TLR mediated XBP1 splicing.

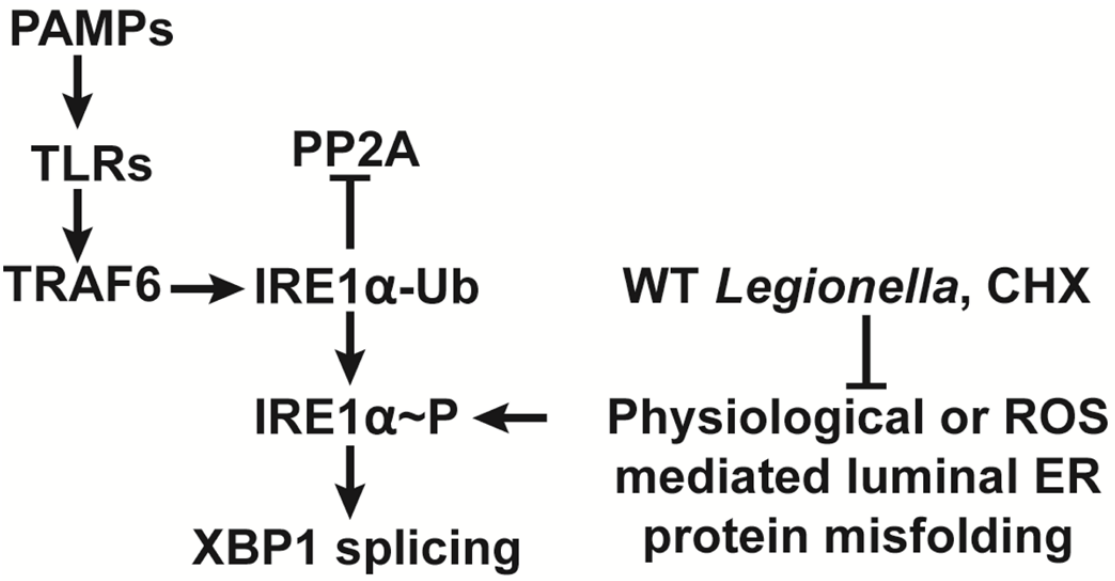
PAMPs
TLRs
TRAF6
PP2A
IRE1α-Ub
IRE1α~P
XBP1 splicing
WT *Legionella*, CHX
Physiological or ROS mediated luminal ER protein misfolding

pathogens similarly interfere with host translation elongation, the mechanism provided here may be a common virulence strategy of pathogens.

5.2.2 Future directions

It was observed that, at late time points, cells challenged by the WT and Δ5 strains showed similar levels of translation. Under these conditions, the Δ5 strain was unable to inhibit a chemically induced splicing, showing that some levels of translation may be occurring in the ER lumen. It is possible that this could be only a few specific proteins, which may not be detectable by global measures of protein translation, that are undergoing folding in the ER lumen during challenge by Δ5. To identify if this is the case and, if so, what these factors are, mass spectrometry could be performed on cells challenged with the WT or Δ5 strains at either early or late time points during infection. This would be combined with treatment of these cells with biotin labeled AHA, which could be immunoprecipitated to identify only proteins that are translated during bacterial challenge. If specific proteins are identified, it would be determined why they are able to overcome the translation block, but only in the absence of the Δ5 effectors. It would be likely that they are translated during blockage of translation initiation, but not elongation, which could be verified using chemical inhibitors.

While the most likely explanation for the lack of inhibition of XBP1 splicing by Δ5 is due to differences in luminal ER translation, if there are no differences in proteins translated during the WT or Δ5 challenges, it is possible that the bacterial translation elongation inhibitors are working by another mechanism. One remaining question is if

WT *Legionella* inhibits IRE1α phosphorylation, which occurs upstream of XBP1 splicing. If it does not, this would indicate that *Legionella* is inhibiting splicing at a step later than the global inhibition of ER protein translation. To determine if IRE1 is phosphorylated during bacterial challenge, a multi-step experiment would need to be performed. Infected cells would need to be sorted under conditions in which dephosphorylation of IRE1α is limited by chemical inhibitors. From the infected cells, IRE1α would then need to be immunoprecipitated and analyzed for phosphorylation by analysis using Phos-tag SDS-PAGE.

If inhibition of IRE1 phosphorylation was not observed, it is possible that the bacterial translation elongation inhibitors may be acting to specifically inhibit the XBP1 splicing step of the IRE1 pathway. It could be that the translation elongation inhibitors are acting directly on the splicing machinery. Intriguingly, while eEF1A is likely the main target of the translocated glucosyltransferases (Lgt1-3), another target, Hbs1, has also been identified (Belyi et al 2009). This factor, in a complex with Dom34, that shows homology to the eukaryotic translation termination factor eRF1, dissociates stalled ribosomes (Shoemaker et al 2010). This results in the endonucleolytic cleavage of the untranslated mRNA in a process known as no-go decay (Doma & Parker 2006). Intriguingly, when ribosome profiling was performed in a *DOM34*Δ or *HBS1*Δ *Saccharomyces cerevisiae* strain, the transcript most highly associated with stalled ribosomes was that of *HAC1* (Guydosh & Green 2014), which encodes the yeast homolog of XBP1. The association of HBS1 with *HAC1* transcript during translational stalling shows that this factor, which is targeted by *L. pneumophila*, plays an important role in the regulation of this mRNA. While there is currently no evidence that this system plays a

role in HAC1 splicing (Guydosh & Green 2014), as DTT induced splicing is unaffected by its absence, there are numerous differences between mammalian XBP1 and yeast HAC1 splicing that may result in the necessity of HBS1 for XBP1 splicing. It is possible that targeting HBS1 by the translocated translation elongation inhibitors may inhibit the endonucleolytic cleavage of this mRNA during XBP1 splicing. This hypothesis could be tested by RNAi knockdown, or CRISPR-Cas9 mediated knockout (Ran et al 2013), of *HBS1*, to determine if it is required for XBP1 splicing in mammalian cells.

5.3 ROLE OF NAD^+ BINDING BY ICMQ

The chaperone/substrate pair IcmQ/IcmR are Icm/Dot components required for the intracellular replication by *L. pneumophila*. The N-terminal region of IcmQ interacts with IcmR, while the C-terminus contains an NAD^+ binding region (Farelli et al 2013). While nicotinic acid, the precursor of NAD^+, has been shown to regulate virulence in *L. pneumophila* (Edwards et al 2013), an intracellular growth defect for the Δ*icmQ* strain expressing IcmQ (D151A), which is defective in NAD^+ binding (Farelli et al 2013), was not observed.

There are many potential explanations for the lack of an intracellular growth defect by strains expressing the NAD^+ binding deficient IcmQ mutant. One possibility is that there may be low levels of NAD^+ bound by this protein when expressed by *Legionella*. As observed by the ability of *L. pneumophila* to replicate during low levels of IcmQ expression, it may be that only a few molecules bound by NAD^+ are necessary for intracellular replication. This would be consistent with the IcmQ (D151A) mutant's low levels (~10%) of NAD^+ binding, relative to the wild type protein, that are observed

during in vitro experiments (Farelli et al 2013). It remains a possibility that NAD^+ binding by IcmQ may not be required for bacterial virulence, though the protein itself is necessary, and NAD^+ binding by IcmQ may play some yet unknown role in another facet of the *L. pneumophila* life cycle.

To address the role of NAD^+ binding by IcmQ during the intracellular replication of *L. pneumophila*, a system was developed to allow for equivalent expression of the wild type and mutant protein that is less stable. This system could be adapted to other *L. pneumophila* proteins to determine what levels of expression are necessary for replication, either in vitro or during host cell challenge. Furthermore, this system could be utilized to generate equivalent levels of wild type and mutant proteins, as was done for IcmQ. As the currently used vector for protein expression in *L. pneumophila* contains a P*tac* promoter, which is not well repressed in *L. pneumophila*, this system could be of great use when regulated levels of protein expression are necessary.

5.4 CONCLUDING REMARKS

The study of the pathogenesis of *L. pneumophila*, and the IDTS it utilizes to manipulate the ER and its signaling pathways, have revealed much about how intracellular pathogens are able to cause disease. The ability of the bacterium to accomplish this results in the construction of an intravacuolar niche that is sequestered away from the dangers of cytosolic innate immune receptors, while also avoiding targeting down the endocytic pathway (Asrat et al 2014a). As the ER also harbors factors important for initiating an immune response, pathogens must also incorporate strategies to overcome this.

In the first part of this study I identified and characterized the IDTS, MavT. When expressed in eukaryotic cells, this factor induces the dramatic reorganization of the ER, as well as causes the fission of mitochondria. It is likely that this activity is dependent on the interaction of MavT with the host cell chaperone machinery as MavT both binds to these factors and encodes a J domain to activate them. While numerous IDTS target the ER, the absence of a single one of these effectors has not been shown to result in an intracellular growth defect, which is likely explained by functional redundancy. As such, Δ*mavT* replicates within hosts at levels similar to WT, which points to MavT playing a role within specific environmental hosts.

In the second part of this study, I showed that *L. pneumophila* was able to inhibit the IRE1α branch of the UPR. The ability of the bacterium to accomplish this was dependent on IDTS that target the host cell translation elongation machinery. This provided the first mechanistic evidence of how a bacterial pathogen is able to block this response. As inhibition of host translation elongation has been observed for a wide variety of pathogens, this may be a common mechanism to block the UPR. Furthermore, *L. pneumophila*, as well as a chemical inhibitor of translation elongation, was able to block TLR induced XBP1 splicing, indicating that pathogens that induce signaling to initiate the response may be able to block its downstream activation. As UPR pathways play an important role in the inflammatory response, understanding how it is manipulated by pathogens will prove essential in efforts to control disease.

These studies have furthered our understanding of the many ways that IDTS manipulate, and interact with, the ER. The activity of these IDTS proteins appears to be broad in span as they also affect processes independent of the ER, through manipulation

of the translation machinery or alterations of mitochondrial structure. This highlights the complexity of the host-bacterium interaction during *L. pneumophila* challenge. Further studies on both MavT and the inhibition of UPR pathways should provide great insight into the mechanisms by which host cells are manipulated to benefit the pathogen.

References

Aachoui Y, Leaf IA, Hagar JA, Fontana MF, Campos CG, et al. 2013. Caspase-11 protects against bacteria that escape the vacuole. *Science* 339: 975-8

Abu Kwaik Y. 1996. The phagosome containing *Legionella pneumophila* within the protozoan *Hartmannella vermiformis* is surrounded by the rough endoplasmic reticulum. *Applied and environmental microbiology* 62: 2022-8

Akazawa Y, Isomoto H, Matsushima K, Kanda T, Minami H, et al. 2013. Endoplasmic reticulum stress contributes to *Helicobacter pylori* VacA-induced apoptosis. *PloS one* 8: e82322

Akira S, Takeda K. 2004. Toll-like receptor signalling. *Nature reviews. Immunology* 4: 499-511

Altman E, Segal G. 2008. The response regulator CpxR directly regulates expression of several *Legionella pneumophila* icm/dot components as well as new translocated substrates. *Journal of bacteriology* 190: 1985-96

Amyot WM, deJesus D, Isberg RR. 2013. Poison domains block transit of translocated substrates via the *Legionella pneumophila* Icm/Dot system. *Infection and immunity* 81: 3239-52

Antonny B, Madden D, Hamamoto S, Orci L, Schekman R. 2001. Dynamics of the COPII coat with GTP and stable analogues. *Nature cell biology* 3: 531-7

Appenzeller-Herzog C, Hauri HP. 2006. The ER-Golgi intermediate compartment (ERGIC): in search of its identity and function. *Journal of cell science* 119: 2173-83

Asrat S, de Jesus DA, Hempstead AD, Ramabhadran V, Isberg RR. 2014a. Bacterial pathogen manipulation of host membrane trafficking. *Annual review of cell and developmental biology* 30: 79-109

Asrat S, Dugan AS, Isberg RR. 2014b. The frustrated host response to *Legionella pneumophila* is bypassed by MyD88-dependent translation of pro-inflammatory cytokines. *PLoS pathogens* 10: e1004229

Bannykh SI, Rowe T, Balch WE. 1996. The organization of endoplasmic reticulum export complexes. *The Journal of cell biology* 135: 19-35

Bardill JP, Miller JL, Vogel JP. 2005. IcmS-dependent translocation of SdeA into macrophages by the *Legionella pneumophila* type IV secretion system. *Molecular microbiology* 56: 90-103

Belyi I, Popoff MR, Cianciotto NP. 2003. Purification and characterization of a UDP-glucosyltransferase produced by *Legionella pneumophila*. *Infection and immunity* 71: 181-6

Belyi Y, Jank T, Aktories K. 2013. Cytotoxic glucosyltransferases of *Legionella pneumophila*. *Current topics in microbiology and immunology* 376: 211-26

Belyi Y, Niggeweg R, Opitz B, Vogelsgesang M, Hippenstiel S, et al. 2006. *Legionella pneumophila* glucosyltransferase inhibits host elongation factor 1A. *Proceedings of the National Academy of Sciences of the United States of America* 103: 16953-8

Belyi Y, Stahl M, Sovkova I, Kaden P, Luy B, Aktories K. 2009. Region of elongation factor 1A1 involved in substrate recognition by *Legionella pneumophila*

glucosyltransferase Lgt1: identification of Lgt1 as a retaining glucosyltransferase. *The Journal of biological chemistry* 284: 20167-74

Bennett JC, Hughes C. 2000. From flagellum assembly to virulence: the extended family of type III export chaperones. *Trends in microbiology* 8: 202-4

Berger KH, Isberg RR. 1993. Two distinct defects in intracellular growth complemented by a single genetic locus in *Legionella pneumophila*. *Molecular microbiology* 7: 7-19

Bertolotti A, Wang X, Novoa I, Jungreis R, Schlessinger K, et al. 2001. Increased sensitivity to dextran sodium sulfate colitis in IRE1beta-deficient mice. *The Journal of clinical investigation* 107: 585-93

Bertolotti A, Zhang Y, Hendershot LM, Harding HP, Ron D. 2000. Dynamic interaction of BiP and ER stress transducers in the unfolded-protein response. *Nature cell biology* 2: 326-32

Bielli A, Haney CJ, Gabreski G, Watkins SC, Bannykh SI, Aridor M. 2005. Regulation of Sar1 NH2 terminus by GTP binding and hydrolysis promotes membrane deformation to control COPII vesicle fission. *The Journal of cell biology* 171: 919-24

Bleazard W, McCaffery JM, King EJ, Bale S, Mozdy A, et al. 1999. The dynamin-related GTPase Dnm1 regulates mitochondrial fission in yeast. *Nature cell biology* 1: 298-304

Boschiroli ML, Ouahrani-Bettache S, Foulongne V, Michaux-Charachon S, Bourg G, et al. 2002. The *Brucella suis* virB operon is induced intracellularly in macrophages. *Proceedings of the National Academy of Sciences of the United States of America* 99: 1544-9

Brosius J, Ullrich A, Raker MA, Gray A, Dull TJ, et al. 1981. Construction and fine mapping of recombinant plasmids containing the *rrnB* ribosomal RNA operon of *E. coli*. *Plasmid* 6: 112-8

Bruckert WM, Abu Kwaik Y. 2015. Complete and Ubiquitinated Proteome of the *Legionella*-Containing Vacuole within Human Macrophages. *Journal of proteome research* 14: 236-48

Burstein D, Zusman T, Degtyar E, Viner R, Segal G, Pupko T. 2009. Genome-scale identification of *Legionella pneumophila* effectors using a machine learning approach. *PLoS pathogens* 5: e1000508

Buscher BA, Conover GM, Miller JL, Vogel SA, Meyers SN, et al. 2005. The DotL protein, a member of the TraG-coupling protein family, is essential for Viability of *Legionella pneumophila* strain Lp02. *Journal of bacteriology* 187: 2927-38

Cambronne ED, Roy CR. 2007. The *Legionella pneumophila* IcmSW complex interacts with multiple Dot/Icm effectors to facilitate type IV translocation. *PLoS pathogens* 3: e188

Campbell KS, Mullane KP, Aksoy IA, Stubdal H, Zalvide J, et al. 1997. DnaJ/hsp40 chaperone domain of SV40 large T antigen promotes efficient viral DNA replication. *Genes & development* 11: 1098-110

Celli J, Salcedo SP, Gorvel JP. 2005. Brucella coopts the small GTPase Sar1 for intracellular replication. *Proceedings of the National Academy of Sciences of the United States of America* 102: 1673-8

Celli J, Tsolis RM. 2015. Bacteria, the endoplasmic reticulum and the unfolded protein response: friends or foes? *Nature reviews. Microbiology* 13: 71-82

Chen J, Reyes M, Clarke M, Shuman HA. 2007. Host cell-dependent secretion and translocation of the LepA and LepB effectors of *Legionella pneumophila*. *Cellular microbiology* 9: 1660-71

Chen X, Shen J, Prywes R. 2002. The luminal domain of ATF6 senses endoplasmic reticulum (ER) stress and causes translocation of ATF6 from the ER to the Golgi. *The Journal of biological chemistry* 277: 13045-52

Cho JA, Lee AH, Platzer B, Cross BC, Gardner BM, et al. 2013. The unfolded protein response element IRE1alpha senses bacterial proteins invading the ER to activate RIG-I and innate immune signaling. *Cell host & microbe* 13: 558-69

Clausen JD, Christiansen G, Holst HU, Birkelund S. 1997. *Chlamydia trachomatis* utilizes the host cell microtubule network during early events of infection. *Molecular microbiology* 25: 441-9

Coers J, Kagan JC, Matthews M, Nagai H, Zuckman DM, Roy CR. 2000. Identification of Icm protein complexes that play distinct roles in the biogenesis of an organelle permissive for *Legionella pneumophila* intracellular growth. *Molecular microbiology* 38: 719-36

Coers J, Vance RE, Fontana MF, Dietrich WF. 2007. Restriction of *Legionella pneumophila* growth in macrophages requires the concerted action of cytokine and Naip5/Ipaf signalling pathways. *Cellular microbiology* 9: 2344-57

Colbert RA, DeLay ML, Klenk EI, Layh-Schmitt G. 2010. From HLA-B27 to spondyloarthritis: a journey through the ER. *Immunological reviews* 233: 181-202

Creasey EA, Isberg RR. 2012. The protein SdhA maintains the integrity of the *Legionella*-containing vacuole. *Proceedings of the National Academy of Sciences of the United States of America* 109: 3481-6

de Felipe KS, Pampou S, Jovanovic OS, Pericone CD, Ye SF, et al. 2005. Evidence for acquisition of *Legionella* type IV secretion substrates via interdomain horizontal gene transfer. *Journal of bacteriology* 187: 7716-26

de Jong MF, Starr T, Winter MG, den Hartigh AB, Child R, et al. 2013. Sensing of bacterial type IV secretion via the unfolded protein response. *mBio* 4: e00418-12

Degtyar E, Zusman T, Ehrlich M, Segal G. 2009. A *Legionella* effector acquired from protozoa is involved in sphingolipids metabolism and is targeted to the host cell mitochondria. *Cellular microbiology* 11: 1219-35

Deng W, Chen L, Peng WT, Liang X, Sekiguchi S, et al. 1999. VirE1 is a specific molecular chaperone for the exported single-stranded-DNA-binding protein VirE2 in *Agrobacterium*. *Molecular microbiology* 31: 1795-807

Dennis PJ, Brenner DJ, Thacker WL, Wait R, Vesey G, et al. 1993. Five new *Legionella* species isolated from water. *International journal of systematic bacteriology* 43: 329-37

Derre I, Isberg RR. 2004. *Legionella pneumophila* replication vacuole formation involves rapid recruitment of proteins of the early secretory system. *Infection and immunity* 72: 3048-53

Derre I, Isberg RR. 2005. LidA, a translocated substrate of the *Legionella pneumophila* type IV secretion system, interferes with the early secretory pathway. *Infection and immunity* 73: 4370-80

Derre I, Swiss R, Agaisse H. 2011. The lipid transfer protein CERT interacts with the *Chlamydia* inclusion protein IncD and participates to ER-*Chlamydia* inclusion membrane contact sites. *PLoS pathogens* 7: e1002092

Dever TE, Green R. 2012. The elongation, termination, and recycling phases of translation in eukaryotes. *Cold Spring Harbor perspectives in biology* 4: a013706

Doma MK, Parker R. 2006. Endonucleolytic cleavage of eukaryotic mRNAs with stalls in translation elongation. *Nature* 440: 561-4

Dorer MS, Kirton D, Bader JS, Isberg RR. 2006. RNA interference analysis of *Legionella* in *Drosophila* cells: exploitation of early secretory apparatus dynamics. *PLoS pathogens* 2: e34

Dumenil G, Isberg RR. 2001. The *Legionella pneumophila* IcmR protein exhibits chaperone activity for IcmQ by preventing its participation in high-molecular-weight complexes. *Molecular microbiology* 40: 1113-27

Dumenil G, Montminy TP, Tang M, Isberg RR. 2004. IcmR-regulated membrane insertion and efflux by the *Legionella pneumophila* IcmQ protein. *The Journal of biological chemistry* 279: 4686-95

Edelstein PH. 1995. Antimicrobial chemotherapy for legionnaires' disease: a review. *Clinical infectious diseases : an official publication of the Infectious Diseases Society of America* 21 Suppl 3: S265-76

Edwards RL, Bryan A, Jules M, Harada K, Buchrieser C, Swanson MS. 2013. Nicotinic acid modulates *Legionella pneumophila* gene expression and induces virulence traits. *Infection and immunity* 81: 945-55

Fan CY, Lee S, Cyr DM. 2003. Mechanisms for regulation of Hsp70 function by Hsp40. *Cell stress & chaperones* 8: 309-16

Farelli JD, Gumbart JC, Akey IV, Hempstead A, Amyot W, et al. 2013. IcmQ in the Type 4b secretion system contains an NAD^+ binding domain. *Structure* 21: 1361-73

Feeley JC, Gibson RJ, Gorman GW, Langford NC, Rasheed JK, et al. 1979. Charcoal-yeast extract agar: primary isolation medium for *Legionella pneumophila*. *Journal of clinical microbiology* 10: 437-41

Feldman M, Segal G. 2004. A specific genomic location within the icm/dot pathogenesis region of different *Legionella* species encodes functionally similar but nonhomologous virulence proteins. *Infection and immunity* 72: 4503-11

Feldman M, Zusman T, Hagag S, Segal G. 2005. Coevolution between nonhomologous but functionally similar proteins and their conserved partners in the *Legionella* pathogenesis system. *Proceedings of the National Academy of Sciences of the United States of America* 102: 12206-11

Fernandez RC, Lee SH, Haldane D, Sumarah R, Rozee KR. 1989. Plaque assay for virulent *Legionella pneumophila*. *Journal of clinical microbiology* 27: 1961-4

Fields BS. 1996. The molecular ecology of legionellae. *Trends in microbiology* 4: 286-90

Fields BS, Barbaree JM, Sanden GN, Morrill WE. 1990. Virulence of a *Legionella anisa* strain associated with Pontiac fever: an evaluation using protozoan, cell culture, and guinea pig models. *Infection and immunity* 58: 3139-42

Fields BS, Benson RF, Besser RE. 2002. *Legionella* and Legionnaires' disease: 25 years of investigation. *Clinical microbiology reviews* 15: 506-26

Fingar DC, Blenis J. 2004. Target of rapamycin (TOR): an integrator of nutrient and growth factor signals and coordinator of cell growth and cell cycle progression. *Oncogene* 23: 3151-71

Folly-Klan M, Alix E, Stalder D, Ray P, Duarte LV, et al. 2013. A novel membrane sensor controls the localization and ArfGEF activity of bacterial RalF. *PLoS pathogens* 9: e1003747

Fontana MF, Banga S, Barry KC, Shen X, Tan Y, et al. 2011. Secreted bacterial effectors that inhibit host protein synthesis are critical for induction of the innate immune response to virulent *Legionella pneumophila*. *PLoS pathogens* 7: e1001289

Fontana MF, Shin S, Vance RE. 2012. Activation of host mitogen-activated protein kinases by secreted *Legionella pneumophila* effectors that inhibit host protein translation. *Infection and immunity* 80: 3570-5

Fourie AM, Sambrook JF, Gething MJ. 1994. Common and divergent peptide binding specificities of hsp70 molecular chaperones. *The Journal of biological chemistry* 269: 30470-8

Fraser DW. 2005. The challenges were legion. *The Lancet. Infectious diseases* 5: 237-41

Friedman JR, Lackner LL, West M, DiBenedetto JR, Nunnari J, Voeltz GK. 2011. ER tubules mark sites of mitochondrial division. *Science* 334: 358-62

Frolova L, Le Goff X, Zhouravleva G, Davydova E, Philippe M, Kisselev L. 1996. Eukaryotic polypeptide chain release factor eRF3 is an eRF1- and ribosome-dependent guanosine triphosphatase. *Rna* 2: 334-41

Fugier E, Salcedo SP, de Chastellier C, Pophillat M, Muller A, et al. 2009. The glyceraldehyde-3-phosphate dehydrogenase and the small GTPase Rab 2 are crucial for *Brucella* replication. *PLoS pathogens* 5: e1000487

Gardner BM, Walter P. 2011. Unfolded proteins are Ire1-activating ligands that directly induce the unfolded protein response. *Science* 333: 1891-4

Genevaux P, Wawrzynow A, Zylicz M, Georgopoulos C, Kelley WL. 2001. DjlA is a third DnaK co-chaperone of *Escherichia coli*, and DjlA-mediated induction of colanic acid capsule requires DjlA-DnaK interaction. *The Journal of biological chemistry* 276: 7906-12

Gerace L, Burke B. 1988. Functional organization of the nuclear envelope. *Annual review of cell biology* 4: 335-74

Gingras AC, Gygi SP, Raught B, Polakiewicz RD, Abraham RT, et al. 1999. Regulation of 4E-BP1 phosphorylation: a novel two-step mechanism. *Genes & development* 13: 1422-37

Glick TH, Gregg MB, Berman B, Mallison G, Rhodes WW, Jr., Kassanoff I. 1978. Pontiac fever. An epidemic of unknown etiology in a health department: I. Clinical and epidemiologic aspects. *American journal of epidemiology* 107: 149-60

Glimcher LH. 2010. XBP1: the last two decades. *Annals of the rheumatic diseases* 69 Suppl 1: i67-71

Goodall JC, Wu C, Zhang Y, McNeill L, Ellis L, et al. 2010. Endoplasmic reticulum stress-induced transcription factor, CHOP, is crucial for dendritic cell IL-23 expression. *Proceedings of the National Academy of Sciences of the United States of America* 107: 17698-703

Guydosh NR, Green R. 2014. Dom34 rescues ribosomes in 3' untranslated regions. *Cell* 156: 950-62
Hackstadt T. 2000. Redirection of host vesicle trafficking pathways by intracellular parasites. *Traffic* 1: 93-9
Halic M, Gartmann M, Schlenker O, Mielke T, Pool MR, et al. 2006. Signal recognition particle receptor exposes the ribosomal translocon binding site. *Science* 312: 745-7
Han D, Lerner AG, Vande Walle L, Upton JP, Xu W, et al. 2009. IRE1alpha kinase activation modes control alternate endoribonuclease outputs to determine divergent cell fates. *Cell* 138: 562-75
Hardiman CA, Roy CR. 2014. AMPylation is critical for Rab1 localization to vacuoles containing *Legionella pneumophila*. *mBio* 5: e01035-13
Harding HP, Zhang Y, Ron D. 1999. Protein translation and folding are coupled by an endoplasmic-reticulum-resident kinase. *Nature* 397: 271-4
Harding HP, Zhang Y, Zeng H, Novoa I, Lu PD, et al. 2003. An integrated stress response regulates amino acid metabolism and resistance to oxidative stress. *Molecular cell* 11: 619-33
Hatch AL, Gurel PS, Higgs HN. 2014. Novel roles for actin in mitochondrial fission. *Journal of cell science* 127: 4549-60
Hay N, Sonenberg N. 2004. Upstream and downstream of mTOR. *Genes & development* 18: 1926-45
Haze K, Yoshida H, Yanagi H, Yura T, Mori K. 1999. Mammalian transcription factor ATF6 is synthesized as a transmembrane protein and activated by proteolysis in response to endoplasmic reticulum stress. *Molecular biology of the cell* 10: 3787-99
Heazlewood CK, Cook MC, Eri R, Price GR, Tauro SB, et al. 2008. Aberrant mucin assembly in mice causes endoplasmic reticulum stress and spontaneous inflammation resembling ulcerative colitis. *PLoS medicine* 5: e54
Hebert DN, Foellmer B, Helenius A. 1995. Glucose trimming and reglucosylation determine glycoprotein association with calnexin in the endoplasmic reticulum. *Cell* 81: 425-33
Hobman TC, Zhao B, Chan H, Farquhar MG. 1998. Immunoisolation and characterization of a subdomain of the endoplasmic reticulum that concentrates proteins involved in COPII vesicle biogenesis. *Molecular biology of the cell* 9: 1265-78
Hollien J, Lin JH, Li H, Stevens N, Walter P, Weissman JS. 2009. Regulated Ire1-dependent decay of messenger RNAs in mammalian cells. *The Journal of cell biology* 186: 323-31
Hollien J, Weissman JS. 2006. Decay of endoplasmic reticulum-localized mRNAs during the unfolded protein response. *Science* 313: 104-7
Horwitz MA. 1983a. Formation of a novel phagosome by the Legionnaires' disease bacterium (*Legionella pneumophila*) in human monocytes. *The Journal of experimental medicine* 158: 1319-31
Horwitz MA. 1983b. The Legionnaires' disease bacterium (*Legionella pneumophila*) inhibits phagosome-lysosome fusion in human monocytes. *The Journal of experimental medicine* 158: 2108-26

Hosokawa N, Wada I, Hasegawa K, Yorihuzi T, Tremblay LO, et al. 2001. A novel ER alpha-mannosidase-like protein accelerates ER-associated degradation. *EMBO reports* 2: 415-22

Hu J, Shibata Y, Zhu PP, Voss C, Rismanchi N, et al. 2009. A class of dynamin-like GTPases involved in the generation of the tubular ER network. *Cell* 138: 549-61

Hu P, Han Z, Couvillon AD, Kaufman RJ, Exton JH. 2006. Autocrine tumor necrosis factor alpha links endoplasmic reticulum stress to the membrane death receptor pathway through IRE1α-mediated NF-kappaB activation and down-regulation of TRAF2 expression. *Molecular and cellular biology* 26: 3071-84

Huang L, Boyd D, Amyot WM, Hempstead AD, Luo ZQ, et al. 2011. The E Block motif is associated with *Legionella pneumophila* translocated substrates. *Cellular microbiology* 13: 227-45

Ingerman E, Perkins EM, Marino M, Mears JA, McCaffery JM, et al. 2005. Dnm1 forms spirals that are structurally tailored to fit mitochondria. *The Journal of cell biology* 170: 1021-7

Ingmundson A, Delprato A, Lambright DG, Roy CR. 2007. Legionella pneumophila proteins that regulate Rab1 membrane cycling. *Nature* 450: 365-9

Ivanov SS, Roy CR. 2013. Pathogen signatures activate a ubiquitination pathway that modulates the function of the metabolic checkpoint kinase mTOR. *Nature immunology* 14: 1219-28

Jackson CL, Casanova JE. 2000. Turning on ARF: the Sec7 family of guanine-nucleotide-exchange factors. *Trends in cell biology* 10: 60-7

Jakob CA, Bodmer D, Spirig U, Battig P, Marcil A, et al. 2001. Htm1p, a mannosidase-like protein, is involved in glycoprotein degradation in yeast. *EMBO reports* 2: 423-30

Jelenska J, van Hal JA, Greenberg JT. 2010. *Pseudomonas syringae* hijacks plant stress chaperone machinery for virulence. *Proceedings of the National Academy of Sciences of the United States of America* 107: 13177-82

Jelenska J, Yao N, Vinatzer BA, Wright CM, Brodsky JL, Greenberg JT. 2007. A J domain virulence effector of *Pseudomonas syringae* remodels host chloroplasts and suppresses defenses. *Current biology : CB* 17: 499-508

Jeong KC, Sutherland MC, Vogel JP. 2015. Novel export control of a *Legionella* Dot/Icm substrate is mediated by dual, independent signal sequences. *Molecular microbiology* 96: 175-88

Kagan JC, Roy CR. 2002. *Legionella* phagosomes intercept vesicular traffic from endoplasmic reticulum exit sites. *Nature cell biology* 4: 945-54

Kagan JC, Stein MP, Pypaert M, Roy CR. 2004. Legionella subvert the functions of Rab1 and Sec22b to create a replicative organelle. *The Journal of experimental medicine* 199: 1201-11

Kaneko M, Niinuma Y, Nomura Y. 2003. Activation signal of nuclear factor-kappa B in response to endoplasmic reticulum stress is transduced via IRE1 and tumor necrosis factor receptor-associated factor 2. *Biological & pharmaceutical bulletin* 26: 931-5

Karin M. 1995. The regulation of AP-1 activity by mitogen-activated protein kinases. *The Journal of biological chemistry* 270: 16483-6

Kelley LA, Sternberg MJ. 2009. Protein structure prediction on the Web: a case study using the Phyre server. *Nature protocols* 4: 363-71

Kelley WL, Georgopoulos C. 1997. The T/t common exon of simian virus 40, JC, and BK polyomavirus T antigens can functionally replace the J-domain of the *Escherichia coli* DnaJ molecular chaperone. *Proceedings of the National Academy of Sciences of the United States of America* 94: 3679-84

Kim PK, Mullen RT, Schumann U, Lippincott-Schwartz J. 2006. The origin and maintenance of mammalian peroxisomes involves a de novo PEX16-dependent pathway from the ER. *The Journal of cell biology* 173: 521-32

Kolter R, Inuzuka M, Helinski DR. 1978. Trans-complementation-dependent replication of a low molecular weight origin fragment from plasmid R6K. *Cell* 15: 1199-208

Korobova F, Ramabhadran V, Higgs HN. 2013. An actin-dependent step in mitochondrial fission mediated by the ER-associated formin INF2. *Science* 339: 464-7

Kubori T, Hyakutake A, Nagai H. 2008. *Legionella* translocates an E3 ubiquitin ligase that has multiple U-boxes with distinct functions. *Molecular microbiology* 67: 1307-19

Kubori T, Koike M, Bui XT, Higaki S, Aizawa S, Nagai H. 2014. Native structure of a type IV secretion system core complex essential for *Legionella* pathogenesis. *Proceedings of the National Academy of Sciences of the United States of America* 111: 11804-9

Labrousse AM, Zappaterra MD, Rube DA, van der Bliek AM. 1999. *C. elegans* dynamin-related protein DRP-1 controls severing of the mitochondrial outer membrane. *Molecular cell* 4: 815-26

Laguna RK, Creasey EA, Li Z, Valtz N, Isberg RR. 2006. A *Legionella pneumophila*-translocated substrate that is required for growth within macrophages and protection from host cell death. *Proceedings of the National Academy of Sciences of the United States of America* 103: 18745-50

Lam SK, Yoda N, Schekman R. 2010. A vesicle carrier that mediates peroxisome protein traffic from the endoplasmic reticulum. *Proceedings of the National Academy of Sciences of the United States of America* 107: 21523-8

Lazinski DW, Camilli A. 2013. Homopolymer tail-mediated ligation PCR: a streamlined and highly efficient method for DNA cloning and library construction. *BioTechniques* 54: 25-34

Lederkremer GZ, Cheng Y, Petre BM, Vogan E, Springer S, et al. 2001. Structure of the Sec23p/24p and Sec13p/31p complexes of COPII. *Proceedings of the National Academy of Sciences of the United States of America* 98: 10704-9

Lee AH, Iwakoshi NN, Glimcher LH. 2003. XBP-1 regulates a subset of endoplasmic reticulum resident chaperone genes in the unfolded protein response. *Molecular and cellular biology* 23: 7448-59

Lee MC, Orci L, Hamamoto S, Futai E, Ravazzola M, Schekman R. 2005. Sar1p N-terminal helix initiates membrane curvature and completes the fission of a COPII vesicle. *Cell* 122: 605-17

Lee SY, Lee MS, Cherla RP, Tesh VL. 2008. Shiga toxin 1 induces apoptosis through the endoplasmic reticulum stress response in human monocytic cells. *Cellular microbiology* 10: 770-80

Li Q, Verma IM. 2002. NF-kappaB regulation in the immune system. *Nature reviews. Immunology* 2: 725-34

Liu Y, Luo ZQ. 2007. The *Legionella pneumophila* effector SidJ is required for efficient recruitment of endoplasmic reticulum proteins to the bacterial phagosome. *Infection and immunity* 75: 592-603

Loson OC, Song Z, Chen H, Chan DC. 2013. Fis1, Mff, MiD49, and MiD51 mediate Drp1 recruitment in mitochondrial fission. *Molecular biology of the cell* 24: 659-67

Lu Y, Liang FX, Wang X. 2014. A synthetic biology approach identifies the mammalian UPR RNA ligase RtcB. *Molecular cell* 55: 758-70

Luo ZQ, Isberg RR. 2004. Multiple substrates of the *Legionella pneumophila* Dot/Icm system identified by interbacterial protein transfer. *Proceedings of the National Academy of Sciences of the United States of America* 101: 841-6

Ma K, Vattem KM, Wek RC. 2002. Dimerization and release of molecular chaperone inhibition facilitate activation of eukaryotic initiation factor-2 kinase in response to endoplasmic reticulum stress. *The Journal of biological chemistry* 277: 18728-35

Machner MP, Isberg RR. 2006. Targeting of host Rab GTPase function by the intravacuolar pathogen *Legionella pneumophila*. *Developmental cell* 11: 47-56

Machner MP, Isberg RR. 2007. A bifunctional bacterial protein links GDI displacement to Rab1 activation. *Science* 318: 974-7

Marra A, Blander SJ, Horwitz MA, Shuman HA. 1992. Identification of a *Legionella pneumophila* locus required for intracellular multiplication in human macrophages. *Proceedings of the National Academy of Sciences of the United States of America* 89: 9607-11

Marston BJ, Lipman HB, Breiman RF. 1994. Surveillance for Legionnaires' disease. Risk factors for morbidity and mortality. *Archives of internal medicine* 154: 2417-22

Martinon F, Chen X, Lee AH, Glimcher LH. 2010. TLR activation of the transcription factor XBP1 regulates innate immune responses in macrophages. *Nature immunology* 11: 411-8

Maurel M, Chevet E, Tavernier J, Gerlo S. 2014. Getting RIDD of RNA: IRE1 in cell fate regulation. *Trends in biochemical sciences* 39: 245-54

McCullough KD, Martindale JL, Klotz LO, Aw TY, Holbrook NJ. 2001. Gadd153 sensitizes cells to endoplasmic reticulum stress by down-regulating Bcl2 and perturbing the cellular redox state. *Molecular and cellular biology* 21: 1249-59

McCusker KT, Braaten BA, Cho MW, Low DA. 1991. *Legionella pneumophila* inhibits protein synthesis in Chinese hamster ovary cells. *Infection and immunity* 59: 240-6

McDade JE, Brenner DJ, Bozeman FM. 1979. Legionnaires' disease bacterium isolated in 1947. *Annals of internal medicine* 90: 659-61

McDade JE, Shepard CC, Fraser DW, Tsai TR, Redus MA, Dowdle WR. 1977. Legionnaires' disease: isolation of a bacterium and demonstration of its role in other respiratory disease. *The New England journal of medicine* 297: 1197-203

Mears JA, Lackner LL, Fang S, Ingerman E, Nunnari J, Hinshaw JE. 2011. Conformational changes in Dnm1 support a contractile mechanism for mitochondrial fission. *Nature structural & molecular biology* 18: 20-6

Mehlitz A, Karunakaran K, Herweg JA, Krohne G, van de Linde S, et al. 2014. The chlamydial organism *Simkania negevensis* forms ER vacuole contact sites and inhibits ER-stress. *Cellular microbiology* 16: 1224-43

Merriam JJ, Mathur R, Maxfield-Boumil R, Isberg RR. 1997. Analysis of the *Legionella pneumophila fliI* gene: intracellular growth of a defined mutant defective for flagellum biosynthesis. *Infection and immunity* 65: 2497-501

Miller E, Antonny B, Hamamoto S, Schekman R. 2002. Cargo selection into COPII vesicles is driven by the Sec24p subunit. *The EMBO journal* 21: 6105-13

Moenner M, Pluquet O, Bouchecareilh M, Chevet E. 2007. Integrated endoplasmic reticulum stress responses in cancer. *Cancer research* 67: 10631-4

Moffat JF, Tompkins LS. 1992. A quantitative model of intracellular growth of *Legionella pneumophila* in *Acanthamoeba castellanii*. *Infection and immunity* 60: 296-301

Monroe KM, McWhirter SM, Vance RE. 2009. Identification of host cytosolic sensors and bacterial factors regulating the type I interferon response to *Legionella pneumophila*. *PLoS pathogens* 5: e1000665

Moreno AA, Mukhtar MS, Blanco F, Boatwright JL, Moreno I, et al. 2012. IRE1/bZIP60-mediated unfolded protein response plays distinct roles in plant immunity and abiotic stress responses. *PloS one* 7: e31944

Mori K, Ogawa N, Kawahara T, Yanagi H, Yura T. 2000. mRNA splicing-mediated C-terminal replacement of transcription factor Hac1p is required for efficient activation of the unfolded protein response. *Proceedings of the National Academy of Sciences of the United States of America* 97: 4660-5

Mukherjee S, Liu X, Arasaki K, McDonough J, Galan JE, Roy CR. 2011. Modulation of Rab GTPase function by a protein phosphocholine transferase. *Nature* 477: 103-6

Muller MP, Peters H, Blumer J, Blankenfeldt W, Goody RS, Itzen A. 2010. The *Legionella* effector protein DrrA AMPylates the membrane traffic regulator Rab1b. *Science* 329: 946-9

Murata T, Delprato A, Ingmundson A, Toomre DK, Lambright DG, Roy CR. 2006. The *Legionella pneumophila* effector protein DrrA is a Rab1 guanine nucleotide-exchange factor. *Nature cell biology* 8: 971-7

Myeni S, Child R, Ng TW, Kupko JJ, 3rd, Wehrly TD, et al. 2013. *Brucella* modulates secretory trafficking via multiple type IV secretion effector proteins. *PLoS pathogens* 9: e1003556

Nagai H, Kagan JC, Zhu X, Kahn RA, Roy CR. 2002. A bacterial guanine nucleotide exchange factor activates ARF on *Legionella* phagosomes. *Science* 295: 679-82

Natoli G. 2009. Control of NF-kappaB-dependent transcriptional responses by chromatin organization. *Cold Spring Harbor perspectives in biology* 1: a000224

Needham PG, Brodsky JL. 2013. How early studies on secreted and membrane protein quality control gave rise to the ER associated degradation (ERAD) pathway: the early history of ERAD. *Biochimica et biophysica acta* 1833: 2447-57

Neunuebel MR, Chen Y, Gaspar AH, Backlund PS, Jr., Yergey A, Machner MP. 2011. De-AMPylation of the small GTPase Rab1 by the pathogen *Legionella pneumophila*. *Science* 333: 453-6

Nicoll WS, Botha M, McNamara C, Schlange M, Pesce ER, et al. 2007. Cytosolic and ER J-domains of mammalian and parasitic origin can functionally interact with DnaK. *The international journal of biochemistry & cell biology* 39: 736-51

Ninio S, Zuckman-Cholon DM, Cambronne ED, Roy CR. 2005. The *Legionella* IcmS-IcmW protein complex is important for Dot/Icm-mediated protein translocation. *Molecular microbiology* 55: 912-26

O'Connor TJ, Adepoju Y, Boyd D, Isberg RR. 2011. Minimization of the *Legionella pneumophila* genome reveals chromosomal regions involved in host range expansion. *Proceedings of the National Academy of Sciences of the United States of America* 108: 14733-40

O'Connor TJ, Boyd D, Dorer MS, Isberg RR. 2012. Aggravating genetic interactions allow a solution to redundancy in a bacterial pathogen. *Science* 338: 1440-4

Ohnishi H, Mizunoe Y, Takade A, Tanaka Y, Miyamoto H, et al. 2004. *Legionella dumoffii* DjlA, a member of the DnaJ family, is required for intracellular growth. *Infection and immunity* 72: 3592-603

Oikawa D, Tokuda M, Hosoda A, Iwawaki T. 2010. Identification of a consensus element recognized and cleaved by IRE1 alpha. *Nucleic acids research* 38: 6265-73

Oliver JD, Roderick HL, Llewellyn DH, High S. 1999. ERp57 functions as a subunit of specific complexes formed with the ER lectins calreticulin and calnexin. *Molecular biology of the cell* 10: 2573-82

Oyadomari S, Mori M. 2004. Roles of CHOP/GADD153 in endoplasmic reticulum stress. *Cell death and differentiation* 11: 381-9

Palade GE. 1955. A small particulate component of the cytoplasm. *The Journal of biophysical and biochemical cytology* 1: 59-68

Palam LR, Baird TD, Wek RC. 2011. Phosphorylation of eIF2 facilitates ribosomal bypass of an inhibitory upstream ORF to enhance CHOP translation. *The Journal of biological chemistry* 286: 10939-49

Park SH, Zhu PP, Parker RL, Blackstone C. 2010. Hereditary spastic paraplegia proteins REEP1, spastin, and atlastin-1 coordinate microtubule interactions with the tubular ER network. *The Journal of clinical investigation* 120: 1097-110

Paton AW, Beddoe T, Thorpe CM, Whisstock JC, Wilce MC, et al. 2006. AB5 subtilase cytotoxin inactivates the endoplasmic reticulum chaperone BiP. *Nature* 443: 548-52

Pavio N, Romano PR, Graczyk TM, Feinstone SM, Taylor DR. 2003. Protein synthesis and endoplasmic reticulum stress can be modulated by the hepatitis C virus envelope protein E2 through the eukaryotic initiation factor 2alpha kinase PERK. *Journal of virology* 77: 3578-85

Pillich H, Loose M, Zimmer KP, Chakraborty T. 2012. Activation of the unfolded protein response by *Listeria monocytogenes*. *Cellular microbiology* 14: 949-64

Qin QM, Pei J, Ancona V, Shaw BD, Ficht TA, de Figueiredo P. 2008. RNAi screen of endoplasmic reticulum-associated host factors reveals a role for IRE1α in supporting *Brucella* replication. *PLoS Pathog* 4: e1000110

Qiu Q, Zheng Z, Chang L, Zhao YS, Tan C, et al. 2013. Toll-like receptor-mediated IRE1α activation as a therapeutic target for inflammatory arthritis. *The EMBO journal* 32: 2477-90

Ran FA, Hsu PD, Wright J, Agarwala V, Scott DA, Zhang F. 2013. Genome engineering using the CRISPR-Cas9 system. *Nature protocols* 8: 2281-308
Raven JF, Koromilas AE. 2008. PERK and PKR: old kinases learn new tricks. *Cell cycle* 7: 1146-50
Raychaudhuri S, Prinz WA. 2008. Nonvesicular phospholipid transfer between peroxisomes and the endoplasmic reticulum. *Proceedings of the National Academy of Sciences of the United States of America* 105: 15785-90
Raychaudhury S, Farelli JD, Montminy TP, Matthews M, Menetret JF, et al. 2009. Structure and function of interacting IcmR-IcmQ domains from a type IVb secretion system in *Legionella pneumophila*. *Structure* 17: 590-601
Richardson CE, Kooistra T, Kim DH. 2010. An essential role for XBP-1 in host protection against immune activation in *C. elegans*. *Nature* 463: 1092-5
Rismanchi N, Soderblom C, Stadler J, Zhu PP, Blackstone C. 2008. Atlastin GTPases are required for Golgi apparatus and ER morphogenesis. *Human molecular genetics* 17: 1591-604
Ritter C, Helenius A. 2000. Recognition of local glycoprotein misfolding by the ER folding sensor UDP-glucose:glycoprotein glucosyltransferase. *Nature structural biology* 7: 278-80
Rizzuto R, Pinton P, Carrington W, Fay FS, Fogarty KE, et al. 1998. Close contacts with the endoplasmic reticulum as determinants of mitochondrial Ca2+ responses. *Science* 280: 1763-6
Robinson CG, Roy CR. 2006. Attachment and fusion of endoplasmic reticulum with vacuoles containing *Legionella pneumophila*. *Cellular microbiology* 8: 793-805
Ron D, Walter P. 2007. Signal integration in the endoplasmic reticulum unfolded protein response. *Nature reviews. Molecular cell biology* 8: 519-29
Rowbotham TJ. 1980. Preliminary report on the pathogenicity of *Legionella pneumophila* for freshwater and soil amoebae. *Journal of clinical pathology* 33: 1179-83
Roy CR, Berger KH, Isberg RR. 1998. *Legionella pneumophila* DotA protein is required for early phagosome trafficking decisions that occur within minutes of bacterial uptake. *Molecular microbiology* 28: 663-74
Rzomp KA, Scholtes LD, Briggs BJ, Whittaker GR, Scidmore MA. 2003. Rab GTPases are recruited to chlamydial inclusions in both a species-dependent and species-independent manner. *Infection and immunity* 71: 5855-70
Sadretdinova OV, Liuk K, Karpova TI, Belyi Iu F, Tartakovskii IS. 2012. [Prevalence of glucosyl transferase Lgt among *Legionella pneumophila* strains isolated from various sources]. *Zhurnal mikrobiologii, epidemiologii, i immunobiologii*: 8-12
Sanders SL, Whitfield KM, Vogel JP, Rose MD, Schekman RW. 1992. Sec61p and BiP directly facilitate polypeptide translocation into the ER. *Cell* 69: 353-65
Sandoz PA, van der Goot FG. 2015. How many lives does CLIMP-63 have? *Biochemical Society transactions* 43: 222-8
Sandvig K, Garred O, Prydz K, Kozlov JV, Hansen SH, van Deurs B. 1992. Retrograde transport of endocytosed Shiga toxin to the endoplasmic reticulum. *Nature* 358: 510-2
Schmidt EK, Clavarino G, Ceppi M, Pierre P. 2009. SUnSET, a nonradioactive method to monitor protein synthesis. *Nature methods* 6: 275-7

Schroder M, Kaufman RJ. 2005. The mammalian unfolded protein response. *Annual review of biochemistry* 74: 739-89

Scorrano L, Oakes SA, Opferman JT, Cheng EH, Sorcinelli MD, et al. 2003. BAX and BAK regulation of endoplasmic reticulum Ca2+: a control point for apoptosis. *Science* 300: 135-9

Segal G, Shuman HA. 1997. Characterization of a new region required for macrophage killing by *Legionella pneumophila*. *Infection and immunity* 65: 5057-66

Segal G, Shuman HA. 1999. Possible origin of the *Legionella pneumophila* virulence genes and their relation to *Coxiella burnetii*. *Molecular microbiology* 33: 669-70

Sexton JA, Pinkner JS, Roth R, Heuser JE, Hultgren SJ, Vogel JP. 2004. The *Legionella pneumophila* PilT homologue DotB exhibits ATPase activity that is critical for intracellular growth. *Journal of bacteriology* 186: 1658-66

Shang J, Lehrman MA. 2004. Discordance of UPR signaling by ATF6 and Ire1p-XBP1 with levels of target transcripts. *Biochemical and biophysical research communications* 317: 390-6

Shen J, Chen X, Hendershot L, Prywes R. 2002a. ER stress regulation of ATF6 localization by dissociation of BiP/GRP78 binding and unmasking of Golgi localization signals. *Developmental cell* 3: 99-111

Shen X, Banga S, Liu Y, Xu L, Gao P, et al. 2009. Targeting eEF1A by a *Legionella pneumophila* effector leads to inhibition of protein synthesis and induction of host stress response. *Cellular microbiology* 11: 911-26

Shen Y, Meunier L, Hendershot LM. 2002b. Identification and characterization of a novel endoplasmic reticulum (ER) DnaJ homologue, which stimulates ATPase activity of BiP in vitro and is induced by ER stress. *The Journal of biological chemistry* 277: 15947-56

Shoemaker CJ, Eyler DE, Green R. 2010. Dom34:Hbs1 promotes subunit dissociation and peptidyl-tRNA drop-off to initiate no-go decay. *Science* 330: 369-72

Smith JA, Khan M, Magnani DD, Harms JS, Durward M, et al. 2013. *Brucella* induces an unfolded protein response via TcpB that supports intracellular replication in macrophages. *PLoS pathogens* 9: e1003785

Solomon JM, Rupper A, Cardelli JA, Isberg RR. 2000. Intracellular growth of *Legionella pneumophila* in *Dictyostelium discoideum*, a system for genetic analysis of host-pathogen interactions. *Infection and immunity* 68: 2939-47

Sonenberg N, Hinnebusch AG. 2009. Regulation of translation initiation in eukaryotes: mechanisms and biological targets. *Cell* 136: 731-45

Song H, Mugnier P, Das AK, Webb HM, Evans DR, et al. 2000. The crystal structure of human eukaryotic release factor eRF1--mechanism of stop codon recognition and peptidyl-tRNA hydrolysis. *Cell* 100: 311-21

Sory MP, Cornelis GR. 1994. Translocation of a hybrid YopE-adenylate cyclase from *Yersinia enterocolitica* into HeLa cells. *Molecular microbiology* 14: 583-94

Starr T, Child R, Wehrly TD, Hansen B, Hwang S, et al. 2012. Selective subversion of autophagy complexes facilitates completion of the *Brucella* intracellular cycle. *Cell host & microbe* 11: 33-45

Starr T, Ng TW, Wehrly TD, Knodler LA, Celli J. 2008. *Brucella* intracellular replication requires trafficking through the late endosomal/lysosomal compartment. *Traffic* 9: 678-94

Stenmark H. 2009. Rab GTPases as coordinators of vesicle traffic. *Nature reviews. Molecular cell biology* 10: 513-25
Su HL, Liao CL, Lin YL. 2002. Japanese encephalitis virus infection initiates endoplasmic reticulum stress and an unfolded protein response. *Journal of virology* 76: 4162-71
Sugito K, Yamane M, Hattori H, Hayashi Y, Tohnai I, et al. 1995. Interaction between hsp70 and hsp40, eukaryotic homologues of DnaK and DnaJ, in human cells expressing mutant-type p53. *FEBS letters* 358: 161-4
Sun EW, Wagner ML, Maize A, Kemler D, Garland-Kuntz E, et al. 2013. *Legionella pneumophila* infection of *Drosophila* S2 cells induces only minor changes in mitochondrial dynamics. *PloS one* 8: e62972
Sussman M. 1987. Cultivation and synchronous morphogenesis of *Dictyostelium* under controlled experimental conditions. *Methods in cell biology* 28: 9-29
Sutherland MC, Nguyen TL, Tseng V, Vogel JP. 2012. The *Legionella* IcmSW complex directly interacts with DotL to mediate translocation of adaptor-dependent substrates. *PLoS pathogens* 8: e1002910
Swanson MS, Isberg RR. 1995. Association of *Legionella pneumophila* with the macrophage endoplasmic reticulum. *Infection and immunity* 63: 3609-20
Swanson MS, Isberg RR. 1996. Identification of *Legionella pneumophila* mutants that have aberrant intracellular fates. *Infection and immunity* 64: 2585-94
Tan Y, Arnold RJ, Luo ZQ. 2011. *Legionella pneumophila* regulates the small GTPase Rab1 activity by reversible phosphorylcholination. *Proceedings of the National Academy of Sciences of the United States of America* 108: 21212-7
Tan Y, Luo ZQ. 2011. *Legionella pneumophila* SidD is a deAMPylase that modifies Rab1. *Nature* 475: 506-9
Tardif KD, Mori K, Kaufman RJ, Siddiqui A. 2004. Hepatitis C virus suppresses the IRE1-XBP1 pathway of the unfolded protein response. *The Journal of biological chemistry* 279: 17158-64
Tardif KD, Mori K, Siddiqui A. 2002. Hepatitis C virus subgenomic replicons induce endoplasmic reticulum stress activating an intracellular signaling pathway. *Journal of virology* 76: 7453-9
Travers KJ, Patil CK, Wodicka L, Lockhart DJ, Weissman JS, Walter P. 2000. Functional and genomic analyses reveal an essential coordination between the unfolded protein response and ER-associated degradation. *Cell* 101: 249-58
Tsai B, Rodighiero C, Lencer WI, Rapoport TA. 2001. Protein disulfide isomerase acts as a redox-dependent chaperone to unfold cholera toxin. *Cell* 104: 937-48
Upton JP, Wang L, Han D, Wang ES, Huskey NE, et al. 2012. IRE1α cleaves select microRNAs during ER stress to derepress translation of proapoptotic Caspase-2. *Science* 338: 818-22
Urano F, Wang X, Bertolotti A, Zhang Y, Chung P, et al. 2000. Coupling of stress in the ER to activation of JNK protein kinases by transmembrane protein kinase IRE1. *Science* 287: 664-6
Urwyler S, Nyfeler Y, Ragaz C, Lee H, Mueller LN, et al. 2009. Proteome analysis of *Legionella* vacuoles purified by magnetic immunoseparation reveals secretory and endosomal GTPases. *Traffic* 10: 76-87

van Schadewijk A, van't Wout EF, Stolk J, Hiemstra PS. 2012. A quantitative method for detection of spliced X-box binding protein-1 (XBP1) mRNA as a measure of endoplasmic reticulum (ER) stress. *Cell stress & chaperones* 17: 275-9

Vance RE, Isberg RR, Portnoy DA. 2009. Patterns of pathogenesis: discrimination of pathogenic and nonpathogenic microbes by the innate immune system. *Cell host & microbe* 6: 10-21

Vattem KM, Wek RC. 2004. Reinitiation involving upstream ORFs regulates ATF4 mRNA translation in mammalian cells. *Proceedings of the National Academy of Sciences of the United States of America* 101: 11269-74

Vincent CD, Buscher BA, Friedman JR, Williams LA, Bardill P, Vogel JP. 2006a. Identification of non-dot/icm suppressors of the *Legionella pneumophila* DeltadotL lethality phenotype. *Journal of bacteriology* 188: 8231-43

Vincent CD, Friedman JR, Jeong KC, Buford EC, Miller JL, Vogel JP. 2006b. Identification of the core transmembrane complex of the *Legionella* Dot/Icm type IV secretion system. *Molecular microbiology* 62: 1278-91

Vincent CD, Friedman JR, Jeong KC, Sutherland MC, Vogel JP. 2012. Identification of the DotL coupling protein subcomplex of the *Legionella* Dot/Icm type IV secretion system. *Molecular microbiology* 85: 378-91

Voeltz GK, Prinz WA, Shibata Y, Rist JM, Rapoport TA. 2006. A class of membrane proteins shaping the tubular endoplasmic reticulum. *Cell* 124: 573-86

Voeltz GK, Rolls MM, Rapoport TA. 2002. Structural organization of the endoplasmic reticulum. *EMBO reports* 3: 944-50

Vogel JP, Andrews HL, Wong SK, Isberg RR. 1998. Conjugative transfer by the virulence system of *Legionella pneumophila*. *Science* 279: 873-6

Wall D, Zylicz M, Georgopoulos C. 1994. The NH2-terminal 108 amino acids of the *Escherichia coli* DnaJ protein stimulate the ATPase activity of DnaK and are sufficient for lambda replication. *The Journal of biological chemistry* 269: 5446-51

Walter P, Blobel G. 1980. Purification of a membrane-associated protein complex required for protein translocation across the endoplasmic reticulum. *Proceedings of the National Academy of Sciences of the United States of America* 77: 7112-6

Walter P, Blobel G. 1982. Signal recognition particle contains a 7S RNA essential for protein translocation across the endoplasmic reticulum. *Nature* 299: 691-8

Wang Y, Shen J, Arenzana N, Tirasophon W, Kaufman RJ, Prywes R. 2000. Activation of ATF6 and an ATF6 DNA binding site by the endoplasmic reticulum stress response. *The Journal of biological chemistry* 275: 27013-20

Wang ZV, Deng Y, Gao N, Pedrozo Z, Li DL, et al. 2014. Spliced X-box binding protein 1 couples the unfolded protein response to hexosamine biosynthetic pathway. *Cell* 156: 1179-92

Wattiau P, Woestyn S, Cornelis GR. 1996. Customized secretion chaperones in pathogenic bacteria. *Molecular microbiology* 20: 255-62

Wolfson JJ, May KL, Thorpe CM, Jandhyala DM, Paton JC, Paton AW. 2008. Subtilase cytotoxin activates PERK, IRE1 and ATF6 endoplasmic reticulum stress-signalling pathways. *Cellular microbiology* 10: 1775-86

Yamamoto K, Tashiro E, Imoto M. 2011. Quinotrierixin inhibited ER stress-induced XBP1 mRNA splicing through inhibition of protein synthesis. *Bioscience, biotechnology, and biochemistry* 75: 284-8

Yamazaki H, Hiramatsu N, Hayakawa K, Tagawa Y, Okamura M, et al. 2009. Activation of the Akt-NF-kappaB pathway by subtilase cytotoxin through the ATF6 branch of the unfolded protein response. *Journal of immunology* 183: 1480-7

Yanagitani K, Imagawa Y, Iwawaki T, Hosoda A, Saito M, et al. 2009. Cotranslational targeting of XBP1 protein to the membrane promotes cytoplasmic splicing of its own mRNA. *Molecular cell* 34: 191-200

Yanagitani K, Kimata Y, Kadokura H, Kohno K. 2011. Translational pausing ensures membrane targeting and cytoplasmic splicing of XBP1u mRNA. *Science* 331: 586-9

Ye J, Rawson RB, Komuro R, Chen X, Dave UP, et al. 2000. ER stress induces cleavage of membrane-bound ATF6 by the same proteases that process SREBPs. *Molecular cell* 6: 1355-64

Yoneyama M, Kikuchi M, Natsukawa T, Shinobu N, Imaizumi T, et al. 2004. The RNA helicase RIG-I has an essential function in double-stranded RNA-induced innate antiviral responses. *Nature immunology* 5: 730-7

Yoshida H, Matsui T, Yamamoto A, Okada T, Mori K. 2001. XBP1 mRNA is induced by ATF6 and spliced by IRE1 in response to ER stress to produce a highly active transcription factor. *Cell* 107: 881-91

Yoshida H, Okada T, Haze K, Yanagi H, Yura T, et al. 2000. ATF6 activated by proteolysis binds in the presence of NF-Y (CBF) directly to the cis-acting element responsible for the mammalian unfolded protein response. *Molecular and cellular biology* 20: 6755-67

Yoshihisa T, Barlowe C, Schekman R. 1993. Requirement for a GTPase-activating protein in vesicle budding from the endoplasmic reticulum. *Science* 259: 1466-8

Zhouravleva G, Frolova L, Le Goff X, Le Guellec R, Inge-Vechtomov S, et al. 1995. Termination of translation in eukaryotes is governed by two interacting polypeptide chain release factors, eRF1 and eRF3. *The EMBO journal* 14: 4065-72

Zhu PP, Patterson A, Lavoie B, Stadler J, Shoeb M, et al. 2003. Cellular localization, oligomerization, and membrane association of the hereditary spastic paraplegia 3A (SPG3A) protein atlastin. *The Journal of biological chemistry* 278: 49063-71

Zhu W, Banga S, Tan Y, Zheng C, Stephenson R, et al. 2011. Comprehensive identification of protein substrates of the Dot/Icm type IV transporter of *Legionella pneumophila*. *PloS one* 6: e17638

Zurek N, Sparks L, Voeltz G. 2011. Reticulon short hairpin transmembrane domains are used to shape ER tubules. *Traffic* 12: 28-41

Zusman T, Aloni G, Halperin E, Kotzer H, Degtyar E, et al. 2007. The response regulator PmrA is a major regulator of the icm/dot type IV secretion system in *Legionella pneumophila* and *Coxiella burnetii*. *Molecular microbiology* 63: 1508-23

Permissions

This is a License Agreement between Andrew D Hempstead ("You") and Springer ("Springer") provided by Copyright Clearance Center ("CCC"). The license consists of your order details, the terms and conditions provided by Springer, and the payment terms and conditions.

All payments must be made in full to CCC. For payment instructions, please see information listed at the bottom of this form.

License Number	3637980708627
License date	May 28, 2015
Licensed content publisher	Springer
Licensed content publication	Springer eBook
Licensed content title	Host Signal Transduction and Protein Kinases Implicated in Legionella Infection
Licensed content author	Andrew D. Hempstead
Licensed content date	Jan 1, 2013
Type of Use	Thesis/Dissertation
Portion	Excerpts
Author of this Springer article	Yes and you are the sole author of the new work
Order reference number	None
Title of your thesis / dissertation	Modulation of the Host Unfolded Protein Response by Legionella pneumophila
Expected completion date	Jun 2015
Estimated size(pages)	1

This is a License Agreement between Andrew D Hempstead ("You") and Elsevier ("Elsevier") provided by Copyright Clearance Center ("CCC"). The license consists of your order details, the terms and conditions provided by Elsevier, and the payment terms and conditions.

All payments must be made in full to CCC. For payment instructions, please see information listed at the bottom of this form.

Supplier	Elsevier Limited The Boulevard,Langford Lane Kidlington,Oxford,OX5 1GB,UK
Registered Company Number	1982084
Customer name	Andrew D Hempstead
Customer address	146 Harrison Ave BOSTON, MA 02111
License number	3656040399361
License date	Jun 25, 2015
Licensed content publisher	Elsevier
Licensed content publication	Structure
Licensed content title	IcmQ in the Type 4b Secretion System Contains an NAD+ Binding Domain
Licensed content author	Jeremiah D. Farelli,James C. Gumbart,Ildikó V. Akey,Andrew Hempstead,Whitney Amyot,James F. Head,C. James McKnight,Ralph R. Isberg,Christopher W. Akey
Licensed content date	6 August 2013
Licensed content volume number	21
Licensed content issue number	8
Number of pages	13
Start Page	1361
End Page	1373
Type of Use	reuse in a thesis/dissertation
Intended publisher of new work	other
Portion	excerpt
Number of excerpts	3
Format	both print and electronic
Are you the author of	Yes

this Elsevier article?	
Will you be translating?	No
Title of your thesis/dissertation	Modulation of the Host Unfolded Protein Response by Legionella pneumophila
Expected completion date	Jun 2015
Estimated size (number of pages)	1

This is a License Agreement between Andrew D Hempstead ("You") and Elsevier ("Elsevier") provided by Copyright Clearance Center ("CCC"). The license consists of your order details, the terms and conditions provided by Elsevier, and the payment terms and conditions.

All payments must be made in full to CCC. For payment instructions, please see information listed at the bottom of this form.

Supplier	Elsevier Limited The Boulevard,Langford Lane Kidlington,Oxford,OX5 1GB,UK
Registered Company Number	1982084
Customer name	Andrew D Hempstead
Customer address	146 Harrison Ave BOSTON, MA 02111
License number	3656040205371
License date	Jun 25, 2015
Licensed content publisher	Elsevier
Licensed content publication	Structure
Licensed content title	IcmQ in the Type 4b Secretion System Contains an NAD+ Binding Domain
Licensed content author	Jeremiah D. Farelli,James C. Gumbart,Ildikó V. Akey,Andrew Hempstead,Whitney Amyot,James F. Head,C. James McKnight,Ralph R. Isberg,Christopher W. Akey
Licensed content date	6 August 2013

Licensed content volume number	21
Licensed content issue number	8
Number of pages	13
Start Page	1361
End Page	1373
Type of Use	reuse in a thesis/dissertation
Portion	figures/tables/illustrations
Number of figures/tables/illustrations	1
Format	both print and electronic
Are you the author of this Elsevier article?	Yes
Will you be translating?	No
Original figure numbers	Figure S5
Title of your thesis/dissertation	Modulation of the Host Unfolded Protein Response by Legionella pneumophila
Expected completion date	Jun 2015
Estimated size (number of pages)	1